University of Southern Queensland

The cytotoxic properties of novel compounds from a *Preussia* sp. isolate on PC-3 prostate cancer cells

A thesis submitted by

Brooke Raphael

Bachelor of Biomedical Science USQ

For the Award of

Bachelor of Science (Honours)

2021

Abstract

Prostate cancer (PCa) is the most commonly diagnosed cancer amongst Australian males. The significant economic and healthcare burden caused by PCa requires immediate action. Although chemotherapies such as docetaxel can be successful as a first line treatment for metastatic castration-resistant PCa (mCRPC), chemo-resistance and disease progression can develop. Therefore, novel drugs are in need of discovery.

Endophytic microfungi have potential as new sources of anticancer chemotherapy agents as they can be sustainably acquired and are capable of large-scale and low-cost production. Many antifungal and antibacterial compounds sourced from endophytes have also been demonstrated to cause cytotoxicity in cancer cell lines. These chemotherapy agents act as mitotic inhibitors, signal transduction disruptors, and topoisomerase inhibitors. The present study investigates the cytotoxic properties that a previously studied endophytic *Preussia* sp. may possess, given that polyketides extracted from this isolate were reported to be antibacterial and antifungal in nature. Cytotoxic polyketides from other *Preussia* spp. have been reported to disrupt the cytoskeleton of prostate cancer cell lines and cause apoptosis. Therefore, evidence of cytoskeletal disruption and apoptosis were the tested mechanisms of action in this study.

The antimicrobial activity of the *Preussia* sp. isolate was initially confirmed by co-culturing with pathogenic bacteria and fungi on solid media. The isolate was next grown in a bulk culture, and ethyl acetate (EtOAc) extracts were obtained and re-tested against *Bacillus cereus* and *Enterococcus faecalis*. EtOAc extracts were then separated into fractions via high performance liquid chromatography (HPLC). These fractions were tested using an *in vitro* model of castration resistant PCa (CRPC), the PC-3 cell line, at varying concentrations in order to investigate any cytotoxic effects. Treated cells were also visualised with fluorescence microscopy to investigate changes to cytoskeletal and nuclear structures.

The cell counting kit (CCK-8) assay revealed that several fractions had a negative effect on cell proliferation and so were potentially cytotoxic at pharmaceutically relevant concentrations. Fraction four at 50 µg/mL decreased live cell number by 16% ($p=0.0355$). Fraction five at 50 µg/mL and 100 µg/mL reduced live cell number by 25% ($p=0.0415$) and 28.5% ($p=0.0082$), respectively. Fraction six at 50 µg/mL and 100 µg/mL decreased live cell number by 32.4% ($p=0.0009$) and 87.4% ($p<0.0001$), respectively. Cytoskeletal and nuclear structure studies using microscopy did not reveal any consistent changes amongst the replicate treated cells suggesting that the decrease in cell number that was observed may have been caused by non-apoptotic mechanisms. Therefore, this study provides significant evidence that this endophytic isolate may contain important anti-cancer compounds.

Keywords

Endophyte, cytotoxic, prostate cancer, anti-cancer, PC-3, antimicrobial, microtubule.

Declaration

I certify that the work reported in this thesis is entirely my own effort, except where otherwise acknowledged. I also certify that the work is original and has not previously been submitted for assessment in any other course of study, at any other University.

Candidate: Brooke Raphael Date:

Endorsement

Principal Supervisor; Dr John Dearnaley Date:

Acknowledgements

I would like to give thanks and acknowledge the contributions to those who have helped me in the pursuit of this project. Firstly, and most importantly, my excellent team of supervisors; Assoc. Prof. John Dearnaley, Assoc. Prof. Eliza Whiteside, and Dr Mark Lynch for your unwavering guidance, feedback, expertise, and assistance throughout this year. An extra thank you for the DA opportunities outside of this project, open-door policies, and most importantly, the coffees. Without the three of you, the completion of this project and thesis would never have been possible. Thank you!

Thank you to soon to be Dr Ashwini Sharma for your support and expertise. I would also like to thank technical staff across W block and D block ILSE laboratories. To all of you, thank you!

An extra special thank you to my examiners Dr Stuart Ellem and Assoc. Prof. Kate Kauter for all of your constructive feedback and advice throughout the year, that has particularly helped me improve my writing. Thank you for your contributions to this. To Dr Joanna Turner, the convenor of this honours program, thank you for your efforts to ensure that I got the most out of this year. I'd also like to thank my fellow students who have provided many an entertaining conversation this year that I am sure has kept us all sane.

Lastly, but certainly not least, the biggest thank you of all must go out to my family and friends who have encouraged me in my pursuit of biomedical science for many years, who have listened to me rant on many occasions about things going wrong in the lab, and always being willing to listen to me talk about this project. You guys are the MVPs, and so I dedicate this thesis to you.

Table of Contents

List of abbreviations

ATCC	American type culture collection
ADT	Androgen deprivation therapy
AR	Androgen receptor
BA	Betulinic acid
BAK	Bcl-2 homologous antagonist killer
BAX	Bcl-2-associated X protein
Bcl-2	B-cell lymphoma 2
CCK-8	Cell counting kit - 8
CRPC	Castration resistant prostate cancer
CZ	Central zone
DMSO	Dimethyl Sulfoxide
DNA	Deoxyribonucleic acid
DU-145	Prostate carcinoma cell line
EMT	Epithelial-mesenchymal transition
EtOAc	Ethyl acetate
EtOH	Ethanol
ETP	Epipolythiodiketopiperazine
Fas/ FasL	Cell surface death receptor
FCE	Fungal crude extract
FCS	Foetal calf serum
HGPIN	High grade prostatic intraepithelial neoplasia
HPLC	High performance liquid chromatography
KDM5D	Lysine-specific demethylase 5D
LC-MS	Liquid chromatography0- mass spectrometry
LEDGF/p75	Lens epithelium-derived growth factor p75
LNCaP	Androgen sensitive lymph node metastases of prostate cancer cell line
MAPK	Mitogen-activated protein kinase
mAU	Milli-absorbance units
mCRPC	Metastatic castration resistant prostate cancer
MEB	Malt extract Broth
MeOH	Methanol

MHB	Mueller-Hinton Broth
MRSA	Methicillin resistant *Staphylococcus aureus*
NCOR	Nuclear receptor corepressor
NMR	Nuclear magnetic resonance
p53	Tumour suppressor protein
PBS	Phosphate buffered saline
PC-3	Grade IV prostate adenocarcinoma cell line
PC-3M	Metastatic prostate adenocarcinoma cell line
PCa	Prostate cancer
PDA	Potato dextrose agar
PIN	Prostatic intraepithelial neoplasia
PS	Penicillin/ streptomycin
PSA	Prostate specific antigen
PUMA	p53 upregulated modulator of apoptosis
PZ	Peripheral zone
ROS	Reactive oxygen species
RPMI	Roswell Park Memorial Institute
SA	Secalonic acid
STA	Sensitest agar
STAT3	Signal transducer and activator of transcription 3
TRAIL	Tumour necrosis factor related apoptosis inducing ligand
TZ	Transitional zone
UV	Ultraviolet

List of figures

List of tables

Chapter 1: Introduction and literature review

1.1 Introduction

Prostate cancer (PCa) is the most commonly diagnosed cancer amongst Australian males with over 19,000 cases recorded in 2017 (Australian Institute of Health and Welfare 2021). This results in approximately 3,000 deaths annually, which is approximately 12% of cancer related deaths. There is a significant healthcare burden that results from PCa, costing Australia over $349 million in 2008-2009 (Prostate Cancer Foundation of Australia 2021). The type of treatment for PCa is usually prescribed based on the age of the patient, the stage and grade of the tumour, and the androgen sensitivity of the tumour. Early stage, low grade tumours are often monitored rather than actively treated however, later stage, localised tumours are treated with radiation or surgical intervention. Late stage metastatic tumours are most commonly treated with androgen deprivation therapy (ADT), and chemotherapy if castration resistance develops (Wang et al. 2018). Docetaxel is a semi-synthetic analogue of paclitaxel and is the primary chemotherapeutic agent used for metastatic (advanced) PCa. Docetaxel elicits its anti-cancer effect via binding to beta tubulin, stabilising the mitotic spindle during cell division (Herbst & Khuri 2003; Weaver 2014). Docetaxel may successfully improve prognosis, but it is not always curative and results in many adverse side effects such as alopecia, fatigue, and anaemia (Tannock et al. 2004; Sathianathen et al. 2018). In addition, resistance to docetaxel is common in patients, so novel approaches for the treatment of advanced PCa are urgently required.

Many existing clinically used medications, including cancer chemotherapy agents like docetaxel, originated from natural sources. One of the most successful anti-cancer drugs discovered thus far is paclitaxel, brand name Taxol, and is the natural origin of docetaxel. Paclitaxel was isolated from the bark of *Taxus brevifolia*, or the Pacific yew tree (Wani et al.

1971), but it was later realised that a micro fungus that resided in the bark of the tree was also capable of producing paclitaxel (Stierle et al. 1993). Microfungi, or endophytes, are organisms which live intercellularly in many plant tissues, and are producers of many different compounds with antibacterial, antifungal, and cytotoxic activity (Aly et al. 2011; Gouda et al. 2016). Endophytes may address the challenges of the slow growth rate and rarity of the *Taxus* trees responsible for paclitaxel production, as endophytes are easy to grow in culture. Therefore, endophytes are a promising source for alternative anti-cancer compounds. In this study, a previously isolated *Preussia* sp. (BSH2.9) endophyte from a local dry rainforest was investigated for antimicrobial and cytotoxic activity against human pathogenic bacteria, fungal pathogens, and prostate cancer cells.

1.2 The prostate gland

The prostate is a secondary sex organ of the male reproductive system, contributing to components of seminal fluid, including enzymes, lipids, amines, and metal ions (Frick & Aulitzky 1991). It is situated inferior to the bladder and surrounds the urethra (McNeal 1981) and can be divided into peripheral (PZ) and central zones (CZ) (Kumar & Majumder 1995). Additionally, a preprostatic sphincter, anterior segment, and transitional zones (TZ) have been identified (Figure 1; (McNeal 1969)). The gland consists of a system of branching ducts which are composed of a fibromuscular stroma that encases a pseudostratified epithelium. The pseudostratified epithelium is comprised of three terminally differentiated cell types; basal,

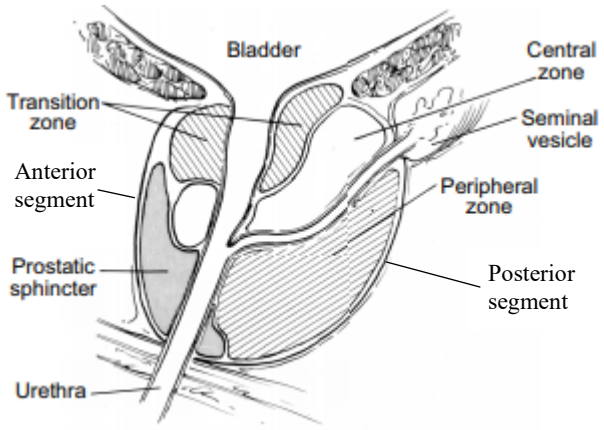

Figure 1: Sagittal section of the adult human prostate (McNeal 1969).

luminal, and neuroendocrine (Toivanen & Shen 2017). The most common pathologies associated with the prostate gland include prostatitis (inflammation), benign prostatic hyperplasia (enlarged prostate), and malignant disease (cancer) (Jemaa et al. 2010; Banerjee et al. 2016). Unfortunately, malignancies of the prostate are difficult to detect as approximately 70% of tumours occur in the PZ and patients are asymptomatic (McNeal et al. 1988; Hoeks et al. 2013; Huang et al. 2019).

1.3 Prostate cancer

1.3.1 The grading method

The Gleason grading system, developed by D.F. Gleason, is a system which categorises PCa tumours based on their histological patterns. The histology of the prostate greatly varies across the grades, where a grade of 1 indicates a healthy, normally differentiated prostate, through to a grade of 5 indicating a poorly differentiated, anaplastic prostate as illustrated in Figure 3 (Gleason & Mellinger 1974). Furthermore, a Gleason score will equal the addition of primary and secondary patterns, resulting in a score ranging from 2-10 (Humphrey 2004; Epstein et al. 2005). However, a score of 2 would indicate a normal prostate, so it is unlikely that lower scores would be seen in a clinical setting. The grouping process has since progressed to a grade grouping system using six groups. Grade Group 1 = Gleason scores ≤ 6, Grade Group 2 = Gleason score 3 + 4 = 7, Grade Group 3 = Gleason score 4 + 3 = 7, Grade Group 4 = Gleason score 4 + 4 = 8, and

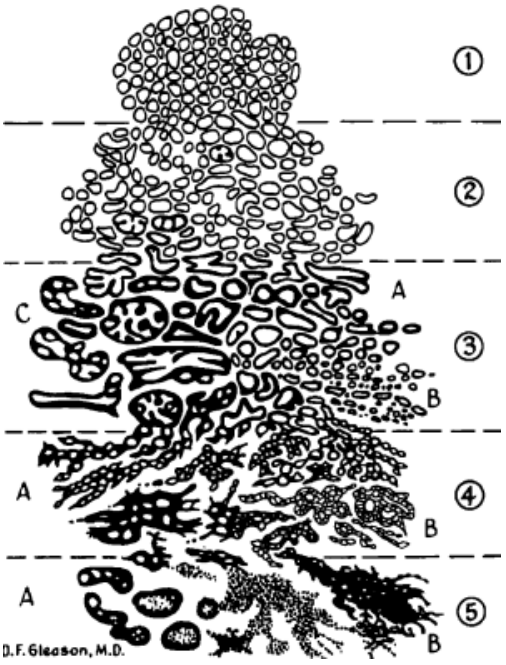

Figure 2: Drawing of the histological patterns of the Gleason grading system (Gleason & Mellinger 1974).

Grade Group 5 = Gleason scores 9 and 10. This updated system has demonstrated improved accuracy in predicting tumour progression (Gordetsky & Epstein 2016). The staging process for PCa is important as diagnosis and prognosis are a result of the association between the given score and the aggressiveness of the tumour (Chen & Zhou 2016). Other mechanisms such as the identification of prostate specific antigen (PSA) concentration are also involved in the staging process (Partin et al. 1996).

1.3.2 Prostate cancer tumorigenesis

The transformation of a benign, normally functioning section of prostate tissue into a malignant, metastatic PCa (illustrated in Figure 3) begins with the progression of a normal epithelium into a localised prostatic intraepithelial neoplasia (PIN) (Wang et al. 2018). PIN is described as a hyperplastic condition of the luminal epithelium with characteristics such as basal cell reduction, nuclear atypia, and cytoplasmic hyperchromasia, occurring primarily in the PZ of the prostate (Bostwick & Brawer 1987; Shappell et al. 2004). PIN lesions usually have a markedly increased expression of proliferation markers, and can be both low- and high-grade (Shappell et al. 2004). High grade PIN (HGPIN) lesions have been demonstrated to be precursors to invasive carcinoma (Bostwick & Qian 2004). Invasive carcinoma in its earlier stages often have altered differentiation markers, which have since been demonstrated in PIN lesions (Nagle et al. 1991).

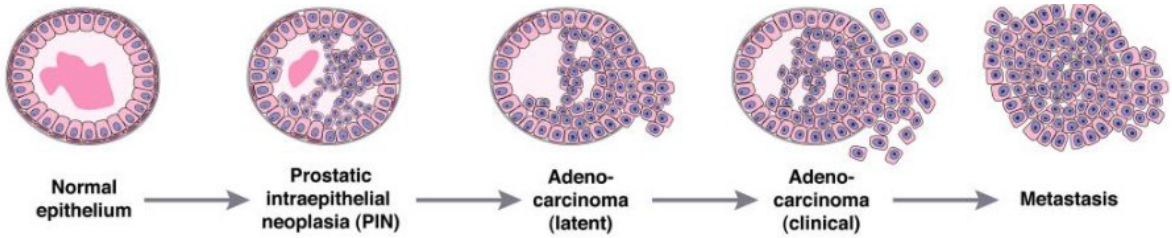

Figure 3: Human prostate cancer progression pathway (Shen & Abate-Shen 2010).

Following the development of PIN, the lesion then progresses to a latent adenocarcinoma, resulting in a complete loss of the basal lamina (Wang et al. 2018). It is suggested that latent carcinomas are a result of a neoplastic transformation event of the prostate which does not

progress to an invasive carcinoma, thus latent adenocarcinoma develops (Yatani et al. 1989). Clinical adenocarcinoma of the prostate develops when developmental signalling pathways for prostate tumorigenesis are reactivated (Shen & Abate-Shen 2010), which begins in a locally advanced stage. At this stage, prostatectomy is common and radiation such as brachytherapy may also be prescribed. In the case of metastatic tumours leading to advanced PCa, treatments such as androgen deprivation therapy (ADT) are prescribed, with or without chemotherapy such as docetaxel (Wang et al. 2018).

The lymph nodes neighbouring the prostate are the primary site for metastases of castration resistant PCa (CRPC) to develop (Datta et al. 2010). CRPC can also metastasise to the liver, lungs, and more commonly, the bones (Wang et al. 2018). Epithelial-mesenchymal transition (EMT) is one of the key explanations for the metastasis of cancers (Kalluri & Weinberg 2009), including PCa (Yeung & Yang 2017). EMT is the trans-differentiation of the epithelial cells into mesenchymal cells which are motile. There is reorganisation of the actin cytoskeleton which promotes cell elongation and directional movement (Lamouille et al. 2014). The membranous, actin rich projections are responsible for the proteolysis of the extracellular matrix, which aids in cell invasion in metastatic disease (Lamouille et al. 2014).

1.3.3 The role of androgen signalling

Androgens signal via the androgen receptor (AR) and are critical in normal prostate function (Fujita & Nonomura 2019). Genomic modifications including loss of nuclear receptor (*NCOR1/2)* AR corepressor, gain of *NCO1/2* AR coactivator and mutations and amplifications of the AR occur in the majority of PCa, including metastatic and primary disease, and contribute to castration resistant PCa (Hodgson et al. 2005; Taylor et al. 2010). The depletion of androgens to below effective concentration is referred to as chemical castration. Castration was first reported as an effective method for reducing prostate tumours in the 1940s (Huggins

& Hodges 1941). Huggins and Hodges (1941) reported that both surgical castration and chemical castration using oestrogen injections significantly reduced the serum concentration of a prostatic enzyme called acid phosphatase. Acid phosphatase was reported to be present in large concentrations within the healthy prostate gland (Kutscher & Wolbergs 1935). Huggins and Hodges (1941) indicated that both surgical castration and oestrogen injections could also reduce prostate tumour growth. Since this discovery, ADT has been a main stay in PCa treatment. However, prolonged use of ADT can result in tumour progression to CRPC (Feng & He 2019). The persistent activation of AR signalling is a result of a lack of the domain responsible for ligand (androgen) binding, therefore driving the progression of PCa to CRPC (Feng & He 2019; Fujita & Nonomura 2019). It is at this stage, where castration resistance develops and chemotherapies such as docetaxel become necessary (Saad & Hotte 2010).

1.3.4 Current chemotherapy regimens for advanced PCa

Docetaxel and chemo-resistance

The treatment regimen prescribed for a specific PCa patient is dependent upon the age, stage and grade from diagnosis and is usually a combination of chemotherapy, radiation, ADT, or surgical intervention (Wang et al. 2018). The most commonly prescribed form of chemotherapy for advanced PCa is docetaxel. Docetaxel is a semi-synthetic taxane diterpene alkaloid which has broad cytotoxic properties and is used for a range of progressed cancers, such as metastatic castration resistant PCa (mCRPC). One mechanism of docetaxel (Figure 4) is inhibition of microtubule disassembly, causing stabilisation of the mitotic spindle which, in turn, causes arrest of the cell cycle and thus, apoptosis occurs. Figure 4 also highlights that microtubule stabilisation by beta-tubulin binding causes cytotoxicity by many pathways (Mikuła-Pietrasik et al. 2019). Docetaxel can also induce apoptosis via caspase-dependent apoptosis by decreasing the expression of the key anti-apoptotic protein, B-cell lymphoma 2

(Bcl-2). An autophagic pathway via lysosomal membrane permeabilisation can also be induced, causing apoptosis (Boya & Kroemer 2008; Mediavilla-Varela et al. 2009).

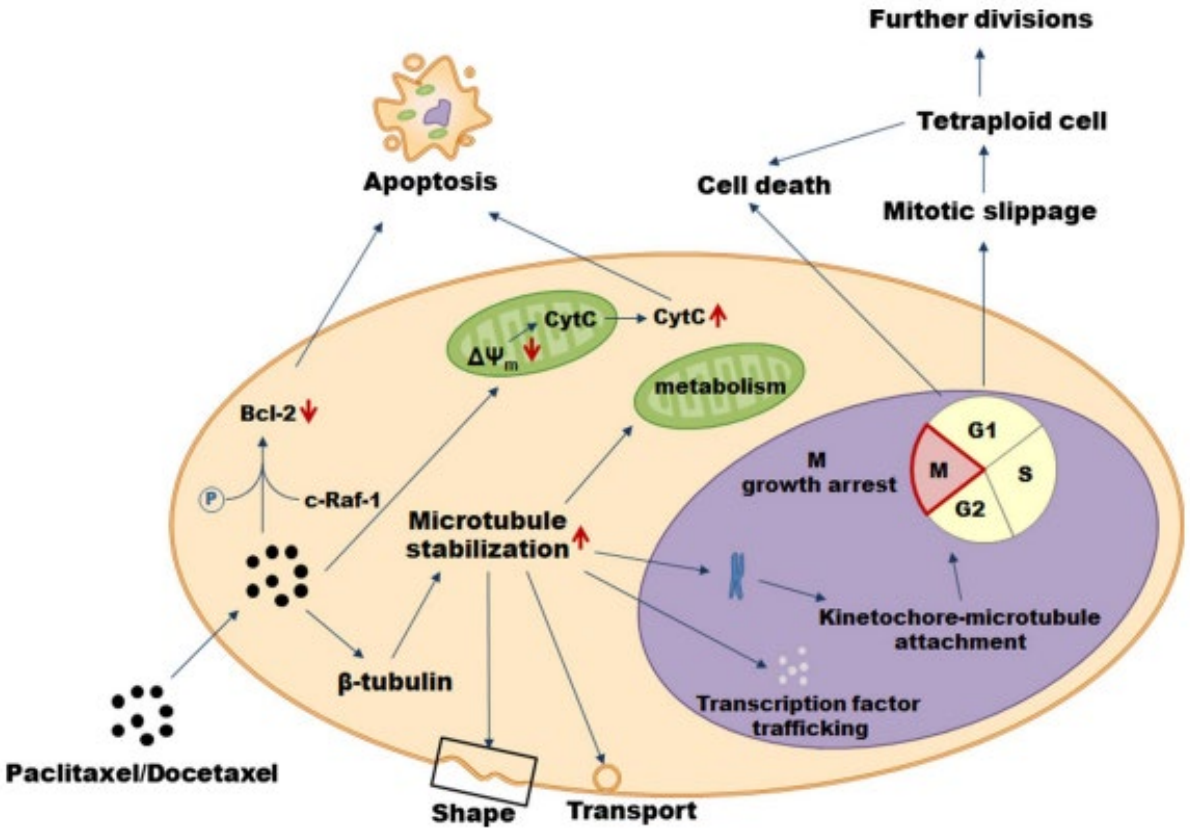

Figure 4: Cytotoxicity mechanisms of paclitaxel and docetaxel (Mikula-Pietrasik et al. 2019).

It is well established that docetaxel administration is effective in improving prognosis of CRPC (Varnai et al. 2019), however, there are adverse side effects. In a phase I trial, 32% of participants reported severe neutropenia, 65% reported alopecia, and 53% reported fatigue. Additionally, thrombocytopaenia and anaemia were reported (Tannock et al. 2004; Sathianathen et al. 2018). Furthermore, CRPC is capable of developing resistance to docetaxel, as well as other chemotherapy drugs, and is therefore rarely curative (Jia et al. 2019). An example of a resistance mechanism to docetaxel is the overexpression of a transcription activator and stress survival autoantigen, lens epithelium-derived growth factor p75 (LEDGF/p75). The implication of LEDGF/p75 in docetaxel resistance has been supported by lysosomal stabilisation resulting from docetaxel exposure. Intriguingly, these protective effects

were not observed for cells that underwent docetaxel induced mitotic cell death or apoptosis caused by tumour necrosis factor related apoptosis inducing ligand (TRAIL) (Mediavilla-Varela et al. 2009). Another potential mechanism for resistance is androgen receptor activation dependent and involves decreased expression of lysine-specific demethylase 5D (KDM5D). KDM5D interacts with the AR, so attenuation of KDM5D deregulates androgen signalling in androgen-dependent tumours (Komura et al. 2016).

Second-line chemotherapy

Cabazitaxel is another taxane-based chemotherapy that is used as a second line treatment when docetaxel resistance develops in CRPC. However, cabazitaxel can only be used for a few months after docetaxel resistance as resistance to cabazitaxel develops quickly. Prednisone, a corticosteroid, has been demonstrated to increase the efficacy of both docetaxel and cabazitaxel (de Bono et al. 2010; Teply et al. 2016).

Estramustine is an oestradiol molecule linked to an alkylating agent (nitrogen mustard) that alkylates deoxyribonucleic acid (DNA) causing cell death resulting in tumour shrinkage (Benson & Hartley-Asp 1990). Vinblastine is a *Vinca* alkaloid that can also be used to treat CRPC. Vinblastine also binds proteins of the microtubules to inhibit correct formation of the mitotic spindle. Studies have demonstrated that the combination of vinblastine with oral estramustine may not improve survival but has slowed progression and decreased PSA when compared to administration of vinblastine alone (Hudes et al. 1999). However, some clinical trials have demonstrated significant deterioration in quality of life and general well-being of patients (Albrecht et al. 2004).

Cisplatin is an alkylating agent which causes overall apoptosis of cancer cells. Cisplatin binds the purine bases of the DNA, forming intra- and inter-strand crosslinks. These DNA adducts then primarily signal tumour protein p53 upregulated modulator of apoptosis (PUMA) and the

Fas/FasL cell surface death receptor apoptosis pathways (Siddik 2003). Cisplatin has also been shown to increase cell stiffness, in turn decreasing metastasis and migration potential of the tumour (Raudenska et al. 2019). Although therapeutic options such as docetaxel and other agents have been demonstrated to be successful in improving PCa prognosis, mCRPC remains an incurable disease. Therefore, the discovery of compounds that are more effective and less likely to lead to resistance mechanisms is essential (Hwang 2012).

1.4 Endophytes

Endophytes are a group of microorganisms, particularly fungi and bacteria, which have an intercellular, endosymbiotic relationship with plants. They have the ability to colonise many areas of the plant including; fruits, buds, leaves, stems, roots, and seeds (Gouda et al. 2016). The relationship between endophytes and their host plants can also be further categorised into obligate or facultative subtypes (Khare et al. 2018). Facultative endophytes naturally live in soils, but will opportunistically colonise plant roots (Hardoim et al. 2015), whereas obligate endophytes require a host plant for their entire life cycle (Card et al. 2016). Endophytes are a highly understudied group of microorganisms, particularly in the rainforests of Queensland. The rich diversity of flora in these regions suggests that many unique and valuable endophyte species await discovery.

Paclitaxel (Taxol) is an anti-cancer agent that was originally isolated from the bark of *Taxus brevifolia* (Stierle et al. 1993). Paclitaxel is also the natural analogue of the primary chemotherapy used for advanced PCa, docetaxel. Due to low yields of paclitaxel from *Taxus,* researchers focussed on identifying other sources in order to satisfy the demand for the drug (Senthil Kumuran et al. 2008). As a result, multiple studies identified other paclitaxel-producing species including an endophyte within *Taxus* bark called *Taxomyces andreanae*

(Stierle et al. 1993). Further study isolated an additional paclitaxel-producing endophyte, *Fusarium solani,* from *Taxus*, and confirmed the anti-cancer activity of the extracted paclitaxel against A459 lung cancer cells in a dose- and time-dependent manner (Kuriakose et al. 2020). *Phyllosticta spinarum*, an endophyte of *Cupressus* species, was also shown to produce paclitaxel, and anti-cancer activity was confirmed against intestinal, leukaemia, breast, and lung cancer cell lines. This latter study identified that the percentage of apoptotic cells were highest at paclitaxel concentrations between 0.05 μM and 0.5 μM (Senthil Kumuran et al. 2008).

Although there is overwhelming evidence supporting the production of paclitaxel by endophytes, there are studies which challenge this idea. One crucial study contradicting the proposed production of paclitaxel from endophytes based this on the finding that there were no genes present in the tested endophytes that could independently synthesise the compound (Heinig et al. 2013). This study used genomic sequencing and phytochemistry techniques on two unidentified endophytes and *T. andreanae* from *Taxus*, and were not able to identify any genes which would be cause for independent biosynthesis of paclitaxel (Heinig et al. 2013).

1.4.1 Cytotoxic compounds from endophytes

Mechanisms of endophyte derived cytotoxic compounds

Endophytes produce an array of cytotoxic compounds including alkaloids, terpenoids, phenols, polyketides, and steroids (see Table 1).

Table 1: Examples of the different types of cytotoxic compounds from varying chemical classes that endophytes have been reported to produce.

Endophytic fungi	Chemical	Chemical class	Cell line	Reference
Fusarium oxysporum	Vincristine	Alkaloid	Not reported	(Zhang et al. 2000)
Mycelia sterile	Vincristine	Alkaloid	Not reported	(Yang et al. 1994)
Phomopsis cassia	3,12-dihydroxydalene	Terpenoid	HeLa cervical cancer	(Silva et al. 2006)
Alternaria sp.	Xanalteric acids	Phenol	Mouse lymphoma (L5178Y)	(Kjer et al. 2009)
Cephalotheca faveolata	Sclerotiorin	Polyketide	Colon cancer (HCT-116)	(Giridharan et al. 2012)
Phoma sp.	5-hydroxyramulosin	Polyketide	Murine leukaemia (P388)	(Santiago et al. 2012)
Aspergillus flavus	Solamargine	Steroid	Not reported	(El-Hawary et al. 2016)

Endophyte cytotoxic compounds, particularly alkaloids and polyketides, have been reported to operate by a variety of mechanisms. Alkaloids have been reported to exhibit their effects by disruption of the cytoskeleton, particularly the arrangement of the mitotic spindle in mitosis. *Vinca* alkaloids, for example target the microtubules of the cell, as do paclitaxel and other taxanes, and prevent correct formation of the mitotic spindle by binding of the beta-tubulin subunits, causing apoptosis (Himes 1991). However, endophytic polyketides have also been reported to inhibit microtubules thereby disrupting normal spindle formation during mitosis, and also causing apoptosis by this mechanism (Noumeur et al. 2017).

Other alkaloid-based compounds have been reported to interrupt topoisomerases. Topoisomerases are responsible for regulating the topology of DNA and inhibition of them results in improper DNA replication and double stranded breaks. Etoposide and teniposide are semi-synthetic analogues of podophyllotoxin (Uzma et al. 2018) that are sourced from endophytes (Kusari et al. 2009) and are examples of alkaloids that inhibit topoisomerases (Li et al. 2006; Montecucco et al. 2015), impacting DNA replication resulting in apoptosis. Some polyketides can also inhibit topoisomerases. Anthracyclines, such as doxorubicin, are examples of polyketide-based compounds that impact DNA replication by topoisomerase inhibition (Zunino & Capranico 1990).

Another pathway in which some cytotoxic compounds act is via the intrinsic caspase-dependent apoptosis pathway. The intrinsic pathway involves the inhibition of the anti-apoptotic proteins belonging to the Bcl-2 family. These proteins preserve the integrity of the mitochondrial membrane (Tsujimoto 1998). However, anticancer therapies typically cause pro-apoptotic members of this family such as Bcl-2-associated X protein (BAX) and Bcl-2 homologous antagonist killer (BAK) proteins to oligomerize the mitochondrial membrane which causes release of cytochrome c, initiating the caspase pathway involving procaspase 9 and caspase 3 that ultimately result in apoptosis (Tzifi et al. 2012). Both alkaloids and polyketides from endophytic fungi have been reported to induce this apoptosis pathway. An alkaloid called pyrrocidine A was reported to have resulted in increased expression of BAX, procaspase 9, and caspase 3 in neutrophilic promyelocyte (HL60) cells, indicating activation of apoptosis via the intrinsic pathway (Uesugi et al. 2016). Secalonic acid (SA) is a polyketide and has also been reported to cause apoptosis via the intrinsic pathway. Caspase 3 cleavage was increased in HL60 and myelogenous leukaemia (K562) cell lines. Furthermore, significant cytotoxicity was observed with IC_{50} of 0.38 ± 0.04 μM and 0.43 ± 0.02 μM for these respective cell lines (Zhang et al. 2009).

STAT3 is a signal transducer and transcription factor which is involved in cell proliferation, and is tightly regulated in a normal cell (Calò et al. 2003). However, increased activation of STAT3 has been correlated to the malignancy of PCa cells, increased Gleason score, and progression of the disease (Mora et al. 2002; Horinaga et al. 2005; Tam et al. 2007). Galiellalactone is a polyketide isolated from endophytic *Galiella rufa* which has been demonstrated to decrease tumour growth in STAT3 positive prostate carcinoma (DU-145) and grade IV prostate adenocarcinoma cell line (PC-3) cells (Don-Doncow et al. 2014) while having no affect in cells which were lacking STAT3 expression (Hellsten et al. 2008). Therefore, endophyte derived alkaloids and polyketides have varying cytotoxic mechanisms, and include signal transduction targets such as STAT3, inhibition of topoisomerases, induction of apoptosis via caspase activation, and disruption of mitosis via inhibition of mitotic spindles.

Endophyte derived compounds causing cytotoxicity in prostate cell lines

Endophytes may contain useful compounds in addressing the current challenges with PCa treatment. Verekar and colleagues (2014) screened a depsipeptide (PM181110) isolated from *Phomopsis glabrae,* an endophyte of *Pongamia pinnata* (Karum or Poonga-Oil tree) for cytotoxicity. The compound was screened against metastatic prostate adenocarcinoma (PC-3M), DU-145, and androgen sensitive lymph node metastases of prostate cancer (LNCaP) cell lines. The compound was effective against all three cell lines with half maximal inhibitory concentrations of 0.047, 0.052, and 0.122 µM, respectively (Verekar et al. 2014).

Tauranin is a compound isolated from *Phyllosticta spinarum,* an endophyte of *Platycladus orientalis* (Chinese arborvitae). Against the PC-3M cell line, tauranin was cytotoxic and had a half maximal inhibitory concentration of 3.5 µM which is comparable, but still less potent than that of the positive control, doxorubicin, which had a half maximal inhibitory concentration of 1.11 µM (Wijeratne et al. 2008).

Epipolythiodiketopiperazines (ETPs) are alkaloids present in many fungal endophytes which have been demonstrated as potent cytotoxic agents. A study isolated ETPs from *Preussia typharum* and identified that they were potently cytotoxic against PC-3 and DU-145 cell lines with a 50% growth inhibition concentration of 15.5 nM and 14.3 nM, respectively. Furthermore, the same compound resulted in 50% apoptosis at concentrations of 208.6 nM and 199.5 nM against the same cell lines, respectively (Du et al. 2014).

Mechanisms of cytotoxicity in prostate cell lines

Six polyketides from *P. similis* called Preussilides A-F demonstrated cytotoxic activity against KB3.1 (HeLa) and U2OS (human osteosarcoma) cell lines. However, these compounds lacked activity (IC_{50} >10 µM) against A431 (squamous carcinoma), A549 (human lung carcinoma), SKOV-3 (ovarian carcinoma), PC-3 and MCF-7 (breast adenocarcinoma) cell lines. Immunofluorescence studies showed changes to the microtubules resulting in multipolar spindles, causing unequal nuclear and cell sizes. As a hallmark of apoptosis, caspase activation was also stained for, and indicated that cells were not apoptotic via this pathway (Noumeur et al. 2017).

SA derivatives isolated from endophytes have also been reported to have cytotoxic activity. *Aspergillus aculeatus* from *Rosa damascena* (Damask rose) was shown to contain SA and this had potent cytotoxic activity against triple negative breast cancer cells with a half maximal inhibitory concentration of 1.66 µM (Farooq et al. 2020). However, this compound was not as potent as paclitaxel against these cells which had an inhibitory concentration of 0.140 ± 2.20 µM. A particularly interesting finding of this study was that the compound may have elicited its effect via complete disintegration of spindle microtubules, indicating that the compound causes mitotic catastrophe (Farooq et al. 2020). Farooq and colleagues (2020) also tested SA for cytotoxicity against PC-3 cells. Although the compound was less effective than against

breast cancer cells, apoptosis was still induced at a half maximal inhibitory concentration of 12.97 ± 0.02 µM (Farooq et al. 2020).

Betulinic acid (BA) is a terpenoid that has been isolated from ethyl acetate (EtOAc) extracts of *Phomopsis* sp. endophytes (Peyrat et al. 2017). It was reported that BA caused ~50% cytotoxicity in LNCaP and DU-145 prostate cell lines when used at a concentration of 20 µM. Furthermore, the mechanism of BA to induce apoptosis in these cells lines was by the p53 PUMA pathway (Shankar et al. 2017). However, other studies have reported different mechanisms, such as an increase of reactive oxygen species (ROS) and caspase cleavage for the intrinsic apoptosis pathway (Ganguly et al. 2007).

1.4.2 Associations between antimicrobial and cytotoxic activity in endophytes

Many studies have reported that crude extracts, fractions, and pure compounds isolated from endophytes could be both antimicrobial and cytotoxic towards cancer cell lines (Cui et al. 2011; Wang et al. 2011; Santiago et al. 2012; Astuti & Nababan 2014).

Antimicrobial and cytotoxic effects of endophyte crude extracts

Crude extracts are a mixture of metabolites that the endophyte produces that can be extracted with varying methods. Considering there are many different chemicals within these extracts, it is likely that they would all have different activities. A crude extract from an endophyte isolated from *Piper crocatum* (Celebes Pepper), inhibited growth of the bacteria *Bacillus subtilus, Escherichia coli,* and *Staphylococcus aureus*, while also having a half maximal inhibitory concentration of 37.43 µg/mL against T-47D human breast cancer cells (Astuti & Nababan 2014). This indicates that endophytes may produce a multitude of compounds, potentially with both antibacterial and cytotoxic activity.

A *Phoma*-like endophyte isolated from *Cinnamomum mollissimum* is also highly cytotoxic and antimicrobial. Of the 88 fractions that were isolated from the EtOAc crude extracts of this

endophyte one had antibacterial activity against *B. subtilis* (96.1% inhibition), antifungal activity against *A. niger* (43.1% inhibition), and was cytotoxic against the P388 murine leukaemia cells (88.60% inhibition) (Santiago et al. 2012).

A crude extract from a strain of *Fusarium oxysporum,* isolated from *Bacopa monnieri* (Herb-of-Grace), was reported to have significant activity against both bacteria and cancer cell lines. This crude extract was bactericidal at 10 µg/mL against *E. coli* and *Pseudomonas aeruginosa* and bacteriostatic against *Salmonella typhyimurium* and *S. aureus* at 10 µg/mL. The extracts were equally effective as streptomycin (Katoch et al. 2014). Katoch and colleagues (2014) also reported that the same extracts from this endophyte exhibited cytotoxic activity against both PC-3 and A549 lung adenocarcinoma cell lines with half maximal inhibitory concentrations of 8 µg/mL and 5 µg/mL, respectively. In comparison, the positive control of paclitaxel had half maximal inhibitory concentrations of 53 µg/mL and 56 µg/mL against the same respective cell lines. The increase of potency of the endophyte extracts in comparison to the clinical paclitaxel positive control is a significant finding as it supports the hypothesis that endophytes may produce important chemicals that can be developed into successful anti-cancer drugs (Katoch et al. 2014).

Another finding that supports the sourcing of antimicrobial and cytotoxic compounds from the same endophyte species is a study on an endophyte called HAB10R12, isolated from a Malaysian rain forest (Ramasamy et al. 2010). The endophyte had reported antibacterial activity, demonstrated by the disc diffusion method. The inhibition zones against *S. aureus* (~28.6% increase), *E. coli* (~34.6% increase), and *B. subtilis* (~20.9% increase) were all larger than the positive controls of ampicillin and gentamycin at equal doses of 10 µg/mL (Ramasamy et al. 2010), indicating significant antibacterial activity. Additionally, Ramasamy and colleagues (2010) reported cytotoxic activity against human colorectal cancer (HCT116 cell lines) and MCF-7 breast adenocarcinoma cell lines at pharmaceutically relevant (IC_{50} <30

µg/mL) concentrations with a half maximal inhibitory concentration of 0.05 ± 0.01 µg/mL and 0.04 ± 0.03 µg/mL, respectively.

Pure endophyte compounds with simultaneous antimicrobial and cytotoxic activity

An example of an endophyte derived pure compound with antimicrobial and cytotoxic activity is Beauvericin. Beauvericin was isolated from an endophytic *Fusarium oxysporum,* had a half maximal inhibitory concentration of 49.5 ± 3.8 µM against PC-3 cells. It was also significantly antibacterial against human pathogen methicillin resistant *S. aureus* (MRSA) and *B. subtilis* which inhabits soil (Wang et al. 2011). Additionally, one purified compound from a *Phoma*-like endophyte, called hydroxyramulosin (a polyketide), inhibited *Aspergillus niger* at a half maximal inhibitory concentration of 1.56 µg/mL and was cytotoxic against P388 cells with a half maximal inhibitory concentration of 2.10 µg/mL (Santiago et al. 2012). This suggests that polyketides isolated from endophytic fungi may exhibit the same effects across both fungal and human eukaryotic cells.

Anthracyclines are endophyte-derived compounds that exhibit both anti-cancer and antibacterial activity (Booser & Hortobagyi 1994). Anthracyclines cause supercoiling of the chromatin by inhibition of topoisomerases which ultimately causes chromatin aggregation, damaging the DNA resulting in apoptosis (Rabbani et al. 1999). Doxorubicin is an example of an anthracycline that has been demonstrated to inhibit growth of PCa tumours (Fan et al. 2016). However, doxorubicin can cause significant cardiotoxicity and hepatotoxicity (Kalender et al. 2005; Zhao & Zhang 2017), and is therefore an undesirable treatment option, although reversal of hepatotoxicity has been reported via administration of vitamin E and catechin to rat models (Kalender et al. 2005).

1.5 Knowledge gaps and project objectives

There is a wealth of endophyte species that are yet to be discovered, and these species are likely to contain many compounds that may be suitable for clinical use. Obtaining paclitaxel from its natural supply is a challenging practice, thus, it is imperative that alternative sources for anti-cancer compounds be identified. Additionally, other chemotherapies such as docetaxel have challenges with resistance and side effects, so the discovery of both taxane and non-taxane compounds is imperative.

Previously, in the USQ fungal pathology laboratory, a *Preussia* sp. endophyte (BSH2.9) was obtained from local rainforests, and pure compounds from this endophyte were isolated from EtOAc extracts. These purified compounds were identified as polyketides and were determined to have antibacterial activity against *Bacillus cereus, Enterococcus faecalis,* and MRSA and antifungal activity against a eukaryotic pathogen, *Candida albicans* (Mapperson et al. 2014). *Preussia* endophytes are being increasingly recognised globally as sources of valuable bioactive compounds (Gonzalez-Menedez et al. 2017). Table 2 summarises *Preussia* species that produce a variety of compounds (predominantly alkaloids and polyketides) with cytotoxic properties.

Table 2: Cytotoxic compounds from *Preussia* species.

Endophytic fungi	Chemical	Cell line	Reference
P. australis	Australifungin	Not reported	(Hensens et al. 1995)
P. typharum	Leptosin A, C Preussiadin A, B	Not reported NCI-60 cell line panel	(Du et al. 2014)
Preussia sp.	Preussiafuran A, B	Rat skeletal (L6)	(Talontsi et al. 2014)
P. africana	Preussochromone A, B, C, D	Human alveolar adenocarcinoma (A549)	(Zhang et al. 2012)
Preussia sp.	Spiropreussione	Human ovarian cancer (A2780) Human hepatoma (BEL-7404)	(Chen et al. 2009)
Preussia sp.	Sporostatin	Not reported	(Kinoshita et al. 1997)

With the knowledge that *Preussia* spp. contain compounds that are cytotoxic and that endophytic polyketides are both antimicrobial and cytotoxic, this study aims to assess the BSH2.9 isolate for cancer inhibiting compounds. Given that previous reports by Noumeur et al. (2017) demonstrated cytoskeleton disruption by polyketides isolated from a *Preussia* sp., it is speculated that the cytotoxic activity is caused via disruption of microtubules or microfilaments.

1.6 Hypothesis

The hypothesis of this study is that fractionated compounds from the ethyl acetate extracts of BSH2.9 will exhibit anti-cancer activities.

1.7 Project aims

This pilot study aims to;

1. Confirm the previously reported antimicrobial activity of BSH2.9 via streak plate and microdilution assay methodologies
2. Achieve a cultured bulk growth of BSH2.9
3. Extract and fractionate compounds from the BSH2.9 bulk growth
4. Evaluate the inhibitory effects of the fractionated compounds on the PC-3 advanced prostate cancer cell line
5. Examine the possible mode of action of bioactive compounds via nuclear and cytoskeletal structure studies

Chapter 2: Materials and methods

2.1 Initial screening for antimicrobial activity

2.1.1 Preparation of microorganisms

All broth and agar recipes used are attached in appendix A. The *Preussia* sp. isolate, BSH2.9, was stored in culture on potato dextrose agar (PDA) plates at 22˚C in the dark. Test bacteria, *Bacillus cereus* (ATCC 14579), and *Enterococcus faecalis* (ATCC 19433) were cultured on sensitest agar (STA) and incubated for 48 hours at 37˚C to confirm previous bioactive behaviour of the isolate against these species (Mapperson 2014). Previous anti-*Candida* activity suggested that that effects of the BSH2.9 isolate may inform cytotoxic activity as cancer cells and *Candida* are both eukaryotes. Therefore, an additional unicellular phylloplane yeast, *Rhodotorula mucilaginosa,* was subcultured on STA and stored at 22˚C for 48 hours for screening.

2.1.2 Streak plate method

Two STA plates were inoculated with 1cm^3 portions of the BSH2.9 isolate and incubated at 22˚C for 48 hours. After 48 hours, a sterile loop was used to streak from the edge of the mycelium in an outwards direction with one of the test bacteria or yeast as illustrated in Figure 5. The loop was sterilised between organisms by submerging the loop into 95% ethanol (EtOH) and then heating it with a blue flame. The second and third plates were then inoculated with the other test microbes. Plates were then incubated at 37˚C for bacterial microbes and 22˚C for the yeast for a further 24-hour period. An inhibition zone between the microbial streaks and the mycelia denoted a positive result.

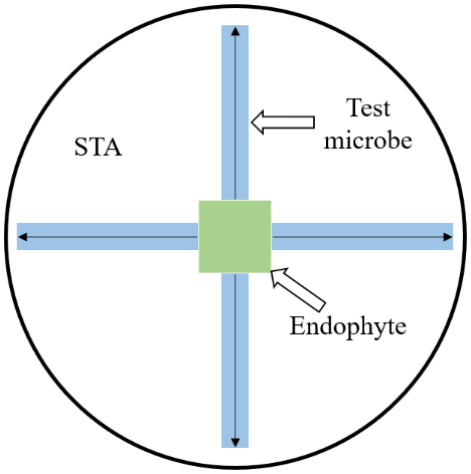

Figure 5: Streak plate method for antimicrobial testing.

2.1.3 Anti-fungal screening

Previous observations of combined anti-fungal and anticancer activity of endophytic fungal extracts suggested that screening of BSH2.9 against other eukaryotes might further inform anti-cancer activity. Therefore, BSH2.9 was also screened against three mycelial fungal isolates from the USQ fungal pathology laboratory. Three BSH2.9 portions of $1cm^3$ were excised from the edges of the culture and transferred to separate STA plates. Cubes ($1cm^3$) of *Pyrenophora teres, Serendipita vermifera* and *Fusarium oxysporum* were similarly excised from their respective active cultures and added to BSH2.9 with a space of 1cm as illustrated in Figure 6. Plates were then incubated at 22°C for up to one week. The plates were checked daily for five days as test organisms each had different growth rates.

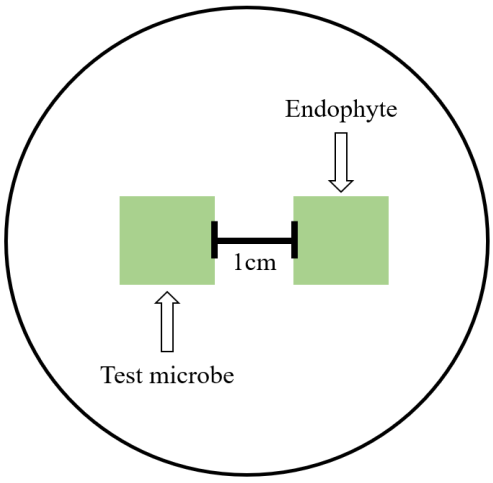

Figure 6: Method for antifungal screening of BSH2.9.

2.2 Bulk growth of the fungal isolate

Six portions of the BSH2.9 mycelium of 1cm^3 were taken from the edge of the active culture and added into six individual McCartney bottles containing 10mL of sterile malt extract broth (MEB). These were incubated at 22˚C for seven days. After seven days, six 1 L conical flasks containing 500mL of MEB were sterilised. The contents of one McCartney bottle were then aseptically transferred into a conical flask. This process was repeated resulting in a total of six 1 L conical flasks and all flasks were stored statically at 22˚C in the dark. After five days of incubation, 500 µL of freshly autoclaved *B. cereus* (ATCC 14579) and *E. faecalis* (ATCC 19433) in a suspension of 0.9% saline was added to each of the conical flasks. After 28 days, the temperature was increased to 25˚C for a further three days to stimulate further production of metabolites.

2.3 Extraction of fractions

2.3.1 Extraction

Upon completion of the growth period, each of the six culture broths were aseptically filtered through sterilised cheese cloth to remove mycelia. Flow throughs from the cheese cloth were collected into 1 L conical flasks. Mycelia were ground using a sterile pipette tip, and 200 mL of EtOAc was poured through the cheese cloth. The flow through was also collected into the conical flask. The total flow through was next poured into a 500 mL separator funnel and allowed to settle so that the water and EtOAc layers could be separated. EtOAc layers from the funnel were collected into 500 mL beakers. The water layers were also collected and combined into 1 L Schott bottles. The EtOAc samples were allowed to evaporate in a fume hood. Once the majority of EtOAc had evaporated, the remainder of the sample was transferred into pre-

weighed scintillation vials via a glass pipette. The remaining EtOAc was allowed to evaporate from the vials and the samples were freeze dried to result in the final crude extract product.

2.3.2 Antimicrobial testing of fungal crude extracts

Fungal crude extracts (FCE) were dissolved in 25% EtOH and sterile H_2O to a concentration of 1 mg/mL. A microdilution assay (Clinical and Laboratory Standard Institute (CLSI) 2018) was used to determine if FCEs were antimicrobial against the same test bacteria from the initial trials (Mapperson et al. 2014). *B. cereus* (ATCC 14579) and *E. faecalis* (ATCC 19433) were cultured onto STA and incubated at 37°C for 48 hours. Test bacteria were suspended in Mueller-Hinton broth (MHB) at 0.5 McFarland standard. Rows A-D and columns one to five of two curved bottom 96-well microdilution plates were aseptically aliquoted with 50 µL of suspended *B. cereus.* Rows E to H and columns one to five of two curved bottom 96-well microdilution plates were aseptically aliquoted with 5 µL of suspended *E. faecalis*. Dissolved crude extract was then aliquoted into columns one and two of rows A to H. Vancomycin at a concentration of 10 µg/mL was aliquoted in all wells of column three as a positive control. 50 µL of sterile H_2O was then added into all wells of column four as a negative control. 50 µL of the 25% EtOH solvent was added into all wells of column five as a solvent control. Finally, 100 µL of MHB was added into wells A to H of column six as a contamination control. The plates were dark incubated at 37°C for 24 hours. STA plates were then streaked with the contents of the test wells using a sterilised inoculation loop to determine bacteriostatic and bactericidal activity of the crude extract, which were then incubated at 37°C for 24 hours.

2.3.3 Fractionation of FCEs

Remaining FCEs underwent semi-preparative high performance liquid chromatography (HPLC) using the Shimadzu Prominence system (C18 150.00mm x 10.00mm silica column, Phenomenex). Remaining FCE was dissolved in 100% methanol (MeOH) at a concentration

of 10 mg/mL. Six fractions were collected over a 40-minute period with a gradient of 90% H_2O and 10% MeOH to 10% H_2O and 90% MeOH, into separate scintillation vials. Volumes of 500 µL of the 10 mg/mL solution was injected through the HPLC system until the total 5 mL volume had been used. Each fraction from each run was collected into separate vials. The fractions from each run were then combined into a round bottom flask for rotary evaporation. Six scintillation vials were weighed. MeOH was used to rinse the dried contents in the round bottom flask to allow transfer of the fractions into the scintillation vials with a glass pipette. This rinsing and transfer process occurred three times per fraction and different fractions were collected into separate vials, resulting in a total of six vials. The MeOH contents of each of the six scintillation vials were evaporated in a fume hood, freeze dried, and weighed for final mass of the fractions.

2.4 Evaluation of the fractions

2.4.1 Treatment of PC-3 cells with fractions

Manufacturer information and lot numbers are all attached in appendix C. PC-3 cells (ATCC CRL-1435) were grown in culture using Roswell Park Memorial Institute (RPMI) 1640 medium containing 10% foetal calf serum (FCS) and 1% penicillin/ streptomycin (PS) at 37˚C and 5% CO_2 in air until 80% confluency was observed in a T175 cell culture flask. Cells were then trypsonised and counted using a TC20 Automated Cell Counter (Biorad, CA, USA). A count of 1.5 x 10^4 cells were then added to the wells of a flat-bottomed 96 well microtiter plate in 100 µL of media. The plate was then incubated for 24 hours at 37˚C and 5% CO_2 in air. A preliminary screening tested a concentration of 1 mg/mL of each of the six fractions to indicate any potential effect of the fractions on the cells. After 24 hours, conditioned media was replaced and BSH2.9 fractions dissolved in dimethyl sulfoxide (DMSO) and fresh media were added to

a total volume of 100 µL with a 1 mg/mL concentration in each well. The plate set up was repeated following the same methodology for testing at pharmaceutically relevant concentrations of 10 µg/mL, 50 µg/mL, and 100 µg/mL. After the addition of each fraction in triplicate, the plate was then incubated for a further 72 hours at 37˚C and 5% CO_2 in air. Negative controls (RPMI media with no fraction or DMSO) were included for comparison to a cell number, proliferating at a normal rate. DMSO solutions of comparable concentrations to the dissolved fractions were used as vehicle controls.

2.4.2 Cytotoxicity assay

A standard curve was produced by adding cell numbers determined using a TC20 Automated Cell Counter into wells of a separate microtiter plate. Cells were added at counts of 6.0 x 10^4, 3.0 x 10^4, 2.25 x 10^4, 1.5 x 10^4, 7.5 x 10^3, 4.5 x 10^3, 3.0 x 10^3, 1.5 x 10^3, and 0 cells/ well. A commercial cell counting kit 8 (CCK-8; Sigma Aldrich, NSW, Australia) containing the WST-8 water soluble tetrazolium salt was used to estimate the cell number in each well. A volume of 10 µL (10% of the total well volume) of the WST-8 solution was added to all wells of the treated cells plate and to the wells of the cells used for the standard curve and both were incubated for four hours at 37˚C and 5% CO_2 in air. The plates were then read in a Varioskan Microplate Reader (Thermo Fisher Scientific Inc., Queensland, Australia) for absorbance at 450 nm. Cell numbers were calculated using the equation of the line from the standard curve.

2.4.3 DNA and cytoskeletal imaging

Cells were prepared for fluorescence microscopy using the Lab-Tek® Chamber Slide™ system (#177437; Thermo Fisher Scientific Inc.) by adding 500 µL of cell suspension in media to each chamber of the slide with a count of 2.5 x 10^4 cells per chamber. The slides were incubated for 72 hours at 37˚C and 5% CO_2 in air so sufficient attachment and confluency could be observed. After 72 hours, conditioned media was removed to be replaced by selected fractions informed

by the preliminary and subsequent CCK-8 assays. The slides were again incubated at 37˚C and 5% CO_2 in air until visible damage to the cells was observed by microscopy (24 hours).

For live cell staining of the microtubules, a solution of 1 µL of BioTracker 488 green microtubule cytoskeleton dye (Sigma/ Merck) and 1 µL of verapamil per 1 mL of RPMI 1640 media was produced. Conditioned media in the chambers of the slides was removed and replaced with 500 µL of the dye/ verapamil/ media mix. The slides were wrapped in aluminium foil and incubated at room temperature for 30 minutes. During incubation, a NucBlue™ (Thermo Fisher Scientific Inc.) stain solution was produced by adding one drop of the stain per millilitre of RPMI 1640 media. After 30 minutes, the media containing the BioTracker dye was removed, and replaced with 500 µL of the NucBlue™ stain/ media solution. The slides were wrapped in aluminium foil and incubated at room temperature for a further 10 minutes. After 10 minutes, the nuclear stain solution was removed, the chambers and gasket were lifted from the slides, and the slides were mounted with a glycerol and gelatine mix and a coverslip for microscopy. Images were then taken with fluorescence microscopy at 400X magnification on a Nikon Eclipse E600 fluorescence microscope (Nikon Imaging Company, Tokyo, Japan) and the Olympus DP26 microscope camera (Olympus Corporation, Tokyo, Japan) using ultraviolet (UV), fluorescein, and rhodamine filters.

As the live cell stain appeared to induce cell death (apoptosis) in the negative control cells, the cells were fixed prior to staining the microfilaments and nucleus. Conditioned media in the chambers of the slides was removed and replaced with 500 µL of 4% paraformaldehyde in sterile phosphate-buffered saline (PBS). This was left for 30 minutes to fix the cells. Paraformaldehyde was then removed, and each chamber was rinsed with PBS three times. Then a fresh 500 µL of PBS with a drop of ActinRed reagent (Thermo Fisher Scientific Inc.) was added to each chamber. The slides were then wrapped in aluminium foil and left to incubate at room temperature for 30 minutes. The PBS and ActinRed was then removed, and chambers

rinsed with PBS. A fresh 500 µL of PBS with a drop of NucBlue™ was added to each chamber, slides were wrapped in aluminium foil and incubated at room temperature for 10 minutes. A gelatine and glycerol mix was heated to approximately 55˚C for mounting coverslips. After 10 minutes the NucBlue™ stain was removed, and chambers were rinsed with PBS three times. The chambers and gasket were detached. A drop of the gelatine and glycerol mix was added to each end of the slide and a coverslip was added. Images were then taken with fluorescence microscopy under oil immersion at 1000X magnification on a Nikon Eclipse E600 fluorescence microscope (Nikon Imaging Company, Tokyo, Japan) and the Olympus DP26 microscope camera (Olympus Corporation, Tokyo, Japan) using UV, fluorescein, and rhodamine filters.

2.5 Statistical analyses

All quantitative data on cell number is presented as the mean ± standard deviation of the mean. A one-way ANOVA with Tukey's post hoc analyses was used to determine statistical significance in all instances. All statistical analyses were performed using version 9.2 of GraphPad Prism (GraphPad Software Inc, California, USA).

Chapter 3: Results

3.1 Initial screening for antimicrobial activity

Figure 7A illustrates the streak plate method for antibacterial testing of BSH2.9 against *B. cereus* after 24 hours of incubation. Figure 7B displays a magnified image of the *B. cereus* streak test plate to highlight inhibition zones. Figures 7A and 7B demonstrate that a zone of inhibition was present, which was approximately 1mm wide. Figure 7C illustrates the streak plate method for antibacterial testing of BSH2.9 against *E. faecalis* after an incubation period of 24 hours. Figure 7D is a magnified image of the *E. faecalis* streak plate test. Figures 7C and 7D demonstrate that there was no inhibition zone for this test microbe.

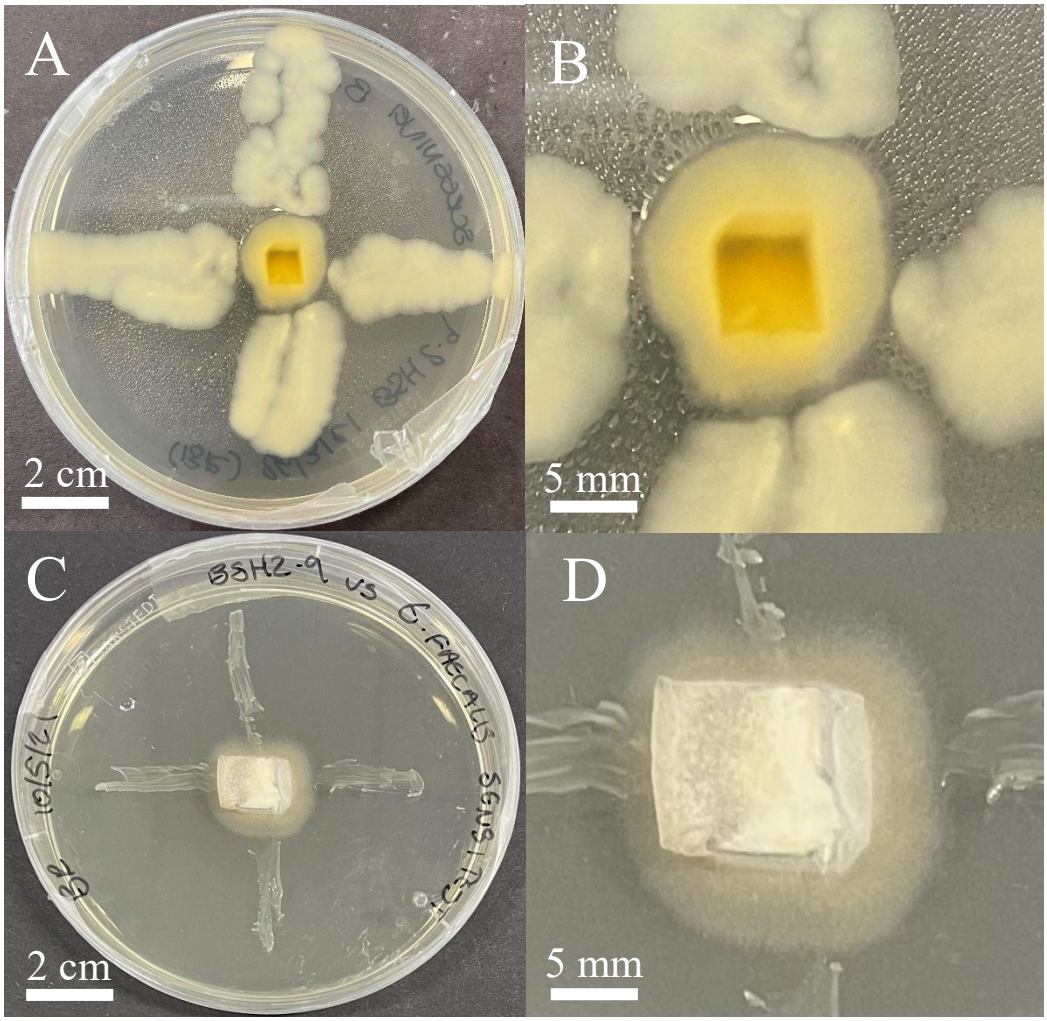

Figure 7: Photographs of BSH2.9 streak plate testing for antimicrobial activity after 24 hours of incubation. **A)** *B. cereus* full plate image; **B)** Magnified inhibition zone of *B. cereus*; **C)** *E. faecalis* full plate image; **D)** Magnified inhibition zone of *E. faecalis*.

Figure 8A illustrates the streak plate method for the phylloplane yeast, *Rhodotorula mucilaginosa*, after 24 hours. Figure 8B illustrates a magnified image of Figure 8A and indicates there is no inhibition zone present.

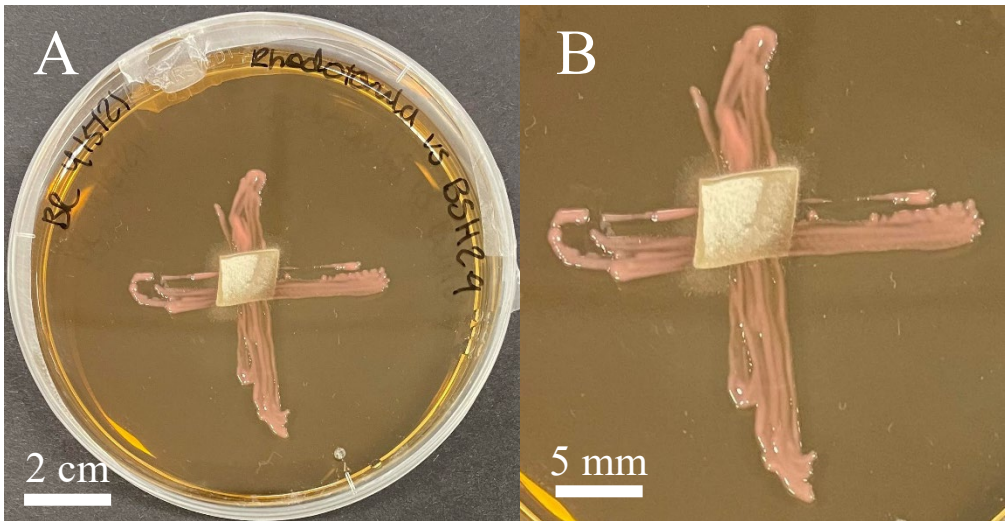

Figure 8: Images of STA screen of *Rhodotorula mucilaginosa.* **A)** Image of *R. mucilaginosa* screening; **B)** Magnified image of *R. mucilaginosa* screening.

Figure 9 displays the results of the anti-fungal screening tests for BSH2.9 against *Pyrenophora teres* (9A), *Serendipita vermifera* (9B), and *Fusarium oxysporum* (9C), respectively. No inhibition zones were observed for any of the test fungi.

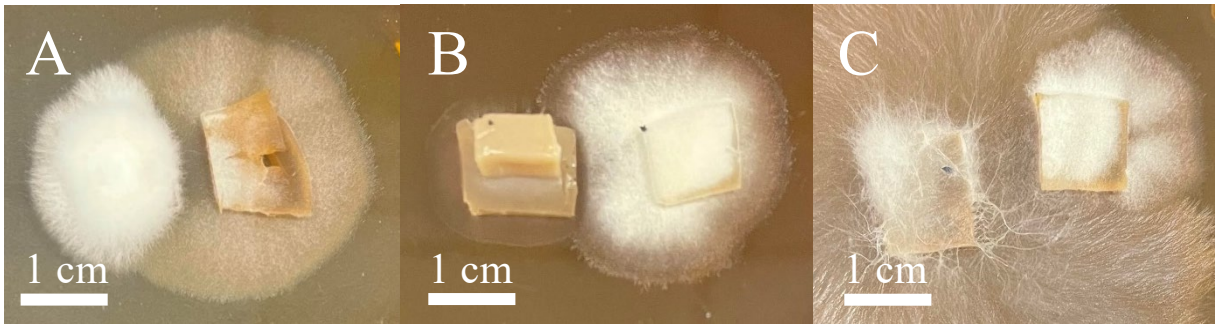

Figure 9: Images of antifungal screens on STA plates. **A)** Screening of *Pyrenophora teres*; **B)** Screening of *Serendipita vermifera*; **C)** Screening of *Fusarium oxysporum*. BSH2.9 mycelium is on the right-hand side on all plates.

3.2 Extraction of compounds

3.2.1 Ethyl acetate extraction

Figure 10 displays the FCEs obtained from EtOAc extraction of the mycelia following bulk growth of BSH2.9. The extracts appear a yellow- brown colour and have a gum-like texture. It is these FCEs that were then processed through semi-preparative HPLC.

Figure 10: Fungal crude extracts (FCEs).

3.2.2 Microdilution assay

Table 3 demonstrates that the crude extract (columns one and two) and vancomycin (column three) both prevented bacterial growth in the wells, while the sterile water (column four) and the 25% EtOH solvent (column five) had no effect on bacterial growth. Additionally, the lack of growth in column six indicates that the MHB was uncontaminated. Results for this assay at 18, 20, and 48 hours are attached in appendix B.

Table 3: Microdilution assay for assessment of antibacterial activity of BSH2.9 FCEs after 24 hours of incubation. – indicates no growth. + indicates a milky appearance to the well. ++ indicates that a button of bacterial growth was observable.

24 HOURS	Crude extract (x2)	Vancomycin	Sterile H_2O	25% EtOH solvent	Plain MH broth
Bacillus cereus	-	-	++	+	-
	-	-	++	+	-
	-	-	++	+	-
	-	-	++	+	-
Enterococcus faecalis	-	-	++	+	-
	-	-	++	+	-
	-	-	++	+	-
	-	-	++	+	-

Figure 11A and 11B demonstrates that both the crude extract and vancomycin were bacteriostatic against *B. cereus*. The bacterial growth present in Figure 11C and 11D indicates that both the crude extract and vancomycin were bacteriostatic against *E. faecalis*.

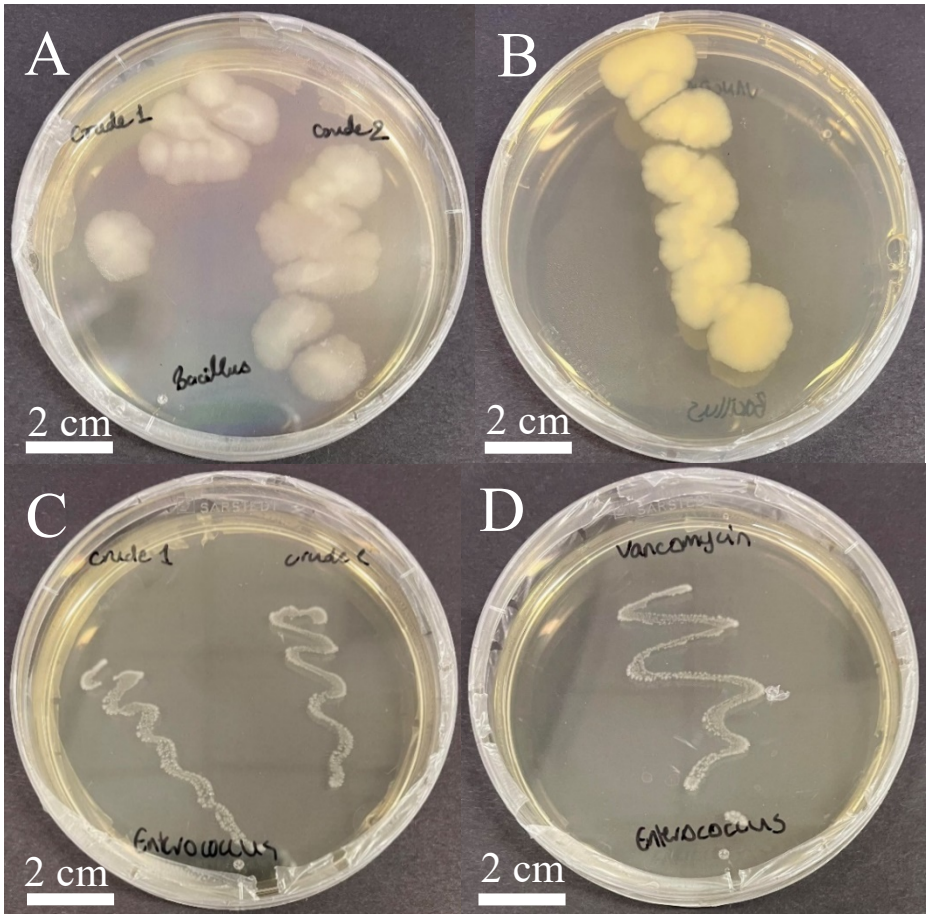

Figure 11: Images of the streaking from crude extract and vancomycin test wells from the microdilution assay after 24 hours of incubation. **A)** The streaking of *B cereus* tested against crude extracts. **B)** The streaking of *B. cereus* treated with vancomycin. **C)** The streaking of *E. faecalis* treated with crude extracts. **D)** The streaking of *E. faecalis* treated with vancomycin.

3.2.3 Semi-preparative HPLC

Figure 12 displays the UV chromatogram for HPLC fractionation of BSH2.9 FCEs. Two clear peaks with more than 2000 milli-absorbance units (mAU) can be seen at four (fraction one) and 23 minutes (fraction three). Two other clear peaks approaching 750 milli-absorbance units can be seen at 15 (fraction two) and 36 (fraction six) minutes. Fractions four and five were collected between 23.5 and 25, and 25 and 34 minutes respectively.

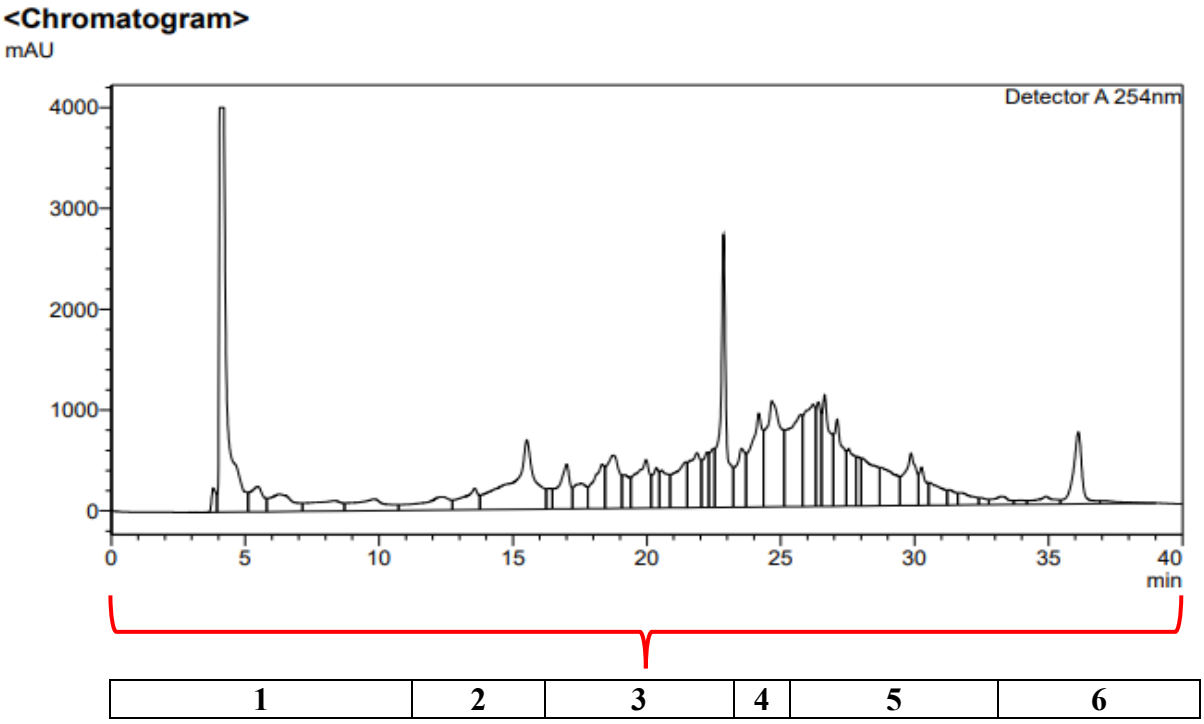

Figure 12: HPLC chromatogram for BSH2.9 crude extract (wavelength = 254nm).

3.4 Evaluation of the effects of the fractions on PC-3 cells

3.4.1 Cell number and viability

Figure 13 depicts the result of the preliminary screen of fractions obtained from HPLC. PC-3 cells were treated with fractions at a concentration of 1 mg/mL after 72 hours. The control cell number after 72 hours was 41.6 x 10^3 cells. Treatment of the cells with 1% DMSO in RPMI media resulted in a significant decrease of cell number to approximately 21.1 x 10^3, an approximate decrease of 50% ($p=0.0130$). Fraction one appeared to increase live cell number in comparison to the 1% DMSO control by approximately 8.0 x 10^3 cells (20%), although this was not statistically significant. Furthermore, fractions three and five also appeared to decrease live cell number by 12 x 10^3 cells (30% decrease) and 17 x 10^3 (40% decrease) of live cell number, respectively, in comparison to the DMSO control. However, these findings were also not statistically significant. Treatment of the cells with fraction two caused a decrease of approximately 3.0 x 10^4 live cells, equating to a 75% decrease ($p=0.0044$). Fraction six also caused a significant decrease ($p<0.0001$) of live cell number by 38 x 10^3 cells, which was approximately a 92% decrease. Fraction four did not appear to have any effect on live cell number in treated cells at this concentration. For all groups, $n=3$.

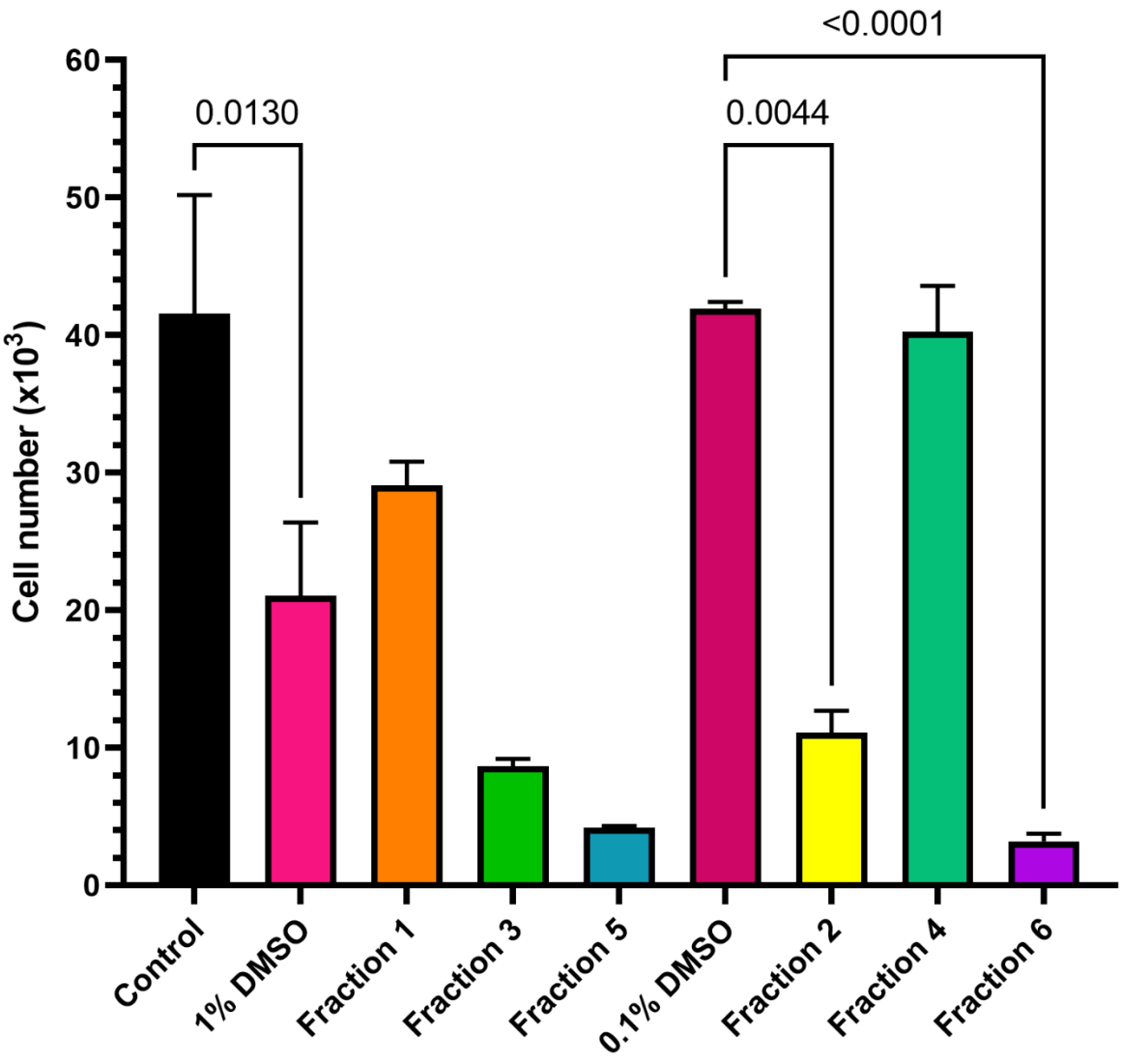

Figure 13: Cell number of PC-3 cells treated with fractions at 1mg/mL after 72 hours of incubation expressed as cell number calculated from the standard curve. Analysis performed was a one-way ANOVA with Tukey's post hoc analysis. Error bars are presented as the means ± standard deviation of the mean. N=3 for all treatment groups.

Figure 14 depicts the estimated number of PC-3 cells (determined by standard curve) after treatment with fractions one to six at concentrations of 10 µg/mL, 50 µg/mL, and 100 µg/mL. DMSO vehicle controls were also used at concentrations of 0.001%, 0.005%, 0.01%, 0.05%, 0.1%, and 1% in RPMI 1640 media.

Control cells averaged a live cell number of 42.4 x 10^3 cells. No DMSO controls resulted in significant changes to cell number except for 1% DMSO which resulted in a significant decrease ($p=0.0130$) of live cell number causing approximately 50% cell death as seen in Figure 14A. Fractions one (Figure 14B), two (Figure 14C) and three (Figure 14D) did not cause any significant changes at any of the pharmaceutically relevant concentrations. Treatment with fraction four at 50 µg/mL caused a decrease in cell number of 6.7 x 10^3 cells, or approximately 16% ($p=0.0355$) as seen in Figure 14E. Treatment of PC-3 cells with 50 µg/mL and 100 µg/mL of fraction five both also resulted in significant decreases of live cell number after the 72-hour incubation period with decreases of 10.4 x 10^3 cells (~25%; $p=0.0415$) and 12.1 x 10^3 cells (~28.5%; $p=0.0082$), respectively, as seen in Figure 14F. Treatment of PC-3 cells with 50 µg/mL and 100 µg/mL of fraction six both resulted in significant decreases of live cell number after the 72-hour incubation period with decreases of 13.7 x 10^3 cells (~32.4%; $p=0.0009$) and 37.1 x 10^3 cells (~87.4%; $p<0.0001$), respectively, as seen in Figure 14G. For all groups, n=3.

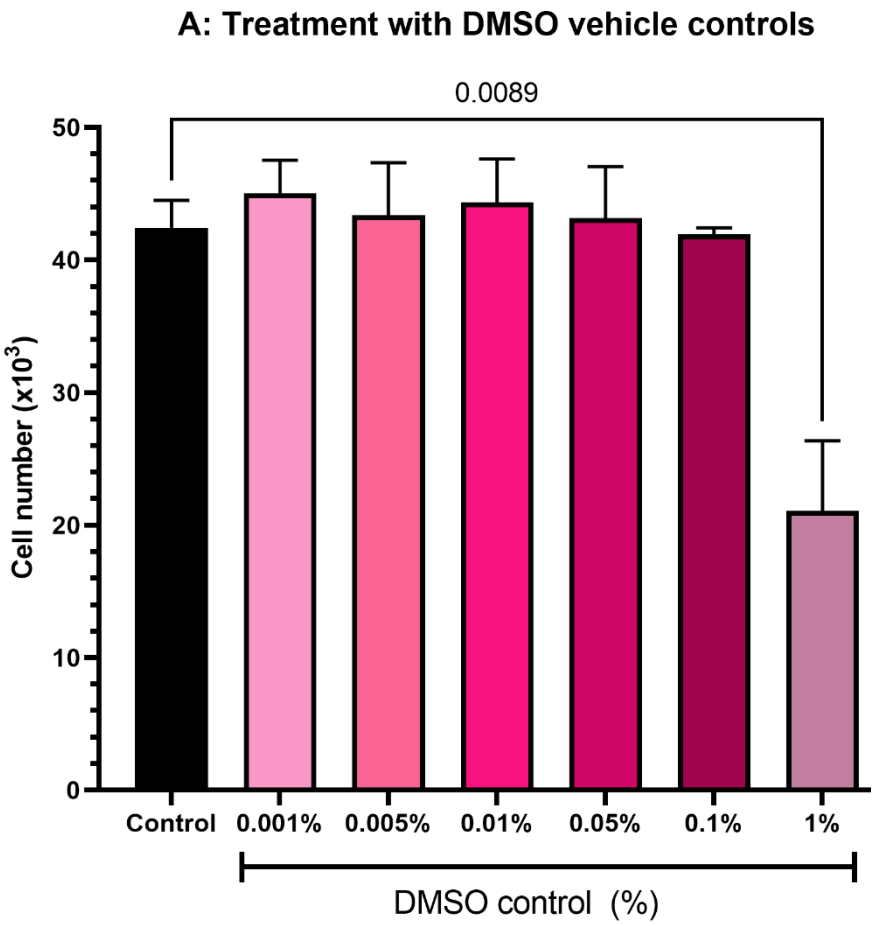
A: Treatment with DMSO vehicle controls
0.0089
Cell number (x10³)
50
40
30
20
10
0
Control
0.001%
0.005%
0.01%
0.05%
0.1%
1%
DMSO control (%)

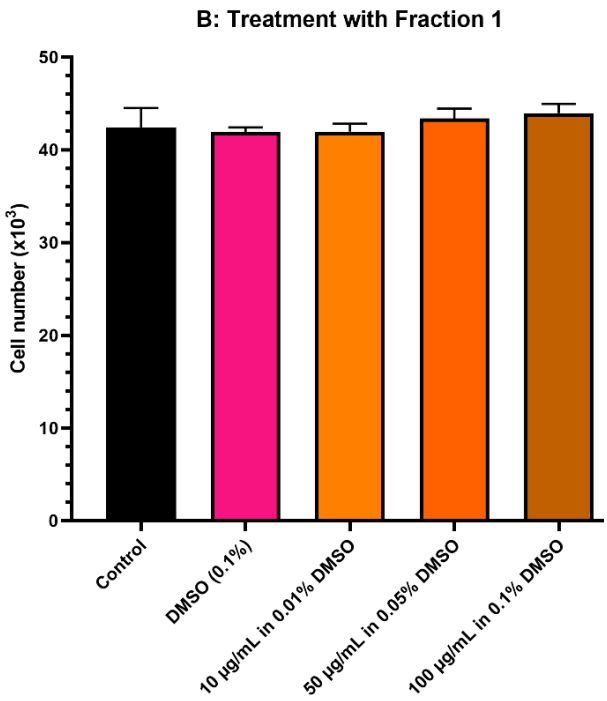
B: Treatment with Fraction 1
Cell number (x10³)
50
40
30
20
10
0
Control
DMSO (0.1%)
10 µg/mL in 0.01% DMSO
50 µg/mL in 0.05% DMSO
100 µg/mL in 0.1% DMSO

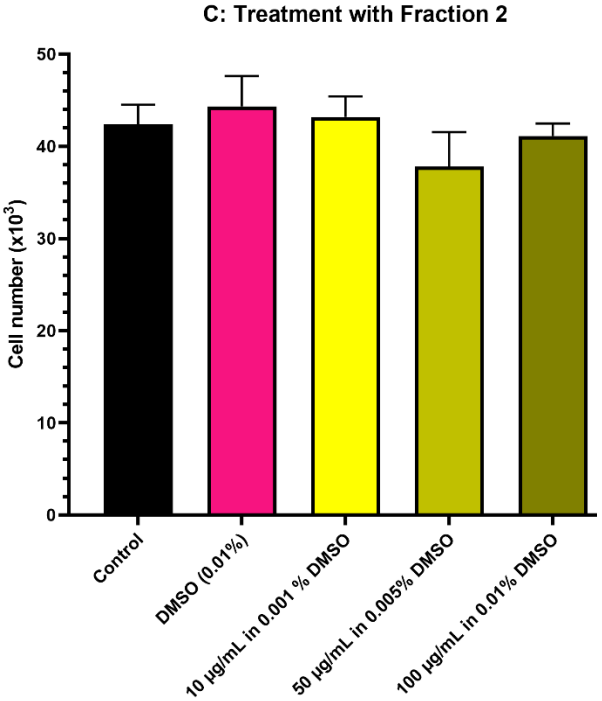
C: Treatment with Fraction 2
Cell number (x10³)
50
40
30
20
10
0
Control
DMSO (0.01%)
10 µg/mL in 0.001 % DMSO
50 µg/mL in 0.005% DMSO
100 µg/mL in 0.01% DMSO

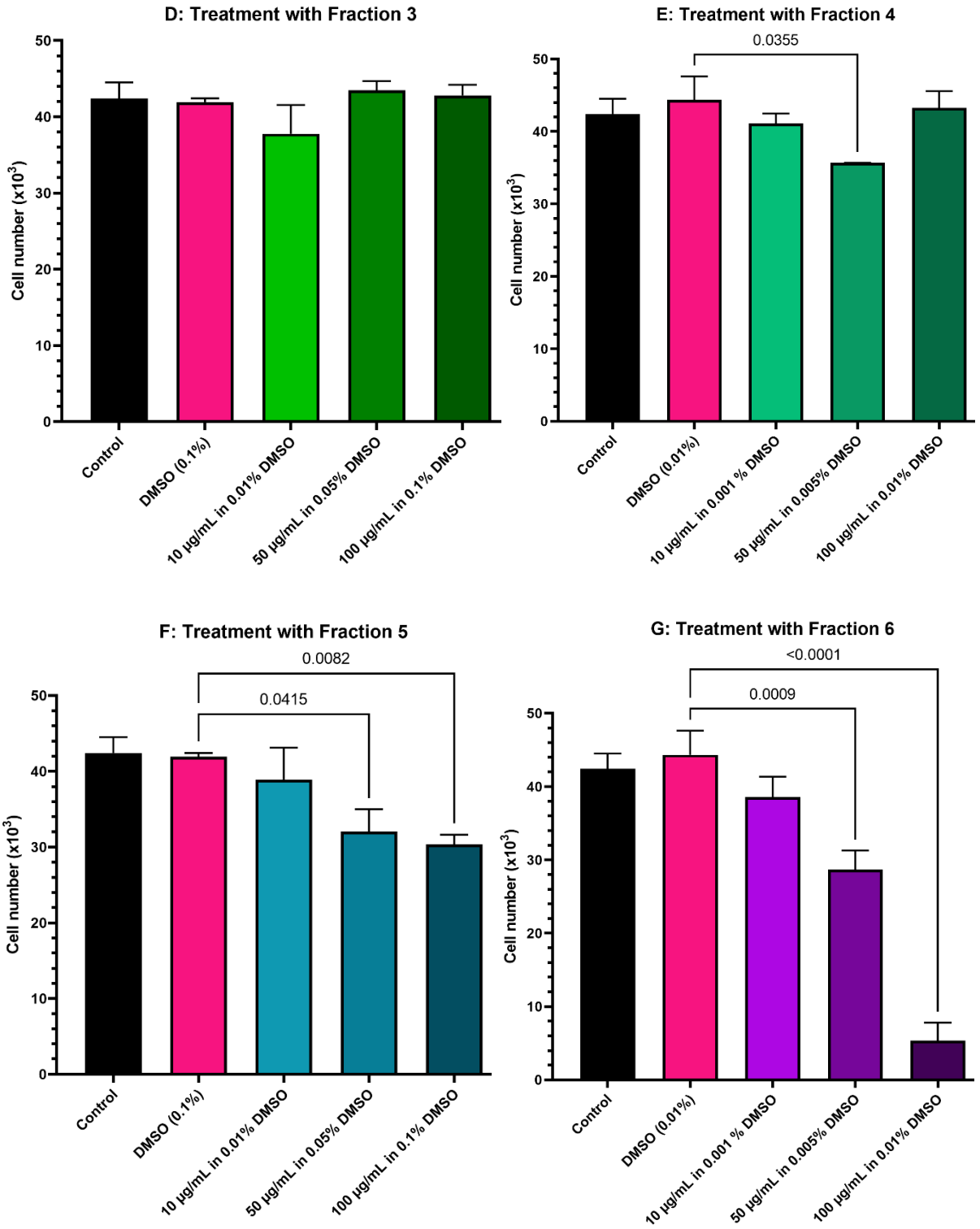

Figure 14: Number of PC-3 cells after treatment with DMSO in RPMI 1640 media vehicle controls and the six fractions at 10 µg/mL, 50 µg/mL, and 100 µg/mL after 72 hours of incubation. **A)** Number of PC-3 cells after treatment with DMSO vehicle controls. **B)** Number of PC-3 cells after treatment with fraction one. **C)** Number of PC-3 cells after treatment with fraction two. **D)** Number of PC-3 cells after treatment with fraction three. **E)** Number of PC-3 cells after treatment with fraction four. **F)** Number of PC-3 cells after treatment with fraction five. **G)** Number of PC-3 cells after treatment with fraction six. Analysis performed was a one-way ANOVA with Tukey's post hoc analysis. Error bars are presented as the means ± standard deviation of the mean. N=3 for all treatment groups.

3.4.2 Microscopy

Figure 15 depicts the results of live cell staining with BioTracker 488 green microtubule cytoskeleton dye and NucBlue™ nuclear stain of untreated cells. Figures 15A, 15B, and 15C are images of the results from the staining of nuclear material, the microtubule staining, and Brightfield microscopy. All images are a sample of untreated cells. Staining of the cell nuclei was successful. However, the live staining of the microtubules of the cell was unsuccessful as no microtubules are clearly fluorescing. A small percentage of the control cells were beginning to form apoptotic blebs (white arrows).

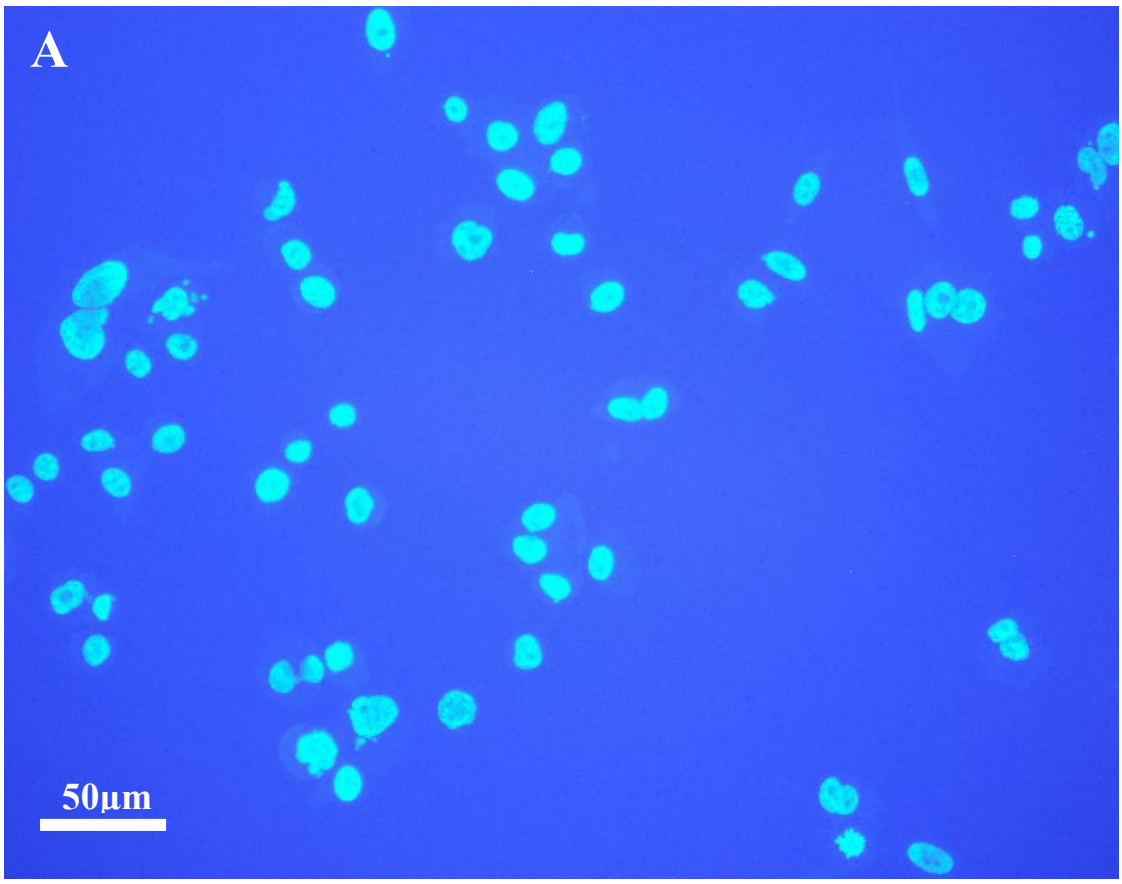

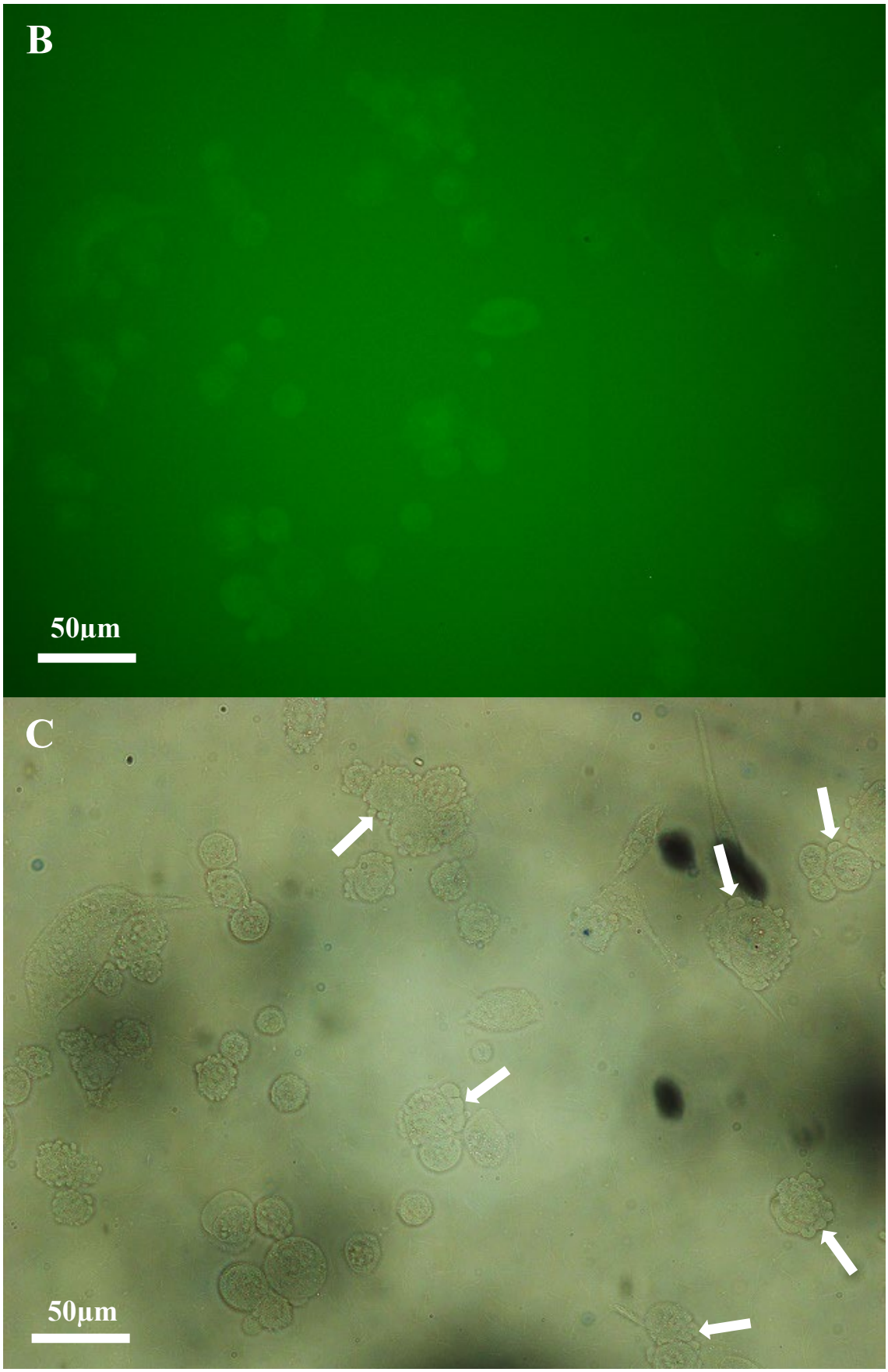

Figure 15: Images of microtubule and nuclear staining of untreated PC-3 cells. **A)** NucBlue™ staining of PC-3 cells. **B)** BioTracker 488 microtubule dye staining of PC-3 cells. **C)** Image of the PC-3 cell using Brightfield microscopy. Blebbing of cells is highlighted with white arrows. Images were taken on 400X magnification.

Figure 16 depicts successful staining of the negative control of PC-3 cells after fixing and staining with phalloidin and NucBlue™. Figure 16A illustrates the staining of microfilaments of the cells. Figure 16B demonstrates the staining of nuclear material of the cells. Clear microfilaments (white arrows) are evident, and the nucleus and nuclear material is not fragmenting. Nuclei are also smooth, rounded and consistently sized.

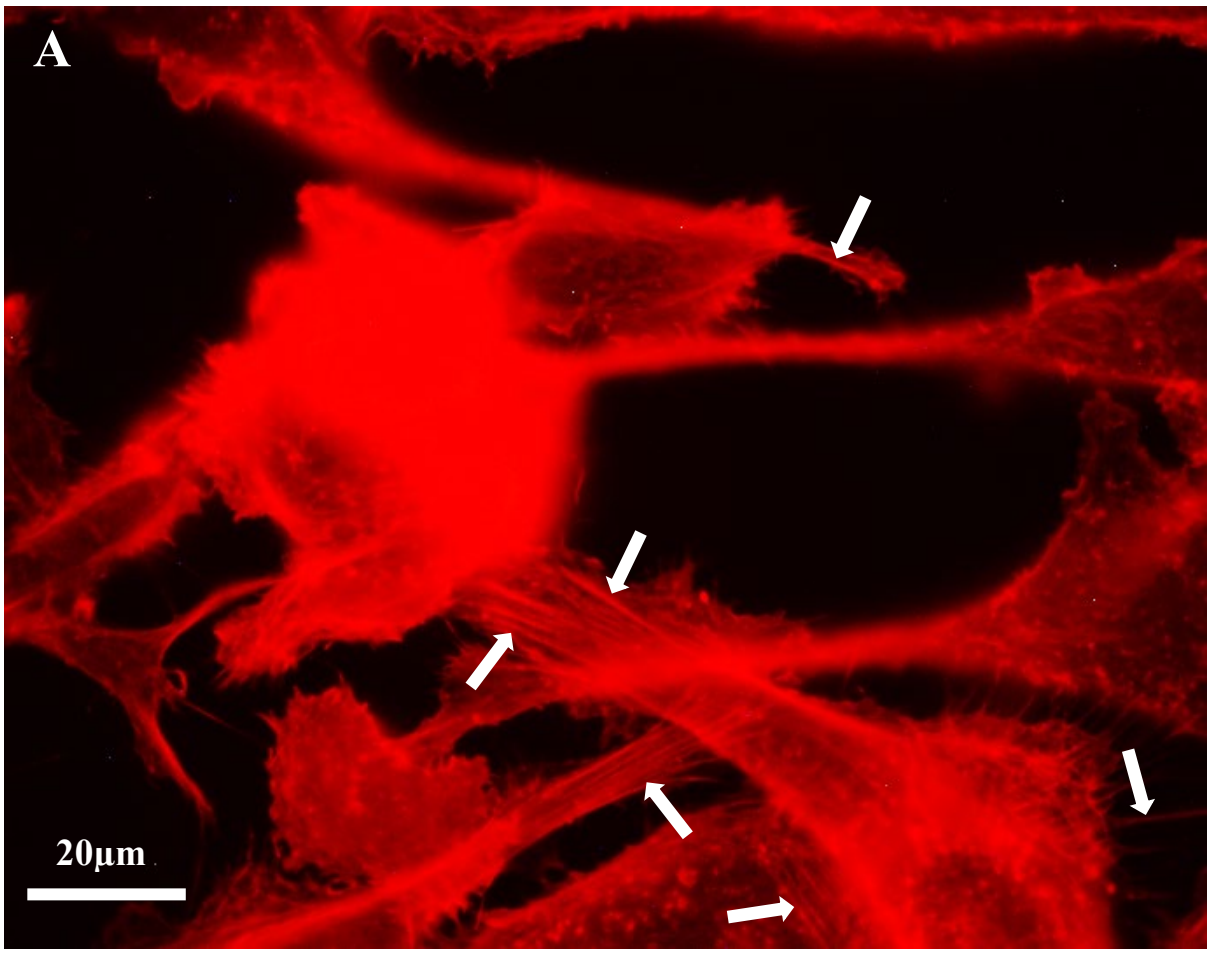

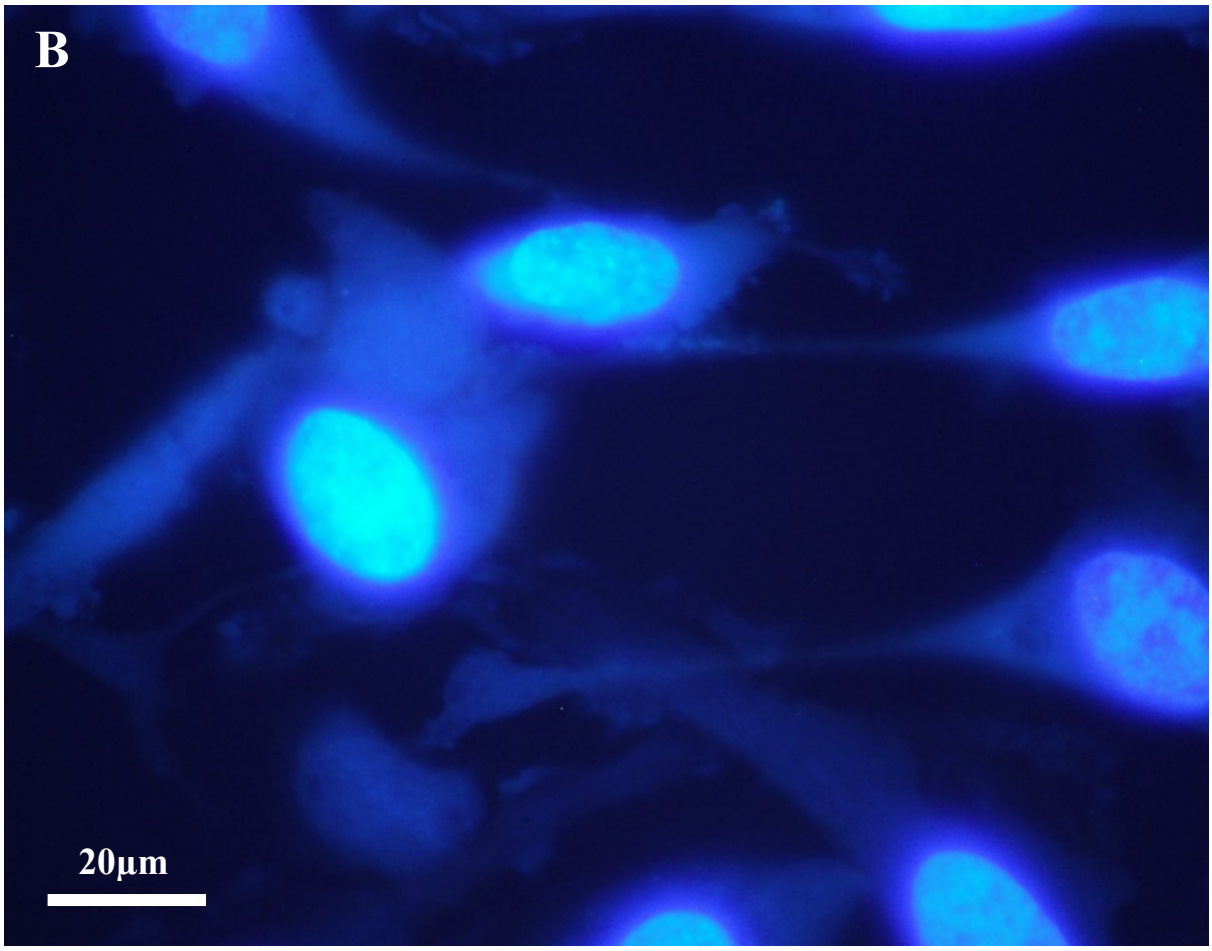

Figure 16: Images of microfilament (white arrows) and nuclear staining of the negative control (untreated) PC-3 cells. **A)** Phalloidin red staining of PC-3 cells. **B)** NucBlue™ staining of PC-3 cells. Images were taken on 1000X magnification.

Figure 17 depicts successful staining of the 0.005% DMSO control group of PC-3 cells after fixing and staining with phalloidin and NucBlue™. Figure 17A illustrates the staining of microfilaments of the cells. Figure 17B demonstrates the staining of nuclear material of the cells. Clear microfilaments (white arrows) are evident in some cells. Additionally, nuclear hypertrophy (yellow arrows) and prominent nucleoli (white arrows) have been observed.

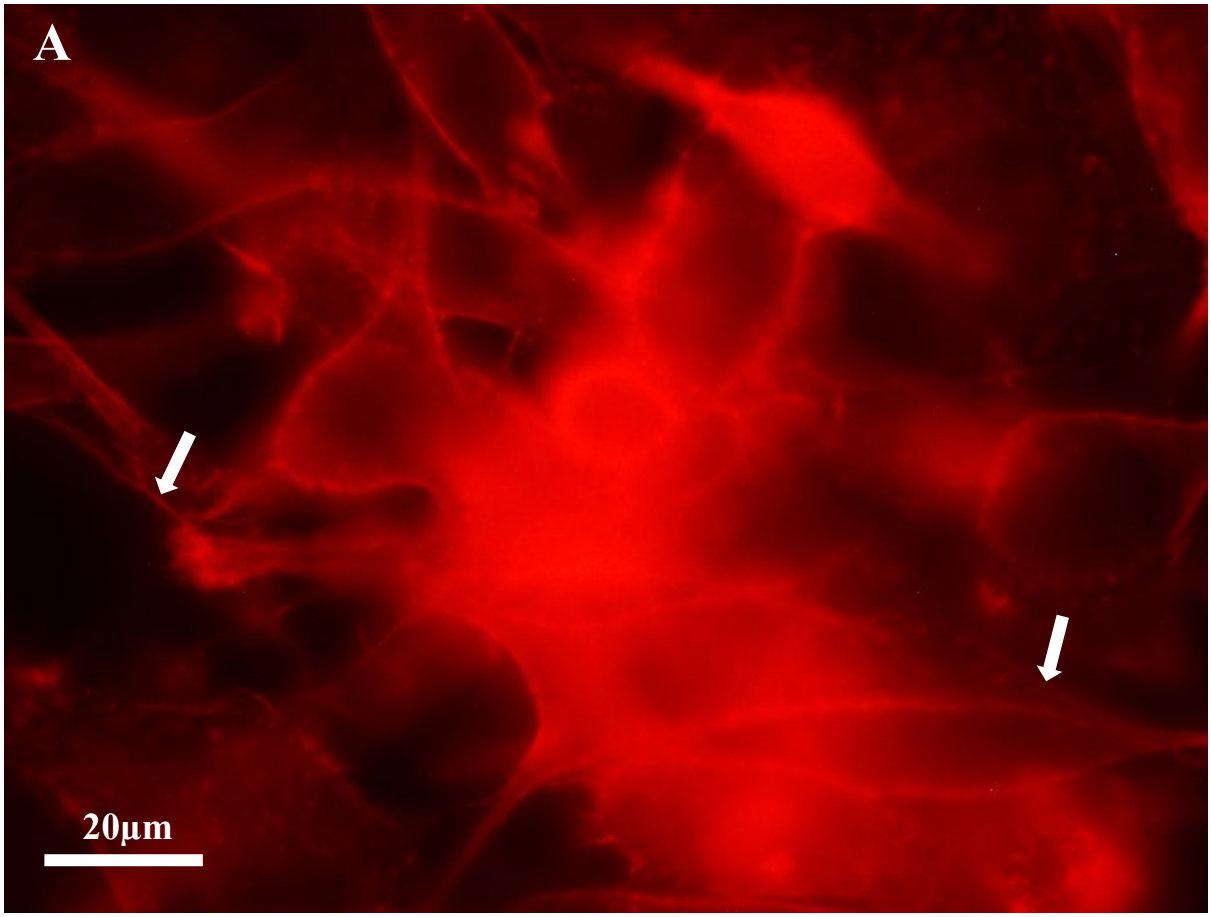

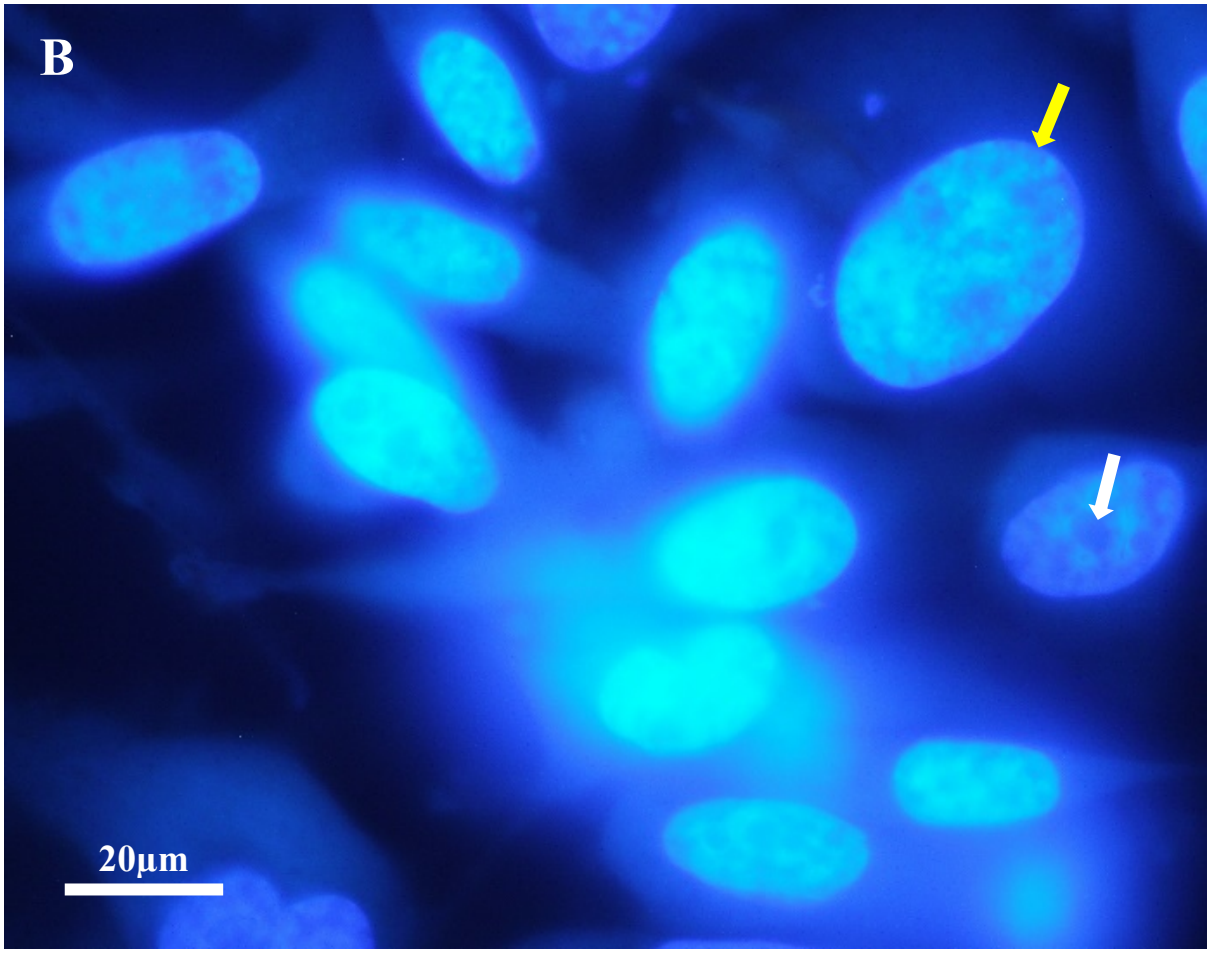

Figure 17: Images of microfilament (white arrows) and nuclear staining of PC-3 cells treated with 0.005% DMSO in RPMI media. **A)** Phalloidin red staining of PC-3 cells. **B)** NucBlue™ staining of PC-3 cells. Yellow arrows highlight hypertrophic nuclei and white arrows highlight prominent nucleoli. Images were taken on 1000X magnification.

Figure 18 depicts successful staining of the 0.01% DMSO control group of PC-3 cells after fixing and staining with phalloidin and NucBlue™. Figure 18A illustrates the staining of microfilaments of the cells. Figure 18B demonstrates the staining of nuclear material of the cells. Clear microfilaments (white arrows) are evident in some cells, although rare. Additionally, prominent nucleoli have been observed and are highlighted with white arrows.

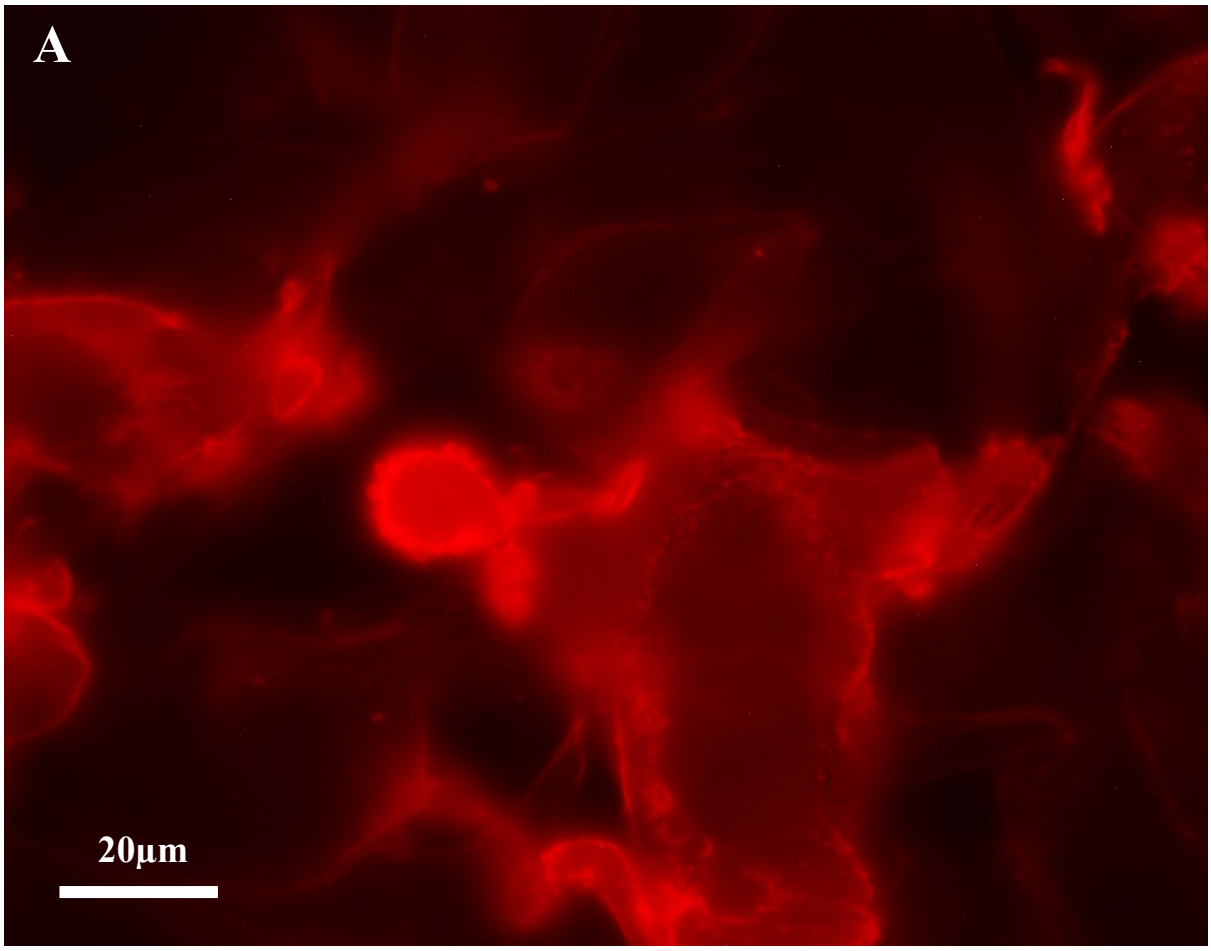

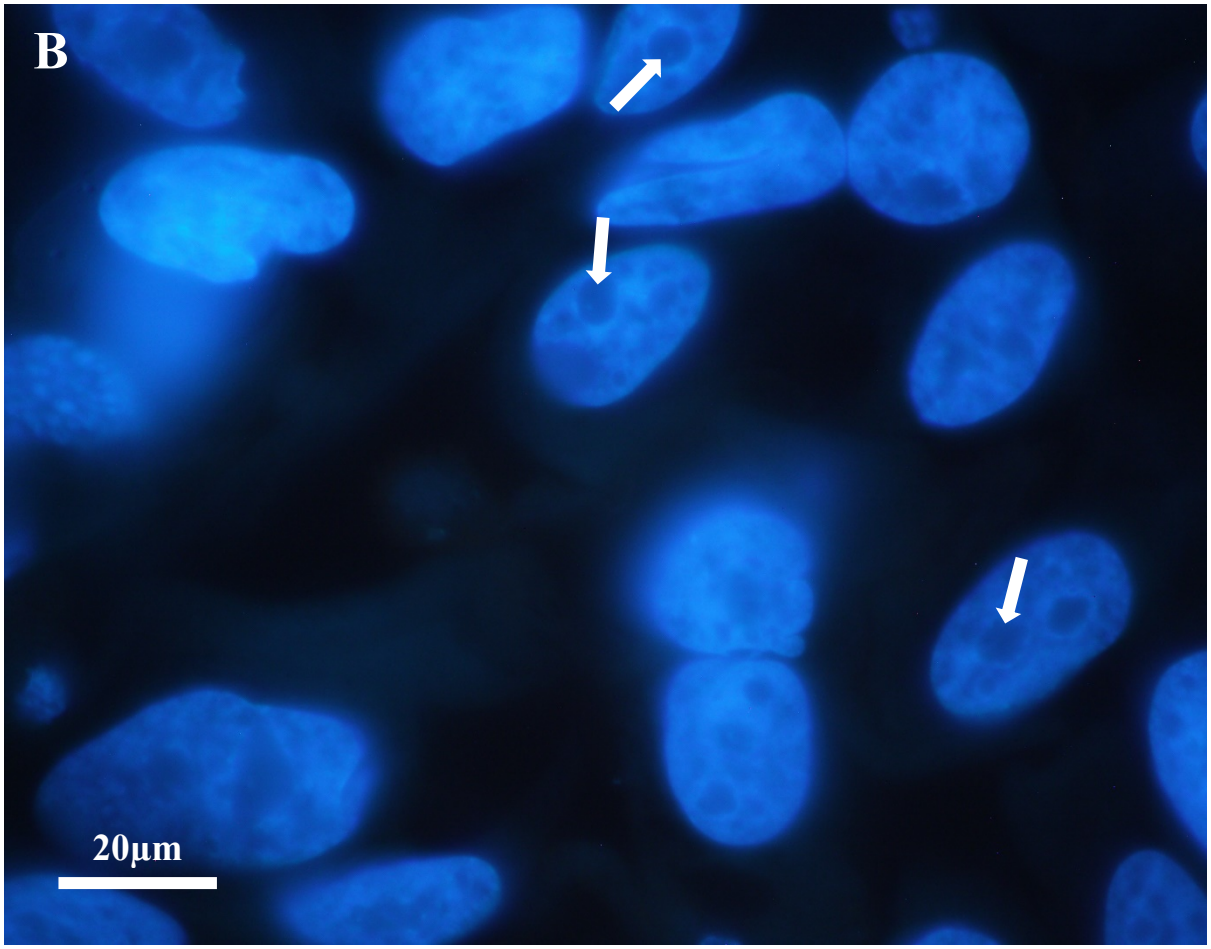

Figure 18: Images of microfilament (white arrows) and nuclear staining of PC-3 cells treated with 0.01% DMSO in RPMI media. **A)** Phalloidin red staining of PC-3 cells. **B)** NucBlue™ staining of PC-3 cells. White arrows highlight prominent nucleoli. Images were taken on 1000X magnification.

Figure 19 depicts successful staining of the 0.05% DMSO control group of PC-3 cells after fixing and staining with phalloidin and NucBlue™. Figure 19A illustrates the staining of microfilaments of the cells. Figure 19B demonstrates the staining of nuclear material of the cells. Clear microfilaments (white arrows) are rare but can be observed in cells. Additionally, prominent nucleoli have been observed and are highlighted with white arrows.

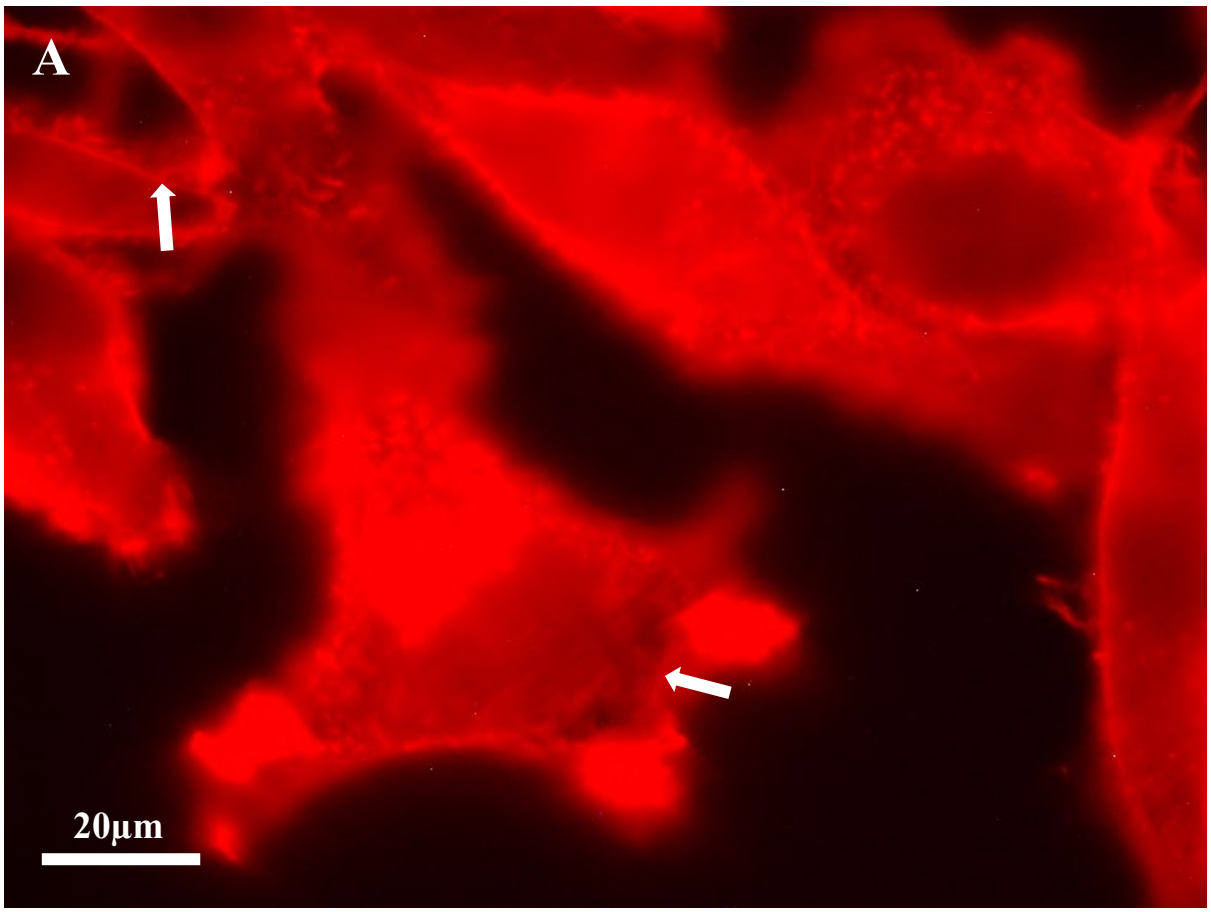

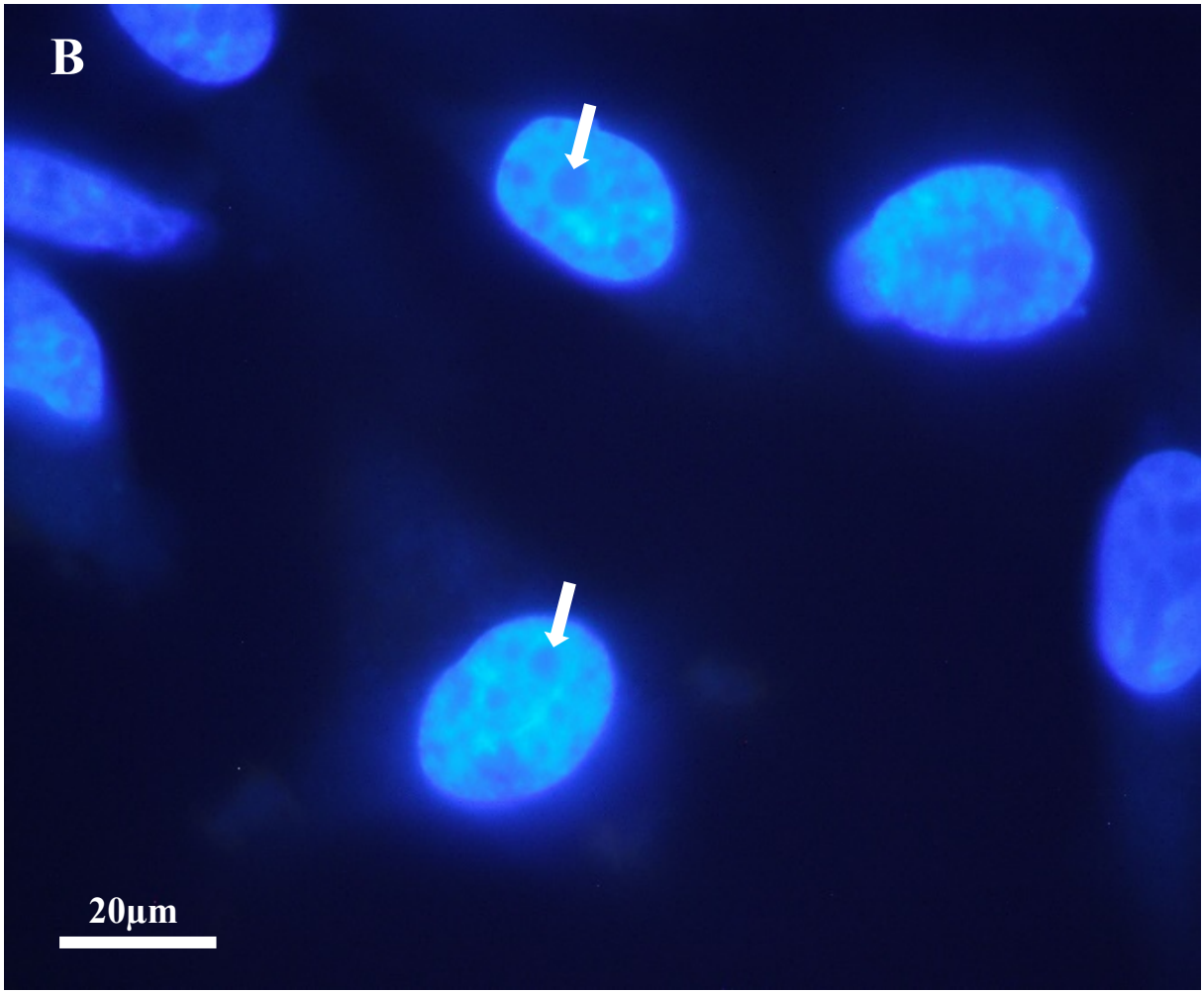

Figure 19: Images of microfilament (white arrows) and nuclear staining of PC-3 cells treated with 0.05% DMSO in RPMI media. **A)** Phalloidin red staining of PC-3 cells. **B)** NucBlue™ staining of PC-3 cells. White arrows highlight prominent nucleoli. Images were taken on 1000X magnification.

Figure 20 depicts successful staining of the 0.1% DMSO control group of PC-3 cells after fixing and staining with phalloidin and NucBlue™. Figure 20A illustrates the staining of microfilaments of the cells. Figure 20B demonstrates the staining of nuclear material of the cells. Clear microfilaments (white arrows) are evident in multiple cells. Additionally, prominent nucleoli have been observed and are highlighted with white arrows.

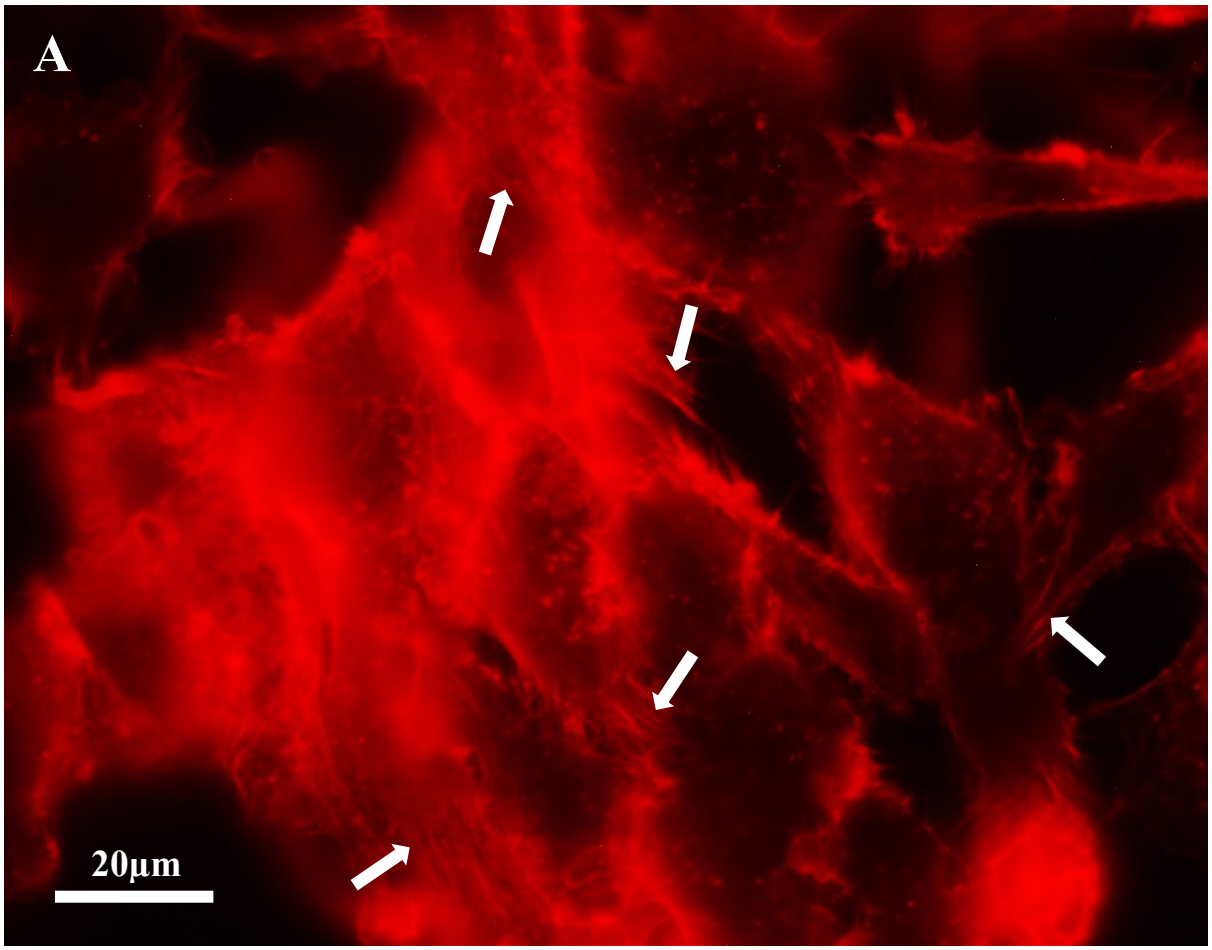

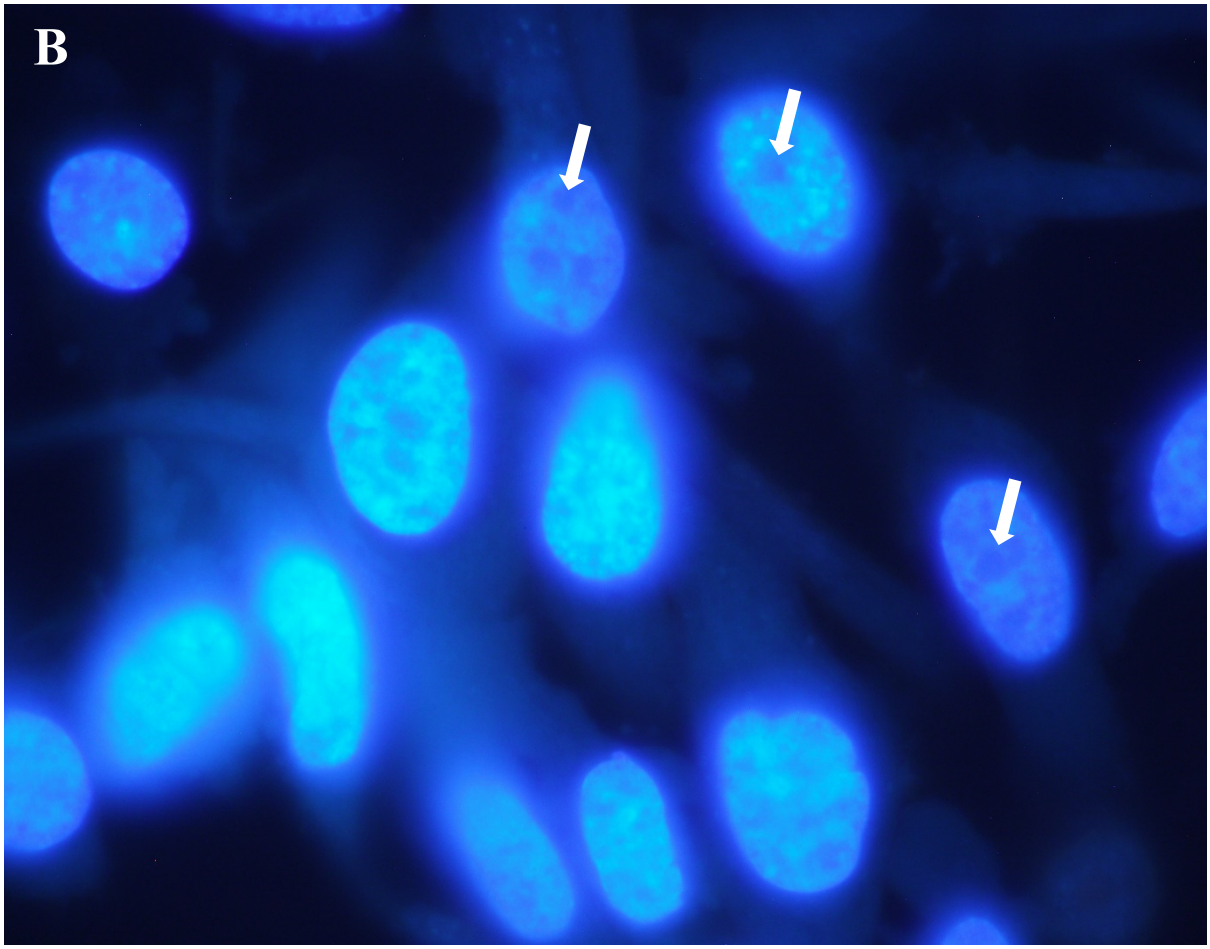

Figure 20: Images of microfilament (white arrows) and nuclear staining of PC-3 cells treated with 0.1% DMSO in RPMI media. **A)** Phalloidin red staining of PC-3 cells. **B)** NucBlue™ staining of PC-3 cells. White arrows highlight prominent nucleoli. Images were taken on 1000X magnification.

Figure 21 depicts successful staining of the PC-3 cells treated with fraction one at a concentration of 50 µg/mL with phalloidin and NucBlue™. Figure 21A illustrates the staining of microfilaments of the cells. Figure 21B illustrates the staining of nuclear material of the cells. Few microfilaments (white arrows) are clear and positive actin staining can be seen. While no obvious differences in nucleus size or shape can be observed in comparison to the DMSO control, two cells have been captured in different phases of mitosis.

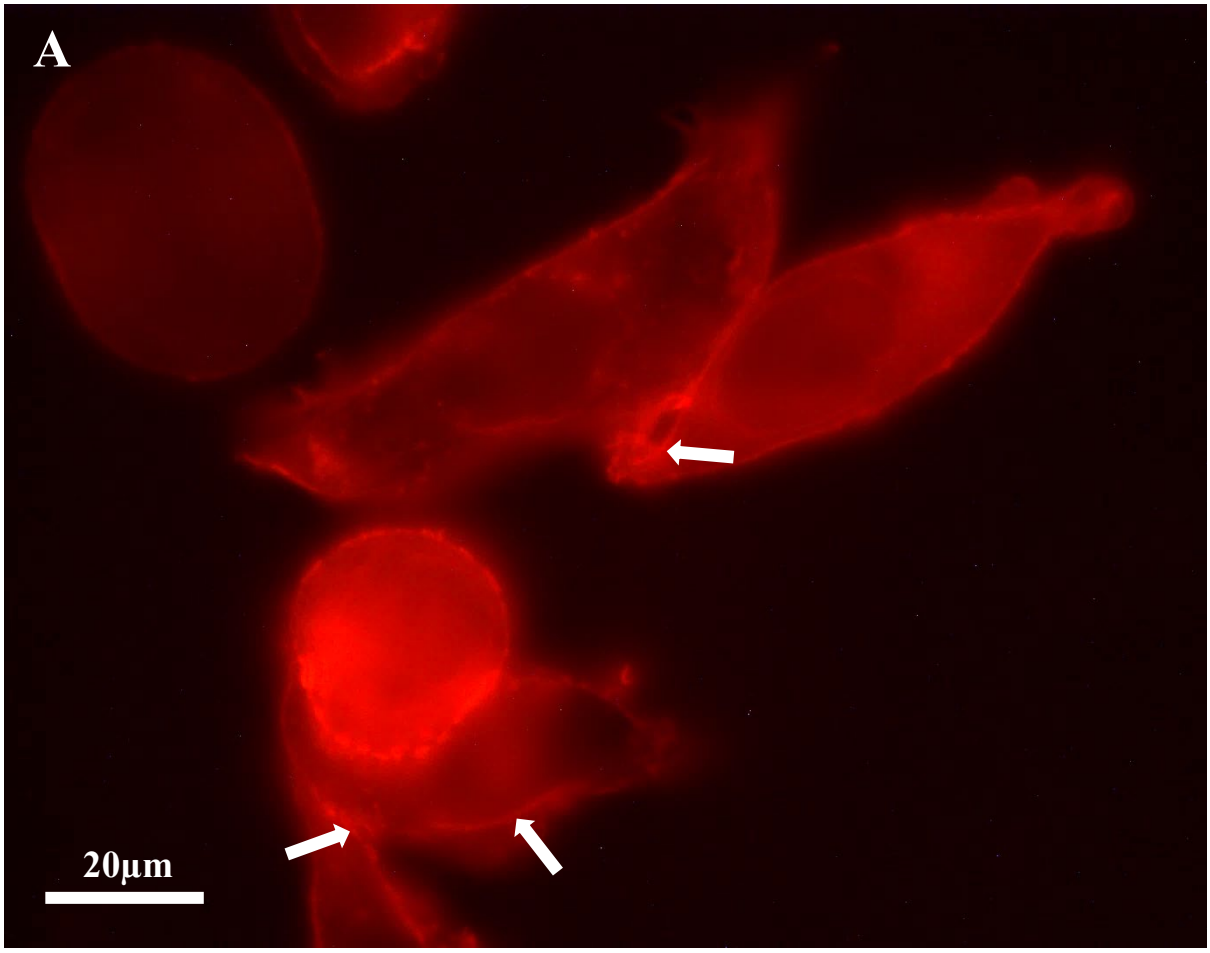

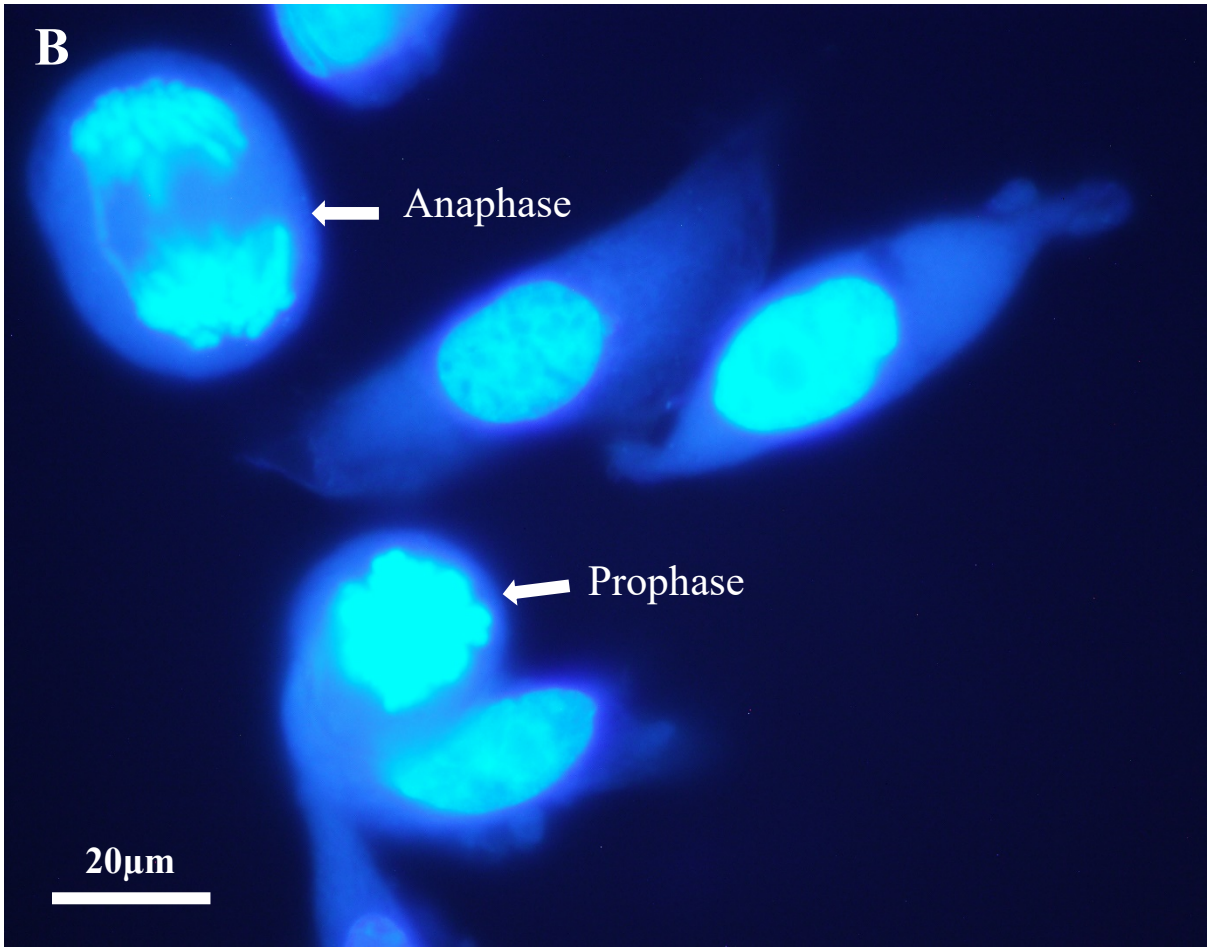

Figure 21: Images of microfilament (white arrows) and nuclear staining of PC-3 cells treated with 50 µg/mL of fraction one. **A)** Phalloidin red staining of PC-3 cells. **B)** NucBlue™ staining of PC-3 cells. Images were taken on 1000X magnification.

Figure 22 depicts successful staining of the PC-3 cells treated with fraction four at a concentration of 50 µg/mL with phalloidin and NucBlue™. Figure 22A illustrates the staining of microfilaments of the cells. Figure 22B illustrates the staining of nuclear material of the cells. Microfilaments have positively stained (white arrows) and can be seen in multiple cells. In some cells, nuclear hypertrophy (yellow arrows) can be seen, however, these were also found in the DMSO controls.

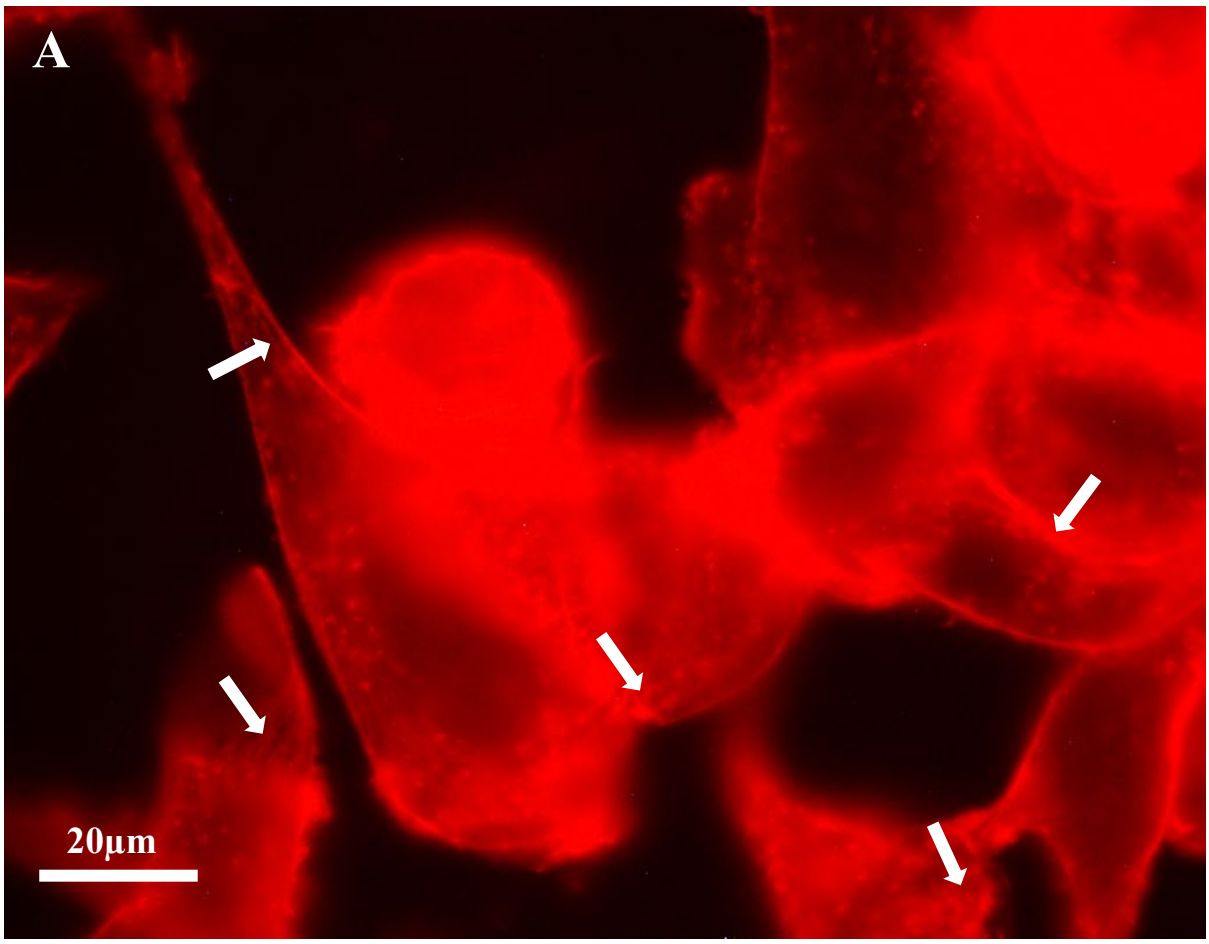

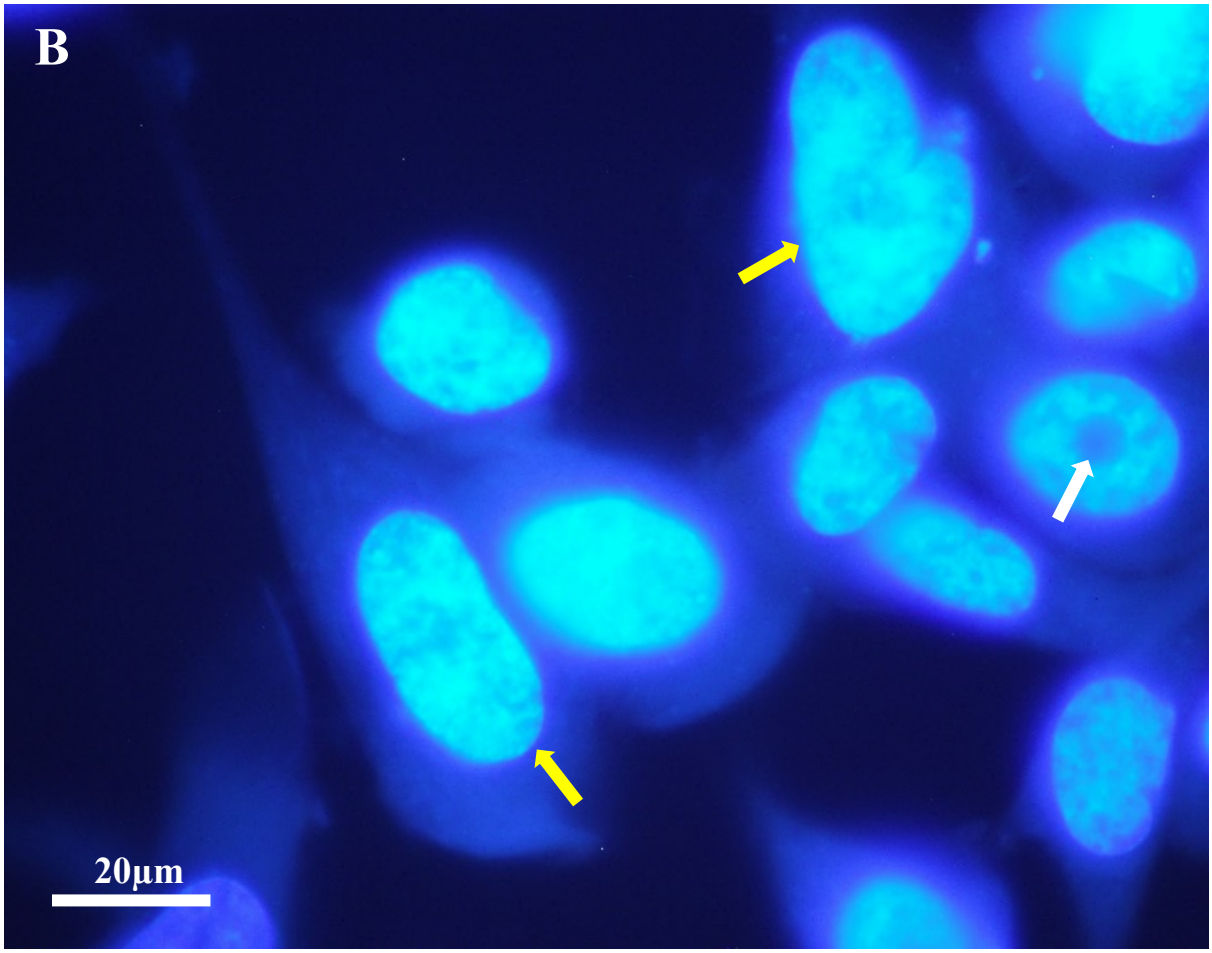

Figure 22: Images of microfilament (white arrows) and nuclear staining of PC-3 cells treated with 50 µg/mL of fraction four. **A)** Phalloidin red staining of PC-3 cells. **B)** NucBlue™ staining of PC-3 cells. Yellow arrows highlight hypertrophic nuclei and white arrows highlight prominent nucleoli. Images were taken on 1000X magnification.

Figure 23 depicts successful staining of the PC-3 cells treated with fraction five at a concentration of 50 µg/mL with phalloidin and NucBlue™. Figure 23A illustrates the staining of microfilaments of the cells. Figure 23B illustrates the staining of nuclear material of the cells. There are many clear microfilaments (white arrows). In some cells, nucleoli can be seen and are highlighted with white arrows in Figure 23B. Additionally, some nuclear hypertrophy has occurred (yellow arrows). However, these changes have also been observed in the DMSO controls.

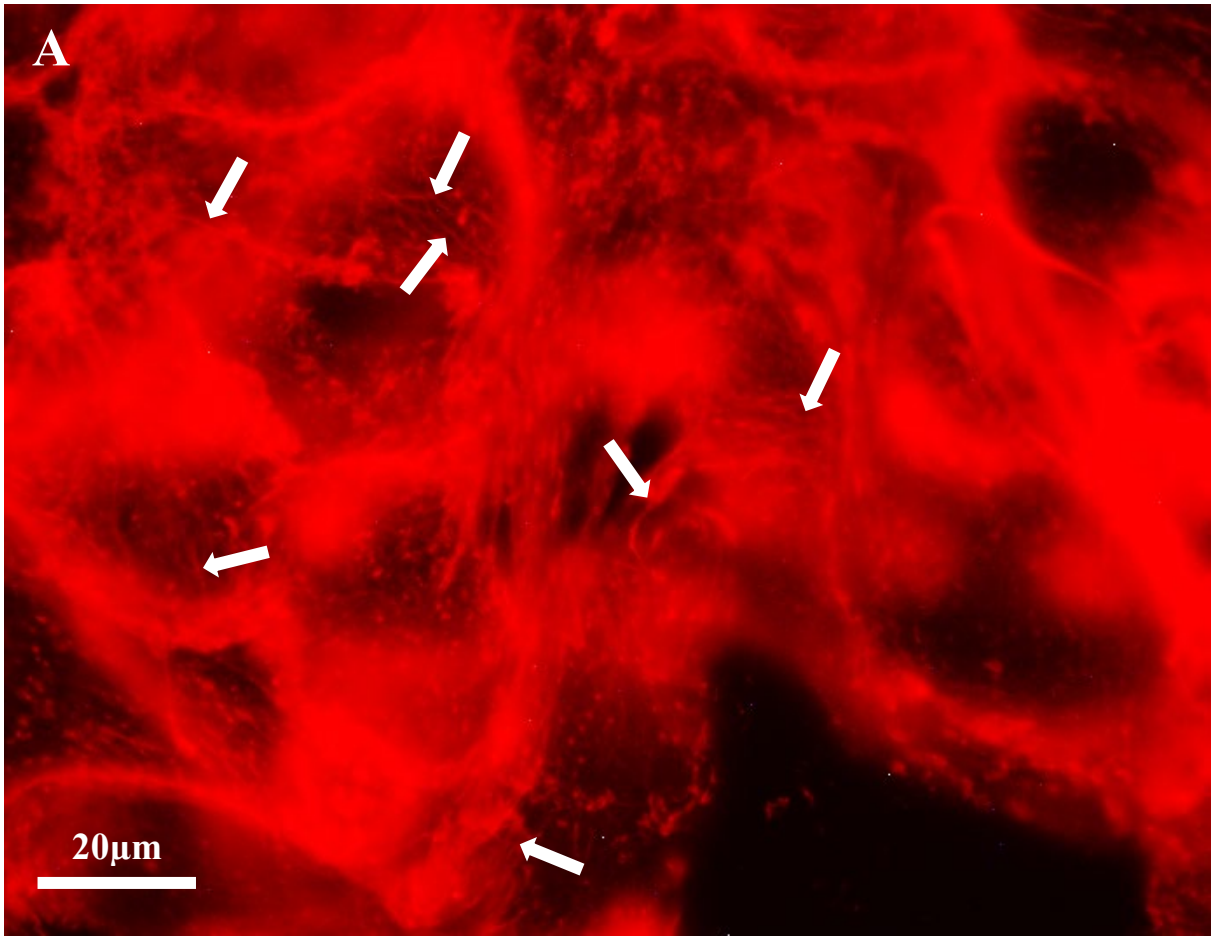

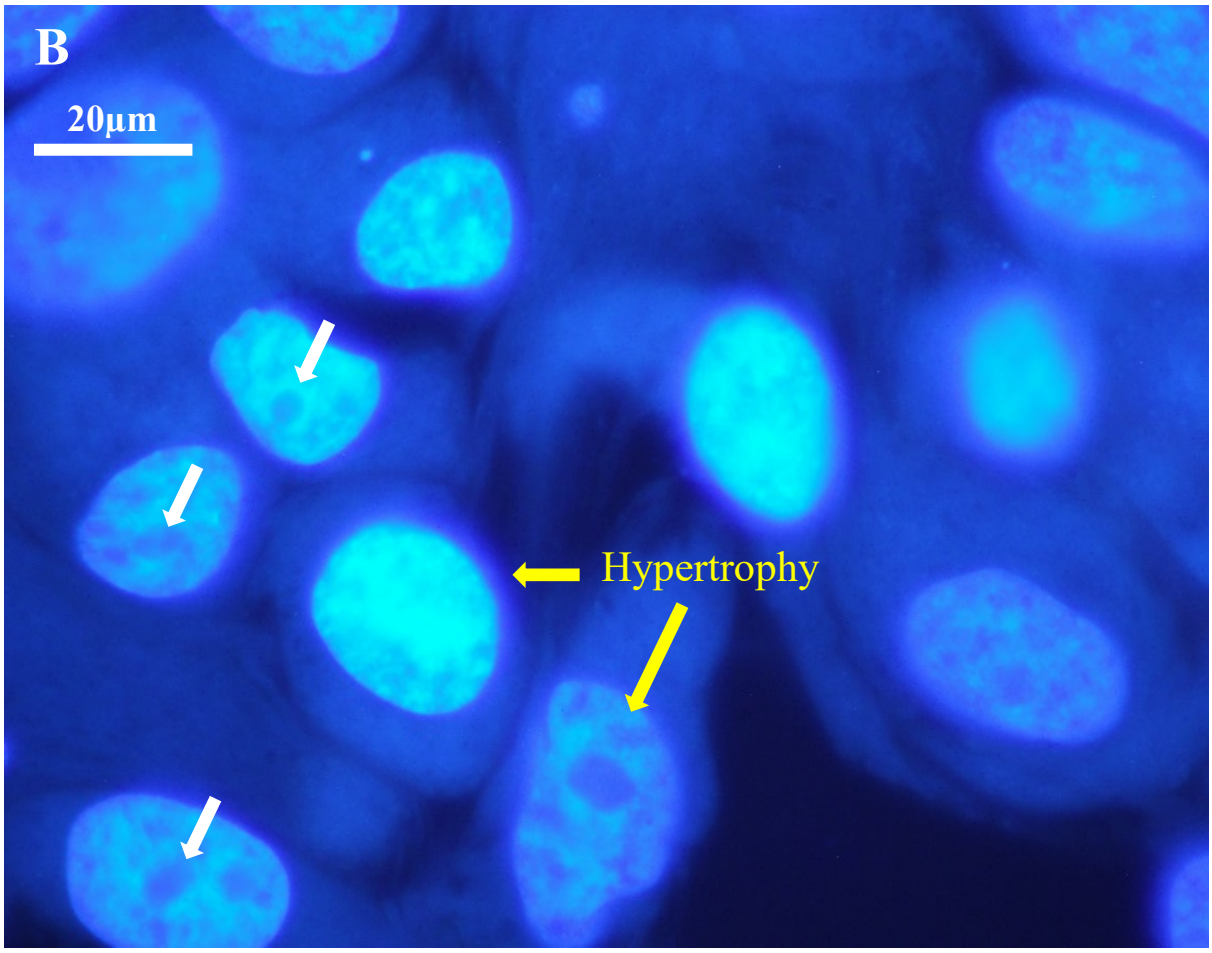

Figure 23: Images of microfilament (white arrows) and nuclear staining of PC-3 cells treated with 50 µg/mL of fraction five. **A)** Phalloidin red staining of PC-3 cells. **B)** NucBlue™ staining of PC-3 cells. White arrows highlight prominent nucleoli and yellow arrows highlight hypertrophic nuclei. Images were taken on 1000X magnification.

Figure 24 depicts successful staining of the PC-3 cells treated with fraction five at a concentration of 100 µg/mL with phalloidin and NucBlue™. Figure 24A illustrates the staining of microfilaments of the cells. Figure 24B illustrates the staining of nuclear material of the cells. Positive staining of microfilaments (white arrows) and hypertrophy of nuclei has occurred (yellow arrow). However, nuclear hypertrophy can also be seen in the DMSO controls.

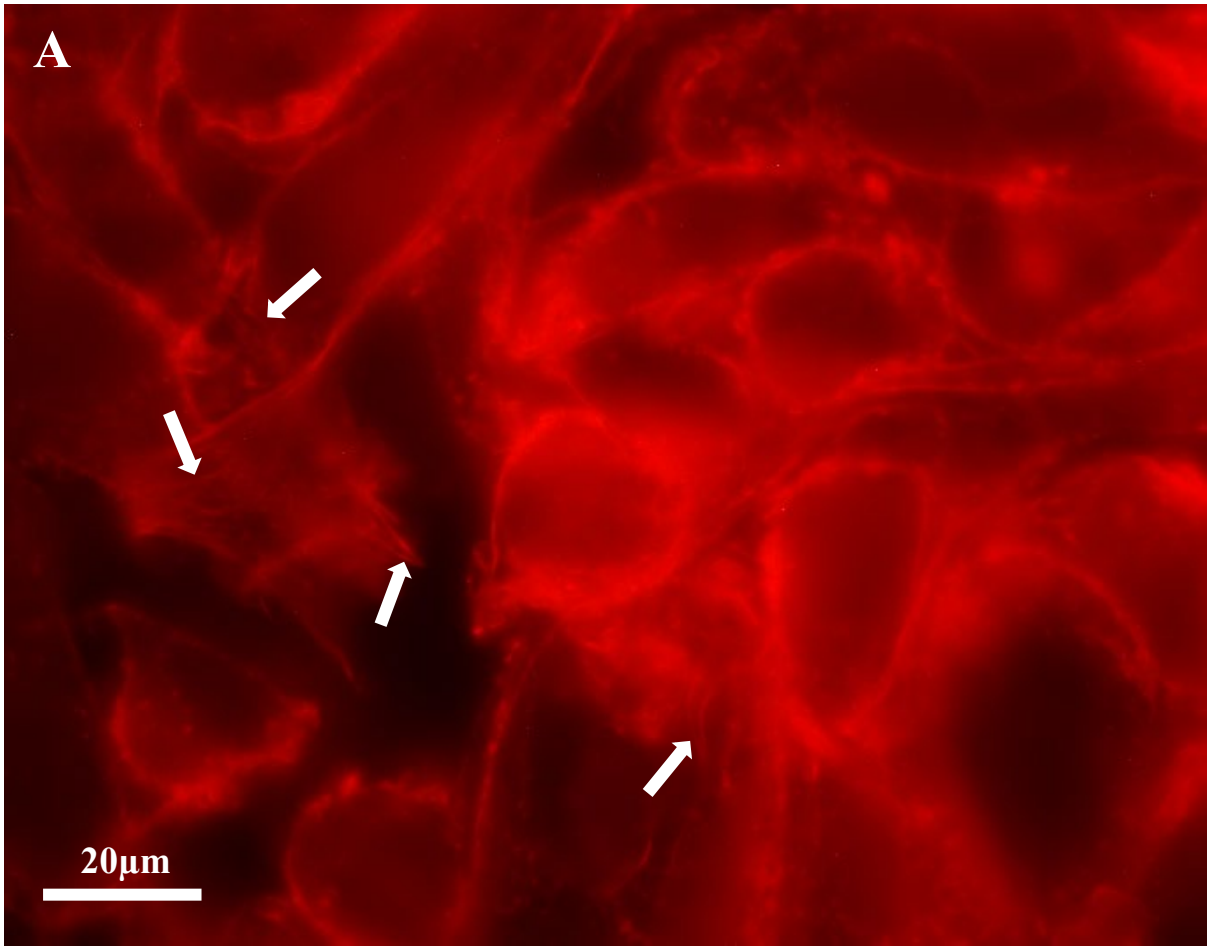

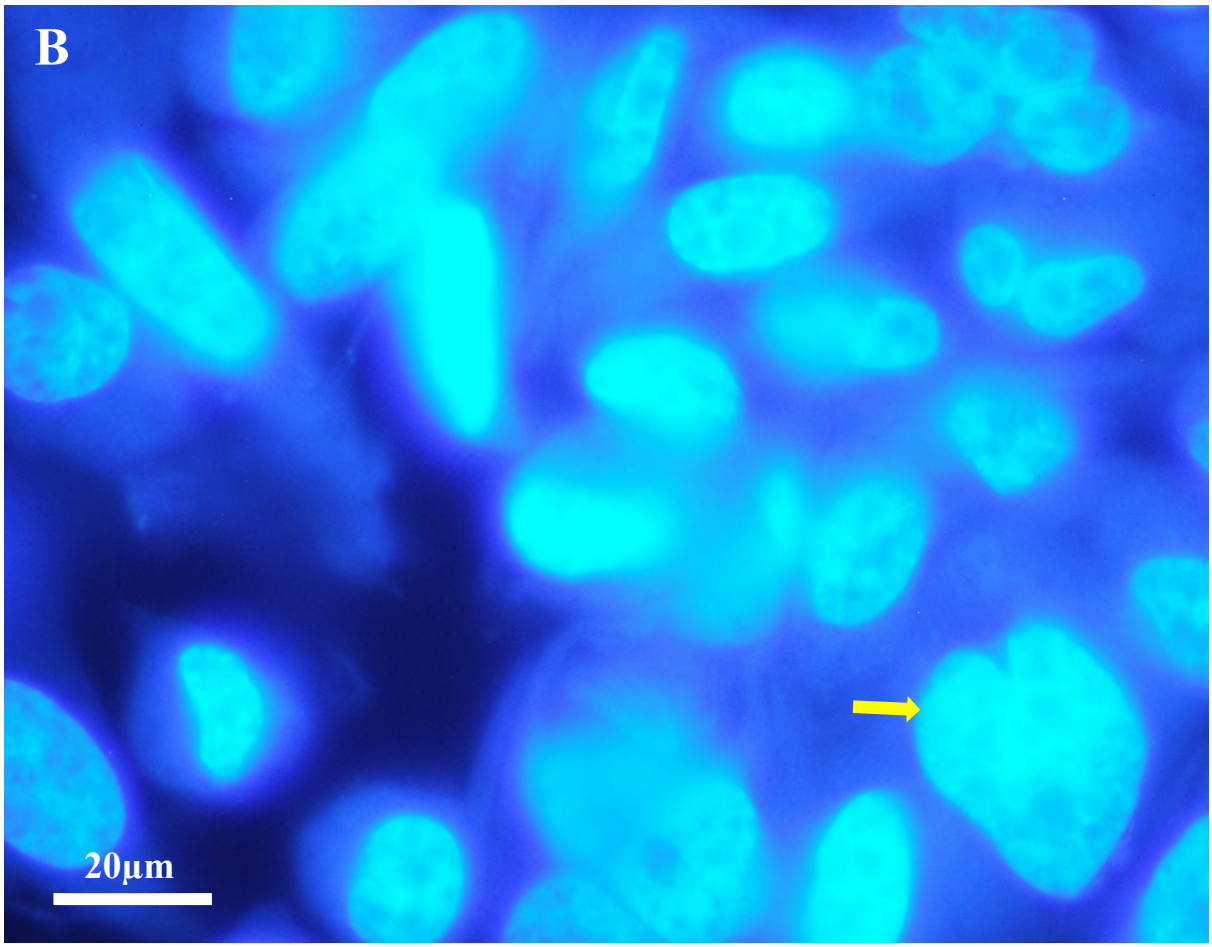

Figure 24: Images of microfilament (white arrows) and nuclear staining of PC-3 cells treated with 100 µg/mL of fraction five. **A)** Phalloidin red staining of PC-3 cells. **B)** NucBlue™ staining of PC-3 cells. Yellow arrows highlight hypertrophic nuclei. Images were taken on 1000X magnification.

Figure 25 depicts successful staining of the PC-3 cells treated with fraction six at a concentration of 50 µg/mL with phalloidin and NucBlue™. Figure 25A illustrates the staining of microfilaments of the cells. Figure 25B illustrates the staining of nuclear material of the cells. Microfilament structures have been stained (white arrows). Prominent nucleoli are highlighted with white arrows. The nuclei of the cells are comparable between the DMSO controls and this treatment group.

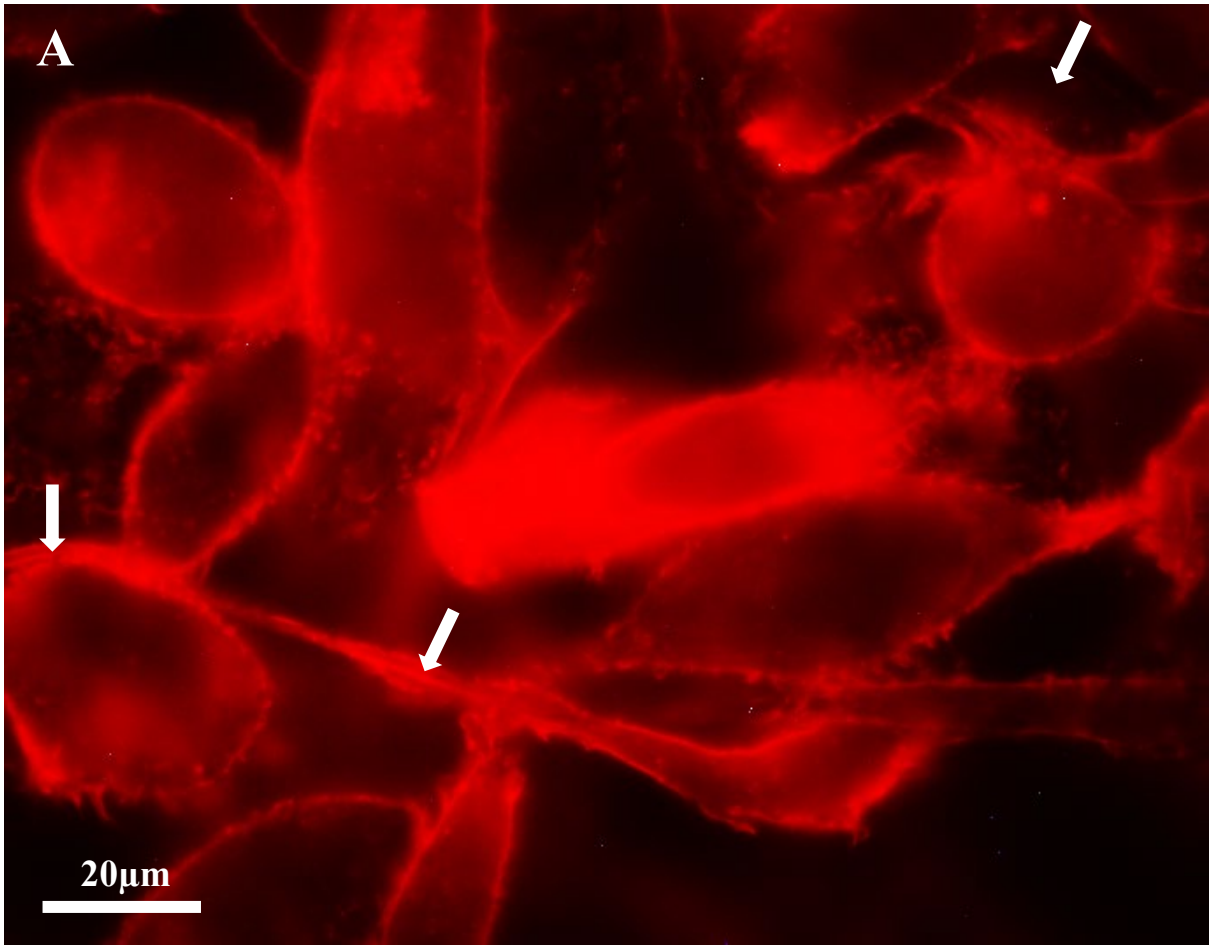

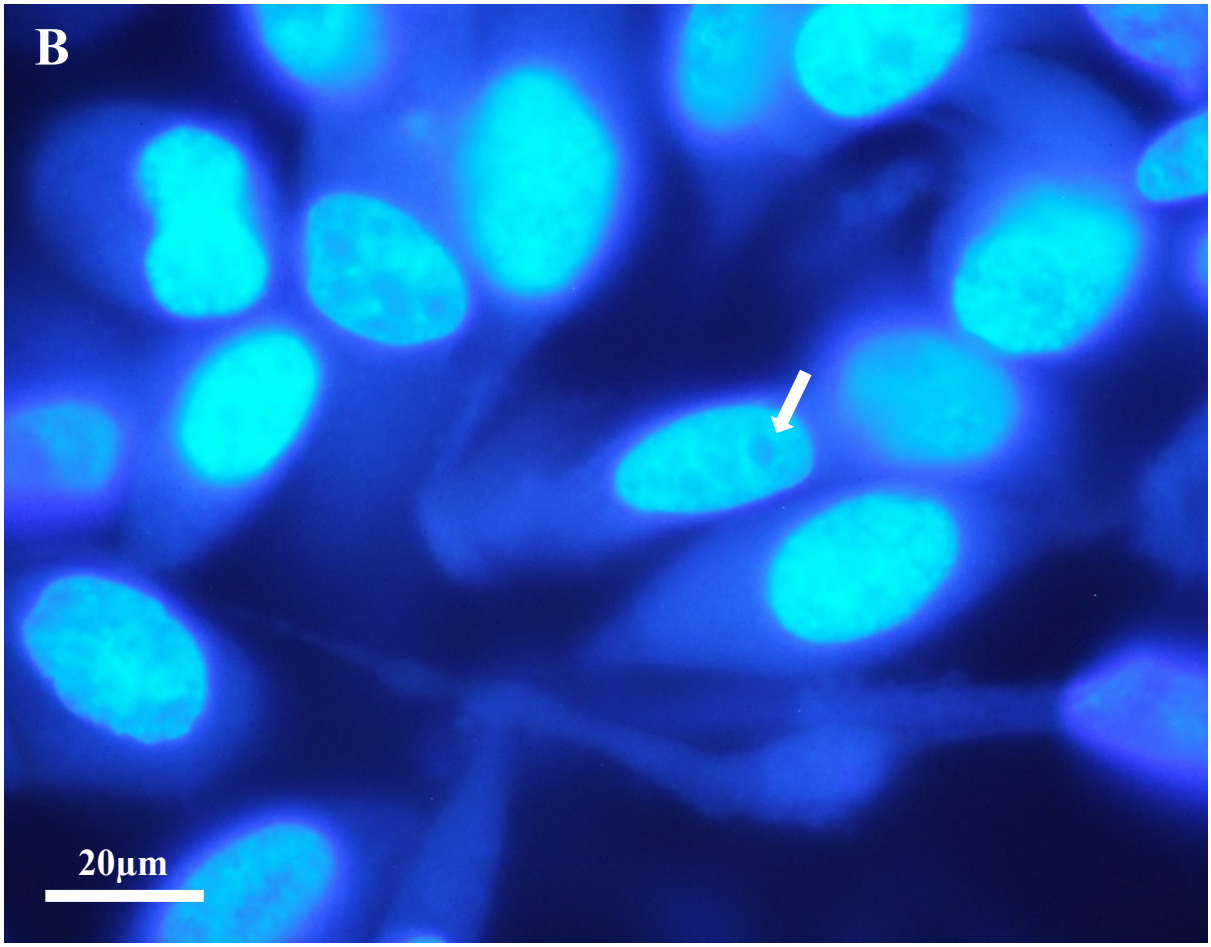

Figure 25: Images of microfilament (white arrows) and nuclear staining of PC-3 cells treated with 50 µg/mL of fraction six. **A)** Phalloidin red staining of PC-3 cells. **B)** NucBlue™ staining of PC-3 cells. White arrows highlight prominent nucleoli. Images were taken on 1000X magnification.

Figure 26 depicts successful staining of the PC-3 cells treated with fraction six at a concentration of 100 µg/mL with phalloidin and NucBlue™. Figure 26A illustrates the staining of microfilaments of the cells. Figure 26B illustrates the staining of nuclear material of the cells. Microfilaments (white arrows) are clear in most cells. Prominent nucleoli have been observed and are highlighted with white arrows. Hypertrophy of nuclei (yellow arrows) has also been observed, although inconsistently, and has occurred across both DMSO control and treatment groups.

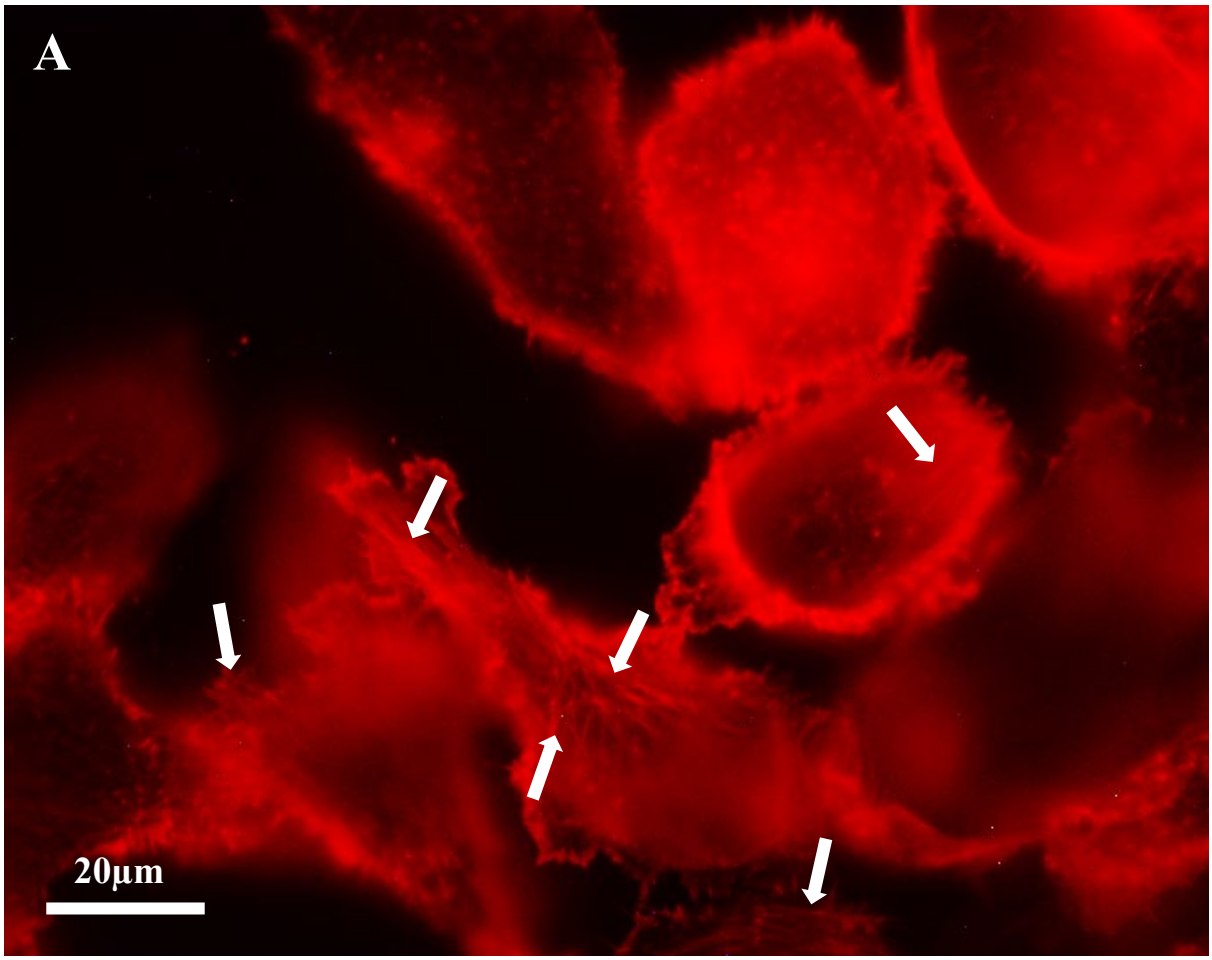

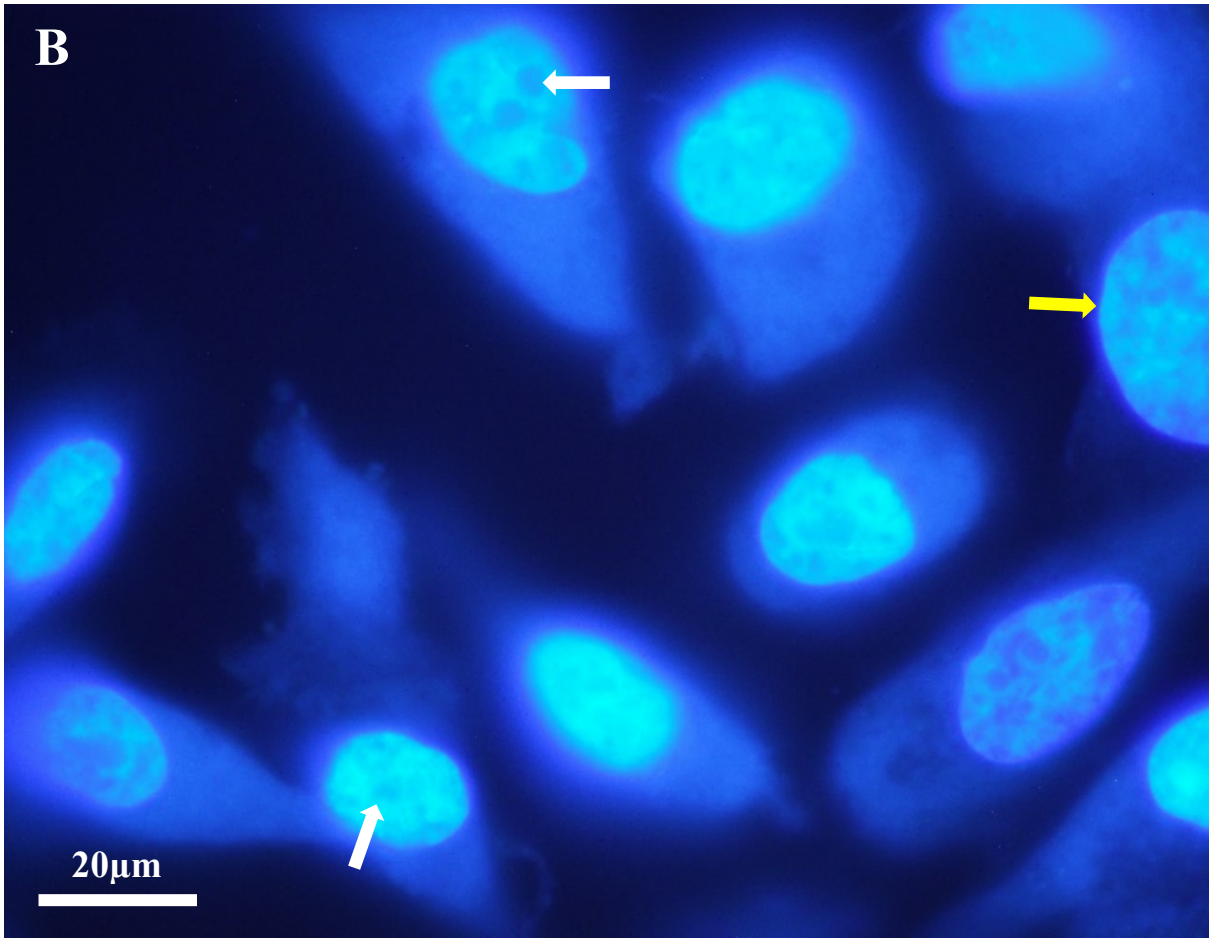

Figure 26: Images of microfilament (white arrows) and nuclear staining of PC-3 cells treated with 100 µg/mL of fraction six. **A)** Phalloidin red staining of PC-3 cells. **B)** NucBlue™ staining of PC-3 cells. White arrows highlight prominent nucleoli and yellow arrows highlight hypertrophic nuclei. Images were taken on 1000X magnification.

Chapter 4: Discussion

The main finding in this investigation was that fractionated compounds from FCEs of BSH2.9 exhibited cytotoxic activity against the PC-3 cell line. In the preliminary screen, the most significant decreases in cell number were seen when PC-3 cells were treated with 1 mg/mL of fractions two and six. Decreases were also observed after treatment with fractions three and five, however these were not statistically significant. A significant decrease in cell number as a result of treatment with fraction four at 50 µg/mL and fractions five and six at 50 µg/mL and 100 µg/mL was also observed. These decreases in cell number indicate that the treatment of the cells with some of the fractions from BSH2.9 may have resulted in cell death, potentially via apoptosis. However, consistent nuclear and cell shrinkage in the treated cells would have been observed if apoptosis had occurred (He et al. 2009).

Antibacterial activity was confirmed for the BSH2.9 isolate by both the streak plate method (for *B. cereus*) and the microdilution assay (*B. cereus* and *E. faecalis*). Previous studies with the BSH2.9 isolate also indicated antibacterial activity. The use of the streak plate methodology resulted in inhibition zones of <5 mm when the isolate was screened against *B. cereus* and *E. faecalis* (Mapperson 2014). Fractions and pure compounds of this fungus continued to show activity against gram positive and negative bacteria (Mapperson 2014). Furthermore, no anti-fungal activity was observed for any of the tested species in this study. Previous studies showed that antifungal activity of this isolate against *C. albicans* required pure compounds to cause inhibition of the species whereas fractions had no activity (Mapperson et al. 2014). The antimicrobial activity of endophytes against a variety of nosocomial and human pathogens is well described (Boddington 2009; Mapperson et al. 2014; Tayung & Jha 2014; Paudal et al. 2018).

One of the compounds isolated in the previous studies with this isolate was bromomethylchlamydosporol (Mapperson 2014), a chlamydosporol derivative. Bromomethylchlamydosporol has been previously identified as a compound with activity against MRSA (Nenkep et al. 2010). However, Mapperson (2014) did not support this finding. Interestingly, other chlamydosporol derivatives have been identified as potential anti-cancer agents as they were cytotoxic against colon cancer (HCT-116), gastric cancer (BGC-823), nonsmall-cell lung carcinoma (NCI-HI650), liver hepatocellular carcinoma (HepG2), and medulloblastoma (Daoy) cell lines (Lai et al. 2020). Given this compound has been demonstrated to exhibit both antimicrobial and anti-cancer activities, it is possible that this chemical was one of the compounds contributing to the activity of the fractions isolated from BSH2.9 in this study.

The primary compounds attributed with the antimicrobial activity of BSH2.9 were tentatively named Africanerones, a group of novel polyketides. Five were isolated, however only three were extracted at masses suitable for testing. The three compounds were active against *C. albicans* while only two of these compounds exhibited activity against MRSA and only for a 24 hour period as opposed to the 48 hours of antifungal activity that was observed (Mapperson 2014). Given these compounds were novel, no studies had investigated their cytotoxic potential. However, many studies describe other bioactive endophytic polyketides and show that these exhibit anti-cancer activity (Nenkep et al. 2010; Santiago et al. 2012; Jahn et al. 2017; Noumeur et al. 2017; Tian et al. 2021). Therefore, the activity observed here may be attributed to polyketides, however, purification and determination of the active chemical's identity is required to confirm this. This may be achieved by purification of the fractions obtained in this study by further use of HPLC, liquid chromatography- mass spectrometry (LC-MS), and nuclear magnetic resonance (NMR) to determine chemical identity before additional screening.

Alkaloids are another class of compounds isolated from endophytes that have anti-cancer activity. Although alkaloids have not been reported from BSH2.9 to date, anti-cancer alkaloids have been found in other *Preussia* sp. Epipolythiodiketopiperazine (ETP) isolated from *P. typharum* was found to be cytotoxic against a wide array of cell lines from the NCI-60 cell line panel (Du et al. 2014). Furthermore, some current clinically used chemotherapies are also alkaloid compounds, such as docetaxel. Although alkaloids have been extracted in EtOAc extracts (Srivastava & Anandrao 2015) other extraction methodologies may need to be employed to increase the yield of these in the obtained extracts (Ali et al. 2019). Differing from the process employed in this study, culture broths would be soaked in absolute EtOH and be concentrated for compounds to be alkalised with ammonium hydroxide (NH_4OH). Alkaloids would be extracted by rinsing with EtOAc (Ali et al. 2019). The utilisation of an extraction process to isolate alkaloids specifically may provide further direction for investigating the anti-cancer activities exhibited by this isolate.

Both fractions two and six had significant activity at the 1 mg/mL concentration trialled in the preliminary screen, but no activity for fraction two was indicated at the pharmaceutically relevant concentrations screened later. It is speculated that this has occurred as a result of the combination of unknown chemicals at unknown ratios within the fractions. That is, there may have been only one compound, potentially amongst many, that had activity and a sufficient amount to elicit the activity was present only at the highest of the tested concentrations. This would support that purification should be completed in future investigations to determine which compounds may have anti-cancer activity in these fractions. Furthermore, the decrease in cell number observed for fractions three and five also warrant further investigation.

An unexpected result obtained from this study was that the preliminary screening of the fractions indicated that fraction one had a protective effect to the cells. In contrast to the other fractions, cells treated with fraction one had ~20% more live cells than the 1% DMSO group

when compared to the negative control. This finding was not reflected in the subsequent screening of this fraction at lower concentrations. Previous accounts of protective effects of extracts are rare. However, proliferating cancer cells synthesise lipids *de novo* to aid in membrane growth, which is essential to producing a new cell, when glutamine or glucose are provided by the nutrient media (Daniëls et al. 2014). Some studies show that cell lines may use other lipids preferentially, such as palmitate (Yao et al. 2016). Given the extracts involved in the study are lipids or lipophilic, it is possible that they may have contained lipids such as palmitate that the cells may use preferentially and may thereby improve cell growth rather than inhibiting it. Boddington (2019) also described a similar result from many of the crude extracts obtained from non-endophytic *Russulaceae* species against colon adenocarcinoma (SW620) and human cervical (HeLa) cell lines. In contrast, a decrease of cell viability was observed in non-cancerous human embryonic (Hek-293) cells (Boddington 2019).

The first cytoskeletal staining protocol used for the PC-3 cells did not reveal any intact microtubules. The staining probe used was a green dye tagged with taxol to allow the cell to uptake the probe into microtubules (Merck 2021). The protocol required the use of verapamil to block calcium channels to prevent the efflux of the stain from the cell (Lukinavičius et al. 2014) and a one-to-one ratio was used. It is speculated that the unsuccessful outcome from this protocol may have been caused by an insufficient ratio of verapamil to stain, and that the presence of taxol may have resulted in a higher efflux rate. Therefore, an increase in the ratio of verapamil to the stain may result in improved future outcomes.

The staining of the cells after fixing with phalloidin red had a more successful outcome with clear microfilaments present. The role of the actin cytoskeleton in EMT suggests that compounds that target actin stabilisation may reduce the metastasis and migration potential of cancer cells and induce apoptosis (Foerster et al. 2014). However, no changes to the actin

cytoskeleton were observed. Therefore, the actin cytoskeleton is unlikely to have had a role in the decrease of live cell number.

Some nuclei appeared hypertrophic in comparison to other cells in the images, however, this was not consistently observed within treatment groups. This was also reflected across DMSO control groups. Furthermore, hypertrophy and folding of the nuclei as well as prominent nucleoli are common features of cancer cells (Zink et al. 2004). Therefore, these structural changes are not necessarily indicative of a mechanism of cell death and are expected. Based on these results, conclusions cannot be drawn as to which pathway of cell death has been activated, if cell death is occurring. Further studies could extend the time frame for the cytoskeletal and nuclear studies to allow more changes to cell structure to occur. This would require the use fewer cells so that they could be incubated for the full 72-hour period without becoming too confluent.

The decrease in live cell number cannot be attributed to cytotoxicity without the measurement of dead cells given that the cytoskeletal and nuclear studies did not indicate any structural changes. Therefore, the decrease of live cell number may have been caused by inhibition of cell proliferation rather than activation of apoptosis, so changes in gene expression and corresponding protein level of proliferation markers could be measured. The Ras–Raf–MEK–ERK mitogen-activated protein kinase (MAPK) signalling pathway has been shown to be involved in cell proliferation (Zhang & Liu 2002) and metastasis of PCa (Pavese et al. 2014). Evaluation of the role of the PI3K/AKT/mTOR pathway may also be of value as inhibition of this pathway appears to result in increased signalling of the Ras-Raf-MEK-ERK pathway in PCa (Butler et al. 2017). Furthermore, this would suggest that the fractions might inhibit a proliferation pathway and this may not be represented by live cell number. For example, fraction four appeared to have no activity as no change in live cell number was indicated. However, this fraction may have inhibited one proliferation pathway, resulting in increased

activity of another, and so no change of cell number was observed. Therefore, future studies could investigate multiple signalling pathways that regulate cell proliferation such as the Ras–Raf–MEK–ERK MAPK and PI3K/AKT/mTOR pathways.

Other signalling mechanisms may also be involved in the reduction of live cell number that was observed. The bioactive molecules observed here may act by inhibition of signalling molecules such as the STAT3 transcription factor. Endophyte derived compounds, including polyketides, have been implicated in reducing growth, or reducing cell proliferation, of PC-3 cells (Don-Doncow et al. 2014), similarly to what may have been observed in this study. Therefore, further studies using cell lines with differing expression of STAT3 and purified *Preussia* spp. derived molecules could also be conducted to evaluate the role this signalling molecule may have had.

This study provides impetus for further investigations into the cytotoxic activity of this *Preussia* sp. isolate, and other *Preussia* spp. endophytes more broadly, as anti-proliferative activity from multiple fractions was evident. *Preussia* spp. appear to be common endophytes in Australian plants (Mapperson et al. 2014; Sharma 2021). It is likely that further efforts to explore understudied Australian habitats such as tropical and subtropical rainforests may isolate additional new *Preussia* species and provide novel compounds useful to cancer treatment.

This study was limited by the use of only one cell line, and the use of fractions of extracts as opposed to purified compounds. The mass of the fractions that was produced limited the number of cell lines that could be screened as evaluation of multiple concentrations was more important to ensure that activity was identified if present. Increasing the yield of fractions would increase the number of cell lines that could be screened and would therefore be a recommendation for future studies. That is, a greater volume of BSH2.9 grown would allow

other cell lines to be tested. This could be achieved by increasing the number of flasks that were supporting fungal growth, and potentially the period of time the growth was allowed to occur. Purification processes such as HPLC could then also be employed.

The evaluation of multiple cancer cell lines in comparison to non-cancerous, normal cell lines against pure compounds may also assist in establishing these endophyte derived compounds as genuine potential treatment alternatives that, in the long term, could be produced into clinically used therapies. This would also require the use of LC-MS and NMR technologies in order to characterise the purified compounds that are causing the anti-cancer activity.

Another key improvement would be to compare the pure compounds to a positive control such as docetaxel. Relationships between existing therapies and newer compounds could also be investigated as they may have a more significant effect when combined. Similar effects have been previously reported in studies evaluating synergistic cytotoxicity of doxorubicin with phytochemicals which decreased cell viability of Jerkat T lymphocyte and HL-60 leukaemia cell lines in comparison to when used alone (Wende et al. 2021). If further studies using multiple cell lines and purified compounds yield positive results, animal models such as xenografts in mice may be used to assist in determining how the compounds impact the overall growth patterns of a tumour.

Chapter 5: Conclusions

This pilot study revealed that several fractions were active against the PC-3 cell line at pharmaceutically relevant concentrations. No mechanism of action was revealed as microfilaments remained intact and there was no observable damage to the nuclei. There was also no evidence of apoptosis as there was no shrinkage of the nuclei or the cells. The protocol used to evaluate cytoskeletal and nuclear changes requires optimisation, and other modes of action should be investigated based on these findings. Therefore, this study does provide significant evidence that this endophytic isolate may contain important anti-cancer compounds. This provides impetus to further evaluate the compounds contained in the EtOAc extracts of the BSH2.9 isolate, potentially with purification measures and other mechanistic studies.

References

Albrecht, W, Van Poppel, H, Horenblas, S, Mickisch, G, Horwich, A, Serretta, V, Casetta, G, Maréchal, J, Jones, W & Kalman, S 2004, 'Randomized Phase II trial assessing estramustine and vinblastine combination chemotherapy vs estramustine alone in patients with progressive hormone-escaped metastatic prostate cancer', *British Journal of Cancer*, vol. 90, no. 1, pp. 100-5.

Ali, E, Abdel-Rahman, T & Ebrahim, H 2019, 'Cytotoxicity and antimicrobial activity of alkaloids extracted from *Catharanthus roseus* associated endophytic fungi', *Malaysian Journal of Microbiology*, vol. 15, no. 1, pp. 16-23.

Aly, AH, Debbab, A & Proksch, P 2011, 'Fungal endophytes: unique plant inhabitants with great promises', *Applied Microbiology and Biotechnology*, vol. 90, no. 6, pp. 1829-45.

Astuti, P & Nababan, OA 2014, 'Antimicrobial and cytotoxic activities of endophytic fungi isolated from *Piper crocatum* Ruiz & Pav', *Asian Pacific Journal of Tropical Biomedicine*, vol. 4, pp. 592-6.

Australian Institute of Health and Welfare 2021, *Cancer data in Australia,* AIoHa Welfare, Canberra, https://www.aihw.gov.au/getmedia/43903b67-3130-4384-8648-39c69bb684b5/Cancer-data-in-Australia.pdf.aspx?inline=true>.

Banerjee, B, Iqbal, BM, Kumar, H, Kambale, T & Bavikar, R 2016, 'Correlation between prostate specific antigen levels and various prostatic pathologies', *Journal of Medical Society*, vol. 30, no. 3, pp. 172-5.

Benson, R & Hartley-Asp, B 1990, 'Mechanisms of action and clinical uses of estramustine', *Cancer Investigation*, vol. 8, no. 3, pp. 375-80.

Boddington, M 2009, 'Discovery and evaluation of novel antimicrobial agents against nosocomial pathogens.', University of Southern Queensland, Toowoomba.

References

Boddington, M 2019, 'The taxonomy, ecology and bioactiv properties of south-east Queensland *Russulaceae*', University of Southern Queensland, Toowoomba.

Booser, DJ & Hortobagyi, GN 1994, 'Anthracycline antibiotics in cancer therapy', *Drugs*, vol. 47, no. 2, pp. 223-58.

Bostwick, DG & Brawer, MK 1987, 'Prostatic intra-epithelial neoplasia and early invasion in prostate cancer', *Cancer*, vol. 59, no. 4, pp. 788-94.

Bostwick, DG & Qian, J 2004, 'High-grade prostatic intraepithelial neoplasia', *Modern Pathology*, vol. 17, no. 3, pp. 360-79.

Boya, P & Kroemer, G 2008, 'Lysosomal membrane permeabilization in cell death', *Oncogene*, vol. 27, no. 50, pp. 6434-51.

Butler, DE, Marlein, C, Walker, HF, Frame, FM, Mann, VM, Simms, MS, Davies, BR, Collins, AT & Maitland, NJ 2017, 'Inhibition of the PI3K/AKT/mTOR pathway activates autophagy and compensatory Ras/Raf/MEK/ERK signalling in prostate cancer', *Oncotarget*, vol. 8, no. 34, pp. 56698-713.

Calò, V, Migliavacca, M, Bazan, V, Macaluso, M, Buscemi, M, Gebbia, N & Russo, A 2003, 'STAT proteins: from normal control of cellular events to tumorigenesis', *Journal of Cellular Physiology*, vol. 197, no. 2, pp. 157-68.

Card, S, Johnson, L, Teasdale, S & Caradus, J 2016, 'Deciphering endophyte behaviour: the link between endophyte biology and efficacious biological control agents', *FEMS Microbiology Ecology*, vol. 92, no. 8, pp. 1-19.

Chen, N & Zhou, Q 2016, 'The evolving Gleason grading system', *Chinese Journal of Cancer Research*, vol. 28, no. 1, pp. 58-64.

References

Chen, X, Shi, Q, Lin, G, Guo, S & Yang, J 2009, 'Spirobisnaphthalene analogues from the endophytic fungus *Preussia* sp', *Journal of Natural Products*, vol. 72, no. 9, pp. 1712-5.

Clinical and Laboratory Standard Institute (CLSI) 2018, *Methods for dilution antimicrobial susceptibility tests for bacteria that grow aerobically: approved standard,* Pennsylvania USA.

Cui, J-l, Guo, S-x & Xiao, P-g 2011, 'Antitumor and antimicrobial activities of endophytic fungi from medicinal parts of *Aquilaria sinensis*', *Journal of Zhejiang University Science B*, vol. 12, no. 5, pp. 385-92.

Daniëls, VW, Smans, K, Royaux, I, Chypre, M, Swinnen, JV & Zaidi, N 2014, 'Cancer cells differentially activate and thrive on de novo lipid synthesis pathways in a low-lipid environment', *PloS One*, vol. 9, no. 9, pp. 1-13.

Datta, K, Muders, M, Zhang, H & Tindall, DJ 2010, 'Mechanism of lymph node metastasis in prostate cancer', *Future Oncology*, vol. 6, no. 5, pp. 823-36.

de Bono, JS, Oudard, S, Ozguroglu, M, Hansen, S, Machiels, J-P, Kocak, I, Gravis, G, Bodrogi, I, Mackenzie, MJ & Shen, L 2010, 'Prednisone plus cabazitaxel or mitoxantrone for metastatic castration-resistant prostate cancer progressing after docetaxel treatment: a randomised open-label trial', *The Lancet*, vol. 376, no. 9747, pp. 1147-54.

Don-Doncow, N, Escobar, Z, Johansson, M, Kjellström, S, Garcia, V, Munoz, E, Sterner, O, Bjartell, A & Hellsten, R 2014, 'Galiellalactone is a direct inhibitor of the transcription factor STAT3 in prostate cancer cells', *Journal of Biological Chemistry*, vol. 289, no. 23, pp. 15969-78.

Du, L, Robles, AJ, King, JB, Mooberry, SL & Cichewicz, RH 2014, 'Cytotoxic dimeric epipolythiodiketopiperazines from the ascomycetous fungus *Preussia typharum*', *Journal of Natural Products*, vol. 77, no. 6, pp. 1459-66.

References

El-Hawary, S, Mohammed, R, AbouZid, S, Bakeer, W, Ebel, R, Sayed, A & Rateb, M 2016, 'Solamargine production by a fungal endophyte of *Solanum nigrum*', *Journal of Applied Microbiology*, vol. 120, no. 4, pp. 900-11.

Epstein, JI, Allsbrook Jr, WC, Amin, MB, Egevad, LL & Committee, IG 2005, 'The 2005 International Society of Urological Pathology (ISUP) consensus conference on Gleason grading of prostatic carcinoma', *The American Journal of Surgical Pathology*, vol. 29, no. 9, pp. 1228-42.

Fan, X, Wang, L, Guo, Y, Xiong, X, Zhu, L & Fang, K 2016, 'Inhibition of prostate cancer growth using doxorubicin assisted by ultrasound-targeted nanobubble destruction', *International Journal of Nanomedicine*, vol. 11, pp. 3585-96.

Farooq, S, Qayum, A, Nalli, Y, Lauro, G, Chini, MG, Bifulco, G, Chaubey, A, Singh, SK, Riyaz-Ul-Hassan, S & Ali, A 2020, 'Discovery of a secalonic acid derivative from *Aspergillus aculeatus*, an endophyte of *Rosa damascena* Mill., triggers apoptosis in MDA-MB-231 triple negative breast cancer cells', *American Chemical Society Omega*, vol. 5, no. 38, pp. 24296-310.

Feng, Q & He, B 2019, 'Androgen receptor signaling in the development of castration-resistant prostate cancer', *Frontiers in Oncology*, vol. 9, pp. 858-67.

Foerster, F, Braig, S, Moser, C, Kubisch, R, Busse, J, Wagner, E, Schmoeckel, E, Mayr, D, Schmitt, S & Huettel, S 2014, 'Targeting the actin cytoskeleton: selective antitumor action via trapping PKC ε', *Cell Death & Disease*, vol. 5, no. 8, pp. 1398-410.

Frick, J & Aulitzky, W 1991, 'Physiology of the prostate', *Infection*, vol. 19, no. 3, pp. 115-8.

Fujita, K & Nonomura, N 2019, 'Role of androgen receptor in prostate cancer: a review', *The World Journal of Men's Health*, vol. 37, no. 3, pp. 288-95.

References

Ganguly, A, Das, B, Roy, A, Sen, N, Dasgupta, SB, Mukhopadhayay, S & Majumder, HK 2007, 'Betulinic acid, a catalytic inhibitor of topoisomerase I, inhibits reactive oxygen species–mediated apoptotic topoisomerase I–DNA cleavable complex formation in prostate cancer cells but does not affect the process of cell death', *Cancer Research*, vol. 67, no. 24, pp. 11848-58.

Giridharan, P, Verekar, SA, Khanna, A, Mishra, P & Deshmukh, SK 2012, 'Anticancer activity of sclerotiorin, isolated from an endophytic fungus *Cephalotheca faveolata* Yaguchi, Nishim. & Udagawa', *Indian Journal of Experimental Biology*, vol. 50, no. 7, pp. 464-8.

Gleason, DF & Mellinger, GT 1974, 'Prediction of prognosis for prostatic adenocarcinoma by combined histological grading and clinical staging', *The Journal of Urology*, vol. 111, no. 1, pp. 58-64.

Gonzalez-Menedez, V, Martin, J, Siles, JA, Gonzalez-Tejero, MR, Reyes, F, Platas, G, Tormo, JR & Genilloud, O 2017, 'Biodiversity and chemotaxonomy of *Preussia* isolates from the Iberian Peninsula', *Mycological Progress*, vol. 17, no. 1, pp. 713-28.

Gordetsky, J & Epstein, J 2016, 'Grading of prostatic adenocarcinoma: current state and prognostic implications', *Diagnostic Pathology*, vol. 11, no. 1, pp. 1-8.

Gouda, S, Das, G, Sen, SK, Shin, H-S & Patra, JK 2016, 'Endophytes: a treasure house of bioactive compounds of medicinal importance', *Frontiers in Microbiology*, vol. 7, pp. 1-8.

Hardoim, PR, Van Overbeek, LS, Berg, G, Pirttilä, AM, Compant, S, Campisano, A, Döring, M & Sessitsch, A 2015, 'The hidden world within plants: ecological and evolutionary considerations for defining functioning of microbial endophytes', *Microbiology and Molecular Biology Reviews*, vol. 79, no. 3, pp. 293-320.

He, B, Lu, N & Zhou, Z 2009, 'Cellular and nuclear degradation during apoptosis', *Current Opinion in Cell Biology*, vol. 21, no. 6, pp. 900-12.

References

Heinig, U, Scholz, S & Jennewein, S 2013, 'Getting to the bottom of Taxol biosynthesis by fungi', *Fungal Diversity*, vol. 60, no. 1, pp. 161-70.

Hellsten, R, Johansson, M, Dahlman, A, Dizeyi, N, Sterner, O & Bjartell, A 2008, 'Galiellalactone is a novel therapeutic candidate against hormone-refractory prostate cancer expressing activated Stat3', *The Prostate*, vol. 68, no. 3, pp. 269-80.

Hensens, OD, Helms, GL, Jones, ETT & Harris, GH 1995, 'Structure elucidation of australifungin, a potent inhibitor of sphinganine N-acyltransferase in sphingolipid biosynthesis from *Sporormiella australis*', *The Journal of Organic Chemistry*, vol. 60, no. 6, pp. 1772-6.

Herbst, RS & Khuri, FR 2003, 'Mode of action of docetaxel–a basis for combination with novel anticancer agents', *Cancer Treatment Reviews*, vol. 29, no. 5, pp. 407-15.

Himes, RH 1991, 'Interactions of the *catharanthus (Vinca)* alkaloids with tubulin and microtubules', *Pharmacology & Therapeutics*, vol. 51, no. 2, pp. 257-67.

Hodgson, MC, Astapova, I, Cheng, S, Lee, LJ, Verhoeven, MC, Choi, E, Balk, SP & Hollenberg, AN 2005, 'The androgen receptor recruits nuclear receptor CoRepressor (N-CoR) in the presence of mifepristone via its N and C termini revealing a novel molecular mechanism for androgen receptor antagonists', *Journal of Biological Chemistry*, vol. 280, no. 8, pp. 6511-9.

Hoeks, CM, Hambrock, T, Yakar, D, Hulsbergen–van de Kaa, CA, Feuth, T, Witjes, JA, Fütterer, JJ & Barentsz, JO 2013, 'Transition zone prostate cancer: detection and localization with 3-T multiparametric MR imaging', *Radiology*, vol. 266, no. 1, pp. 207-17.

Horinaga, M, Okita, H, Nakashima, J, Kanao, K, Sakamoto, M & Murai, M 2005, 'Clinical and pathologic significance of activation of signal transducer and activator of transcription 3 in prostate cancer', *Urology*, vol. 66, no. 3, pp. 671-5.

References

Huang, G, Lebovic, G & Vlachou, PA 2019, 'Diagnostic value of ct in detecting peripheral zone prostate cancer', *American Journal of Roentgenology*, vol. 213, no. 4, pp. 831-5.

Hudes, G, Einhorn, L, Ross, E, Balsham, A, Loehrer, P, Ramsey, H, Sprandio, J, Entmacher, M, Dugan, W & Ansari, R 1999, 'Vinblastine versus vinblastine plus oral estramustine phosphate for patients with hormone-refractory prostate cancer: a Hoosier Oncology Group and Fox Chase Network phase III trial', *Journal of Clinical Oncology*, vol. 17, no. 10, pp. 3160-6.

Huggins, C & Hodges, CV 1941, 'Studies on prostatic cancer. I. The effect of castration, of estrogen and of androgen injection on serum phosphatases in metastatic carcinoma of the prostate', *Cancer Research*, vol. 1, no. 4, pp. 293-7.

Humphrey, PA 2004, 'Gleason grading and prognostic factors in carcinoma of the prostate', *Modern Pathology*, vol. 17, no. 3, pp. 292-306.

Hwang, C 2012, 'Overcoming docetaxel resistance in prostate cancer: a perspective review', *Therapeutic Advances in Medical Oncology*, vol. 4, no. 6, pp. 329-40.

Jahn, L, Schafhauser, T, Wibberg, D, Rückert, C, Winkler, A, Kulik, A, Weber, T, Flor, L, van Pée, K-H & Kalinowski, J 2017, 'Linking secondary metabolites to biosynthesis genes in the fungal endophyte *Cyanodermella asteris*: The anti-cancer bisanthraquinone skyrin', *Journal of Biotechnology*, vol. 257, pp. 233-9.

Jemaa, AB, Bouraoui, Y, Sallami, S, Banasr, A, Rais, NB, Ouertani, L, Nouira, Y, Horchani, A & Oueslati, R 2010, 'Co-expression and impact of prostate specific membrane antigen and prostate specific antigen in prostatic pathologies', *Journal of Experimental & Clinical Cancer Research*, vol. 29, no. 1, pp. 1-9.

Jia, J, Zhang, H-B, Shi, Q, Yang, C, Ma, J-B, Jin, B, Wang, X, He, D & Guo, P 2019, 'KLF5 downregulation desensitizes castration-resistant prostate cancer cells to docetaxel by

increasing BECN1 expression and inducing cell autophagy', *Theranostics*, vol. 9, no. 19, pp. 5464-77.

Kalender, Y, Yel, M & Kalender, S 2005, 'Doxorubicin hepatotoxicity and hepatic free radical metabolism in rats: the effects of vitamin E and catechin', *Toxicology*, vol. 209, no. 1, pp. 39-45.

Kalluri, R & Weinberg, RA 2009, 'The basics of epithelial-mesenchymal transition', *The Journal of Clinical Investigation*, vol. 119, no. 6, pp. 1420-8.

Katoch, M, Singh, G, Sharma, S, Gupta, N, Sangwan, PL & Saxena, AK 2014, 'Cytotoxic and antimicrobial activities of endophytic fungi isolated from *Bacopa monnieri* (L.) Pennell *(Scrophulariaceae)*', *BMC Complementary and Alternative Medicine*, vol. 14, no. 1, pp. 1-8.

Khare, E, Mishra, J & Arora, NK 2018, 'Multifaceted interactions between endophytes and plant: developments and prospects', *Frontiers in Microbiology*, vol. 9, pp. 1-12.

Kinoshita, K, Sasaki, T, Awata, M, Takada, M & Yaginuma, S 1997, 'Structure of sporostatin (M5032), an inhibitor of cyclic adenosine 3', 5'-monophosphate phosphodiesterase', *The Journal of Antibiotics*, vol. 50, no. 11, pp. 961-4.

Kjer, J, Wray, V, Edrada-Ebel, R, Ebel, R, Pretsch, A, Lin, W & Proksch, P 2009, 'Xanalteric acids I and II and related phenolic compounds from an endophytic *Alternaria* sp. isolated from the mangrove plant *Sonneratia alba*', *Journal of Natural Products*, vol. 72, no. 11, pp. 2053-7.

Komura, K, Jeong, SH, Hinohara, K, Qu, F, Wang, X, Hiraki, M, Azuma, H, Lee, G-SM, Kantoff, PW & Sweeney, CJ 2016, 'Resistance to docetaxel in prostate cancer is associated with androgen receptor activation and loss of KDM5D expression', *Proceedings of the National Academy of Sciences*, vol. 113, no. 22, pp. 6259-64.

References

Kumar, V & Majumder, P 1995, 'Prostate gland: structure, functions and regulation', *International Urology and Nephrology*, vol. 27, no. 3, pp. 231-43.

Kuriakose, GC, Arathi, BP, Lakshmanan, MD, Jiby, MV, Gudde, RS & Jayabhaskaran, C 2020, 'Sub-acute toxicity assessment of taxol isolated from *Fusarium solani*, an endophytic fungus of *Taxus brevifolia*, in wistar rats and analyzing its cytotoxicity and apoptotic potential in lung cancer cells', *Frontiers in Oncology*, vol. 10, pp. 1-12.

Kusari, S, Lamshöft, M & Spiteller, M 2009, '*Aspergillus fumigatus* Fresenius, an endophytic fungus from *Juniperus communis* L. Horstmann as a novel source of the anticancer pro-drug deoxypodophyllotoxin', *Journal of Applied Microbiology*, vol. 107, no. 3, pp. 1019-30.

Kutscher, W & Wolbergs, H 1935, 'Prostataphosphatase ', *Journal of Physical Chemistry*, vol. 236, pp. 237-40.

Lai, D, Mao, Z, Zhou, Z, Zhao, S, Xue, M, Dai, J, Zhou, L & Li, D 2020, 'New chlamydosporol derivatives from the endophytic fungus *Pleosporales* sp. Sigrf05 and their cytotoxic and antimicrobial activities', *Scientific Reports*, vol. 10, no. 1, pp. 1-9.

Lamouille, S, Xu, J & Derynck, R 2014, 'Molecular mechanisms of epithelial–mesenchymal transition', *Nature Reviews Molecular Cell Biology*, vol. 15, no. 3, pp. 178-96.

Li, J, Chen, W, Zhang, P & Li, N 2006, 'Topoisomerase II trapping agent teniposide induces apoptosis and G2/M or S phase arrest of oral squamous cell carcinoma', *World Journal of Surgical Oncology*, vol. 4, no. 1, pp. 1-7.

Lukinavičius, G, Reymond, L, D'este, E, Masharina, A, Göttfert, F, Ta, H, Güther, A, Fournier, M, Rizzo, S & Waldmann, H 2014, 'Fluorogenic probes for live-cell imaging of the cytoskeleton', *Nature Methods*, vol. 11, no. 7, pp. 731-3.

References

Mapperson, R 2014, 'Diversity of fungal endophytes in the semi evergreen vine thickets of the southern Brigalow Belt bioregion and their production of antimicrobial secondary metabolites', University of Southern Queensland, Toowoomba.

Mapperson, R, Kotiw, M, Davis, RA & Dearnaley, JDW 2014, 'The diversity and antimicrobial activity of *Preussia* sp. endophytes isolated from Australian dry rainforests', *Current Microbiology*, vol. 68, no. 1, pp. 30-7.

McNeal, JE 1969, 'Origin and development of carcinoma in the prostate', *Cancer*, vol. 23, no. 1, pp. 24-34.

McNeal, JE 1981, 'The zonal anatomy of the prostate', *The Prostate*, vol. 2, no. 1, pp. 35-49.

McNeal, JE, Redwine, EA, Freiha, FS & Stamey, TA 1988, 'Zonal distribution of prostatic adenocarcinoma. Correlation with histologic pattern and direction of spread', *The American Journal of Surgical Pathology*, vol. 12, no. 12, pp. 897-906.

Mediavilla-Varela, M, Pacheco, FJ, Almaguel, F, Perez, J, Sahakian, E, Daniels, TR, Leoh, LS, Padilla, A, Wall, NR & Lilly, MB 2009, 'Docetaxel-induced prostate cancer cell death involves concomitant activation of caspase and lysosomal pathways and is attenuated by LEDGF/p75', *Molecular Cancer*, vol. 8, no. 1, pp. 1-15.

Merck 2021, *SCT142 Sigma-Aldrich BioTracker 488 Green Microtubule Cytoskeleton Dye*, Germany, https://www.merckmillipore.com/AU/en/product/BioTracker-488-Green-Microtubule-Cytoskeleton-Dye,MM_NF-SCT142>.

Mikuła-Pietrasik, J, Witucka, A, Pakuła, M, Uruski, P, Begier-Krasińska, B, Niklas, A, Tykarski, A & Książek, K 2019, 'Comprehensive review on how platinum-and taxane-based chemotherapy of ovarian cancer affects biology of normal cells', *Cellular and Molecular Life Sciences*, vol. 76, no. 4, pp. 681-97.

References

Montecucco, A, Zanetta, F & Biamonti, G 2015, 'Molecular mechanisms of etoposide', *Experimental and Clinical Sciences Journal*, vol. 14, pp. 95-108.

Mora, LB, Buettner, R, Seigne, J, Diaz, J, Ahmad, N, Garcia, R, Bowman, T, Falcone, R, Fairclough, R & Cantor, A 2002, 'Constitutive activation of Stat3 in human prostate tumors and cell lines: direct inhibition of Stat3 signaling induces apoptosis of prostate cancer cells', *Cancer Research*, vol. 62, no. 22, pp. 6659-66.

Nagle, RB, Brawer, MK, Kittelson, J & Clark, V 1991, 'Phenotypic relationships of prostatic intraepithelial neoplasia to invasive prostatic carcinoma', *The American Journal of Pathology*, vol. 138, no. 1, pp. 119-28.

Nenkep, V, Yun, K, Zhang, D, Choi, HD, Kang, JS & Son, BW 2010, 'Induced production of bromomethylchlamydosporols A and B from the marine-derived fungus *Fusarium tricinctum*', *Journal of Natural Products*, vol. 73, no. 12, pp. 2061-3.

Noumeur, SR, Helaly, SE, Jansen, R, Gereke, M, Stradal, TEB, Harzallah, D & Stadler, M 2017, 'Preussilides A−F, bicyclic polyketides from the endophytic fungus *Preussia similis* with antiproliferative activity', *Journal of Natural Products*, vol. 80, no. 5, pp. 1531-40.

Partin, AW, Catalona, WJ, Southwick, PC, Subong, EN, Gasior, GH & Chan, DW 1996, 'Analysis of percent free prostate-specific antigen (PSA) for prostate cancer detection: influence of total PSA, prostate volume, and age', *Urology*, vol. 48, no. 6, pp. 55-61.

Paudal, B, Bhattarai, K & Bhattarai, HD 2018, 'Antimicrobial and antioxidant activities of two polyketides from lichen-endophytic fungus *Preussia* sp', *Journal for Nature Research*, vol. 73, no. 3, pp. 161-3.

Pavese, JM, Ogden, IM, Voll, EA, Huang, X, Xu, L, Jovanovic, B & Bergan, RC 2014, 'Mitogen-activated protein kinase kinase 4 (MAP2K4) promotes human prostate cancer metastasis', *PloS One*, vol. 9, no. 7, pp. 1-12.

References

Peyrat, LA, Eparvier, V, Eydoux, C, Guillemot, JC, Litaudon, M & Stien, D 2017, 'Betulinic acid, the first lupane-type triterpenoid isolated from both a *Phomopsis* sp. and its host plant *Diospyros carbonaria* Benoist', *Chemistry & Biodiversity*, vol. 14, no. 1, pp. 1-21.

Prostate Cancer Foundation of Australia 2021, *Prostate cancer; A guide for newly diagnosed men*, PCFA, St Leonards, NSW, Australia, https://issuu.com/prostatecancerfoundationaus/docs/pcf13457_-_prostate_cancer_-_a_guide_for_newly_dia>.

Rabbani, A, Iskandar, M & Ausió, J 1999, 'Daunomycin-induced unfolding and aggregation of chromatin', *Journal of Biological Chemistry*, vol. 274, no. 26, pp. 18401-6.

Ramasamy, K, Lim, SM, Bakar, HA, Ismail, N, Ismail, MS, Ali, MF, Faizal Weber, JF & Cole, AL 2010, 'Antimicrobial and cytotoxic activities of Malaysian endophytes', *Phytotherapy Research: An International Journal Devoted to Pharmacological and Toxicological Evaluation of Natural Product Derivatives*, vol. 24, no. 5, pp. 640-3.

Raudenska, M, Kratochvilova, M, Vicar, T, Gumulec, J, Balvan, J, Polanska, H, Pribyl, J & Masarik, M 2019, 'Cisplatin enhances cell stiffness and decreases invasiveness rate in prostate cancer cells by actin accumulation', *Scientific Reports*, vol. 9, no. 1, pp. 1-11.

Saad, F & Hotte, SJ 2010, 'Guidelines for the management of castrate-resistant prostate cancer', *Canadian Urological Association Journal*, vol. 4, no. 6, pp. 380-4.

Santiago, C, Fitchett, C, Munro, MH, Jalil, J & Santhanam, J 2012, 'Cytotoxic and antifungal activities of 5-hydroxyramulosin, a compound produced by an endophytic fungus isolated from *Cinnamomum mollisimum*', *Evidence-Based Complementary and Alternative Medicine*, vol. 2012, pp. 1-6.

Sathianathen, NJ, Philippou, YA, Kuntz, GM, Konety, BR, Gupta, S, Lamb, AD & Dahm, P 2018, 'Taxane-based chemohormonal therapy for metastatic hormone-sensitive prostate cancer', *Cochrane Database of Systematic Reviews*, vol. 10, pp. 1-51.

References

Senthil Kumuran, R, Muthumary, J & Hur, B 2008, 'Production of Taxol from *Phyllosticta spinarum*, an endophytic fungus of *Cupressus* sp', *Engineering in Health Sciences*, vol. 4, no. 1, pp. 438-46.

Shankar, E, Zhang, A, Franco, D & Gupta, S 2017, 'Betulinic acid-mediated apoptosis in human prostate cancer cells involves p53 and nuclear factor-kappa B (NF-κB) pathways', *Molecules*, vol. 22, no. 2, pp. 264-77.

Shappell, SB, Thomas, GV, Roberts, RL, Herbert, R, Ittmann, MM, Rubin, MA, Humphrey, PA, Sundberg, JP, Rozengurt, N & Barrios, R 2004, 'Prostate pathology of genetically engineered mice: definitions and classification. The consensus report from the Bar Harbor meeting of the Mouse Models of Human Cancer Consortium Prostate Pathology Committee', *Cancer Research*, vol. 64, no. 6, pp. 2270-305.

Sharma, A 2021, 'Investigation of Queensland dry rainforest endophytes and their production of antimicrobial agents', University of Southern Queensland, Toowoomba.

Shen, MM & Abate-Shen, C 2010, 'Molecular genetics of prostate cancer: new prospects for old challenges', *Genes & Development*, vol. 24, no. 18, pp. 1967-2000.

Siddik, ZH 2003, 'Cisplatin: mode of cytotoxic action and molecular basis of resistance', *Oncogene*, vol. 22, no. 47, pp. 7265-79.

Silva, GH, Teles, HL, Zanardi, LM, Young, MCM, Eberlin, MN, Hadad, R, Pfenning, LH, Costa-Neto, CM, Castro-Gamboa, I & da Silva Bolzani, V 2006, 'Cadinane sesquiterpenoids of *Phomopsis cassiae*, an endophytic fungus associated with *Cassia spectabilis* (*Leguminosae*)', *Phytochemistry*, vol. 67, no. 17, pp. 1964-9.

Srivastava, A & Anandrao, RK 2015, 'Antimicrobial potential of fungal endophytes isolated from leaves of *Prosopis juliflora* (SW.) DC. an important weed', *International Journal of Pharmacy and Pharmaceutical Sciences*, vol. 7, no. 12, pp. 128-36.

References

Stierle, A, Strobel, G & Stierle, D 1993, 'Taxol and taxane production by *Taxomyces andreanae,* an endophytic fungus of Pacific yew', *Science*, vol. 260, no. 5105, pp. 214-6.

Talontsi, FM, Lamshöft, M, Douanla-Meli, C, Kouam, SF & Spiteller, M 2014, 'Antiplasmodial and cytotoxic dibenzofurans from *Preussia* sp. harboured in *Enantia chlorantha* Oliv', *Fitoterapia*, vol. 93, pp. 233-8.

Tam, L, McGlynn, LM, Traynor, P, Mukherjee, R, Bartlett, JM & Edwards, J 2007, 'Expression levels of the JAK/STAT pathway in the transition from hormone-sensitive to hormone-refractory prostate cancer', *British Journal of Cancer*, vol. 97, no. 3, pp. 378-83.

Tannock, IF, De Wit, R, Berry, WR, Horti, J, Pluzanska, A, Chi, KN, Oudard, S, Théodore, C, James, ND & Turesson, I 2004, 'Docetaxel plus prednisone or mitoxantrone plus prednisone for advanced prostate cancer', *New England Journal of Medicine*, vol. 351, no. 15, pp. 1502-12.

Taylor, BS, Schultz, N, Hieronymus, H, Gopalan, A, Xiao, Y, Carver, BS, Arora, VK, Kaushik, P, Cerami, E & Reva, B 2010, 'Integrative genomic profiling of human prostate cancer', *Cancer Cell*, vol. 18, no. 1, pp. 11-22.

Tayung, K & Jha, D 2014, 'Identification and characterization of antimicrobial metabolite from an endophytic fungus, *Fusarium solani* isolated from bark of Himalayan yew', *Annual Review of Plant Pathology*, vol. 6, pp. 299-334.

Teply, BA, Luber, B, Denmeade, SR & Antonarakis, ES 2016, 'The influence of prednisone on the efficacy of docetaxel in men with metastatic castration-resistant prostate cancer', *Prostate Cancer and Prostatic Diseases*, vol. 19, no. 1, pp. 72-8.

Tian, L-L, Ren, H, Xi, J-M, Fang, J, Zhang, JZ & Wu, Q-X 2021, 'Diverse anti-inflammation and anti-cancer polyketides isolated from the endophytic fungi *Alternaria* sp. MG1', *Fitoterapia*, vol. 153, pp. 1-9.

References

Toivanen, R & Shen, MM 2017, 'Prostate organogenesis: tissue induction, hormonal regulation and cell type specification', *Development*, vol. 144, no. 8, pp. 1382-98.

Tsujimoto, Y 1998, 'Role of Bcl-2 family proteins in apoptosis: apoptosomes or mitochondria?', *Genes to Cells*, vol. 3, no. 11, pp. 697-707.

Tzifi, F, Economopoulou, C, Gourgiotis, D, Ardavanis, A, Papageorgiou, S & Scorilas, A 2012, 'The role of BCL2 family of apoptosis regulator proteins in acute and chronic leukemias', *Advances in Hematology*, vol. 2012, pp. 1-14.

Uesugi, S, Fujisawa, N, Yoshida, J, Watanabe, M, Dan, S, Yamori, T, Shiono, Y & Kimura, K-i 2016, 'Pyrrocidine A, a metabolite of endophytic fungi, has a potent apoptosis-inducing activity against HL60 cells through caspase activation via the Michael addition', *The Journal of Antibiotics*, vol. 69, no. 3, pp. 133-40.

Uzma, F, Mohan, CD, Hashem, A, Konappa, NM, Rangappa, S, Kamath, PV, Singh, BP, Mudili, V, Gupta, VK & Siddaiah, CN 2018, 'Endophytic fungi—alternative sources of cytotoxic compounds: a review', *Frontiers in Pharmacology*, vol. 9, no. 39, pp. 1-31.

Varnai, R, Koskinen, LM, Mäntylä, LE, Szabo, I, FitzGerald, LM & Sipeky, C 2019, 'Pharmacogenomic biomarkers in docetaxel treatment of prostate cancer: from discovery to implementation', *Genes*, vol. 10, no. 8, pp. 599-621.

Verekar, SA, Mishra, PD, Sreekumar, ES, Deshmukh, SK, Fiebig, H-H, Kelter, G & Maier, A 2014, 'Anticancer activity of new depsipeptide compound isolated from an endophytic fungus', *The Journal of Antibiotics*, vol. 67, no. 10, pp. 697-701.

Wang, G, Zhao, D, Spring, DJ & DePinho, RA 2018, 'Genetics and biology of prostate cancer', *Genes & Development*, vol. 32, no. 17, pp. 1105-40.

References

Wang, Q-X, Li, S-F, Zhao, F, Dai, H-Q, Bao, L, Ding, R, Gao, H, Zhang, L-X, Wen, H-A & Liu, H-W 2011, 'Chemical constituents from endophytic fungus *Fusarium oxysporum*', *Fitoterapia*, vol. 82, no. 5, pp. 777-81.

Wani, MC, Taylor, HL, Wall, ME, Coggon, P & McPhail, AT 1971, 'Plant antitumor agents. VI. Isolation and structure of taxol, a novel antileukemic and antitumor agent from *Taxus brevifolia*', *Journal of the American Chemical Society*, vol. 93, no. 9, pp. 2325-7.

Weaver, BA 2014, 'How Taxol/paclitaxel kills cancer cells', *Molecular Biology of the Cell*, vol. 25, no. 18, pp. 2677-81.

Wende, M, Sithole, S, Fru, CG, Stevens, MY & Mukanganyama, S 2021, 'The Effects of Combining Cancer Drugs with Compounds Isolated from *Combretum zeyheri* Sond. and *Combretum platypetalum* Welw. ex MA Lawson (*Combretaceae*) on the Viability of Jurkat T Cells and HL-60 Cells', *BioMed research international*, vol. 2021, pp. 1-10.

Wijeratne, EK, Paranagama, PA, Marron, MT, Gunatilaka, MK, Arnold, AE & Gunatilaka, AL 2008, 'Sesquiterpene quinones and related metabolites from *Phyllosticta spinarum*, a fungal strain endophytic in *Platycladus orientalis* of the Sonoran Desert', *Journal of Natural Products*, vol. 71, no. 2, pp. 218-22.

Yang, X, Zhang, L, Guo, B & Guo, S 1994, 'Preliminary study of a vincristine-producing endophytic fungus isolated from leaves of *Catharanthus roseus*', *Chinese Traditional and Herbal Drugs*, vol. 35, no. 1, pp. 79-81.

Yao, C-H, Fowle-Grider, R, Mahieu, NG, Liu, G-Y, Chen, Y-J, Wang, R, Singh, M, Potter, GS, Gross, RW & Schaefer, J 2016, 'Exogenous fatty acids are the preferred source of membrane lipids in proliferating fibroblasts', *Cell Chemical Biology*, vol. 23, no. 4, pp. 483-93.

References

Yatani, R, Kusano, I, Shiraishi, T, Hayashi, T & Stemmermann, GN 1989, 'Latent prostatic carcinoma: Pathological and epidemiological aspects', *Japanese Journal of Clinical Oncology*, vol. 19, no. 4, pp. 319-26.

Yeung, KT & Yang, J 2017, 'Epithelial–mesenchymal transition in tumor metastasis', *Molecular Oncology*, vol. 11, no. 1, pp. 28-39.

Zhang, F, Li, L, Niu, S, Guo, L, Jiang, X & Che, Y 2012, 'A thiopyranchromenone and other chromone derivatives from an endolichenic fungus, *Preussia africana*', *Journal of Natural Products*, vol. 75, no. 2, pp. 230-7.

Zhang, J-y, Tao, L-y, Liang, Y-j, Yan, Y-y, Dai, C-l, Xia, X-k, She, Z-g, Lin, Y-c & Fu, L-w 2009, 'Secalonic acid D induced leukemia cell apoptosis and cell cycle arrest of G1 with involvement of GSK-3β/β-catenin/c-Myc pathway', *Cell Cycle*, vol. 8, no. 15, pp. 2444-50.

Zhang, L, Guo, B, Li, H, Zeng, S, Shao, H, Gu, S & Wei, R 2000, 'Preliminary study on the isolation of endophytic fungus of *Catharanthus roseus* and its fermentation to produce products of therapeutic value', *Chinese Traditional and Herbal Drugs*, vol. 31, no. 11, pp. 805-7.

Zhang, W & Liu, HT 2002, 'MAPK signal pathways in the regulation of cell proliferation in mammalian cells', *Cell Research*, vol. 12, no. 1, pp. 9-18.

Zhao, L & Zhang, B 2017, 'Doxorubicin induces cardiotoxicity through upregulation of death receptors mediated apoptosis in cardiomyocytes', *Scientific Reports*, vol. 7, no. 1, pp. 1-11.

Zink, D, Fischer, AH & Nickerson, JA 2004, 'Nuclear structure in cancer cells', *Nature Reviews Cancer*, vol. 4, no. 9, pp. 677-87.

Zunino, F & Capranico, G 1990, 'DNA topoisomerase II as the primary target of anti-tumor anthracyclines', *Anti-cancer Drug Design*, vol. 5, no. 4, pp. 307-17.

Appendices

Appendix A: Media recipes for fungal culture

DIFCO Potato Dextrose Agar (PDA)

Dissolve 15.6g of PDA powder into 400mL of dH_2O and autoclave at 121°C for 15 minutes. Cool agar to 50°C in an incubator shaker. Pour 20 agar plates in the biohazard cabinet once cooled.

Oxoid Sensitest Agar (STA)

Dissolve 12.8g of STA powder in 400mL of dH_2O and autoclave at 121°C for 15 minutes. Cool agar to 50°C in an incubator shaker. Pour 20 agar plates in the biohazard cabinet once cooled.

Sigma Aldrich Malt Extract Broth (MEB)

Dissolve 20g of MEB powder into 1 L of dH_2O and autoclave at 121°C for 15 minutes. Store broth at room temperature.

Oxoid Mueller-Hinton Broth (MHB)

Dissolve 8.4g of MHB powder in 400mL of dH_2O and autoclave at 121°C for 15 minutes. Store broth at room temperature.

Appendix B: Microdilution assay data

Table 4: Microdilution assay for assessment of antibacterial activity of BSH2.9 FCEs after 18 hours of incubation.

18 HOURS	Crude extract	Crude extract	Vancomycin	Sterile H_2O	25% EtOH solvent	Plain MH broth
Bacillus cereus	-	-	-	+	-	-
	-	-	-	+	-	-
	-	-	-	+	-	-
	-	-	-	+	-	-
Enterococcus faecalis	-	-	-	++	-	-
	-	-	-	++	-	-
	-	-	-	++	-	-
	-	-	-	++	-	-

Table 5: Microdilution assay for assessment of antibacterial activity of BSH2.9 FCEs after 20 hours of incubation.

20 HOURS	Crude extract	Crude extract	Vancomycin	Sterile H_2O	25% EtOH solvent	Plain MH broth
Bacillus cereus	-	-	-	+	+	-
	-	-	-	+	+	-
	-	-	-	+	+	-
	-	-	-	+	+	-
Enterococcus faecalis	-	-	-	++	+	-
	-	-	-	++	+	-
	-	-	-	++	+	-
	-	-	-	++	+	-

Table 6: Microdilution assay for assessment of antibacterial activity of BSH2.9 FCEs after 48 hours of incubation.

48 HOURS	Crude extract	Crude extract	Vancomycin	Sterile H_2O	25% EtOH solvent	Plain MH broth
Bacillus cereus	-	-	-	++	++	-
	-	-	-	++	++	-
	-	-	-	++	++	-
	-	-	-	++	++	-
Enterococcus faecalis	-	-	-	++	++	-
	-	-	-	++	++	-
	-	-	-	++	++	-
	-	-	-	++	++	-

Key

-	No growth observed
+	Milky appearance in the well indicating microbial growth
++	Both a visible growth button and milkiness were observed

Appendix C: Equipment and reagent details

PC-3 grade IV prostate adenocarcinoma cell line

- ATCC CRL-1435
- Gifted by Dr. Patrick Thomas (Translational Research Institute/ Queensland University of Technology)

RPMI-1640 Culture Medium

- Manufacturer; Sigma-Aldrich
- Containing L-glutamine and sodium bicarbonate
- Lot #RNBK2587

Cell counting kit 8

- Manufacturer; Sigma Aldrich
- Lot # BCCD4662

Lab-Tek® Chamber Slide™ system 177347

- Manufacturer; Thermo Fisher Scientific Inc.
- Lot #1287760

BioTracker 488 green microtubule cytoskeleton dye

- Manufacturer; Sigma/ Merck
- Lot # K1471210

ActinRed™ 555 ReadyProbes™ reagent

- Manufacturer; Invitrogen by Thermo Fisher Scientific
- Lot #2204191

NucBlue™ Live Cell Stain ReadyProbes™ reagent

- Manufacturer; Invitrogen by Thermo Fisher Scientific
- Hoechst33342 special formulation
- Lot #2214511